

N72-33743

NASA CR-120914



TF34 TURBOFAN QUIET ENGINE STUDY

FINAL REPORT

by D.P. Edkins, R. Hirschkron, R. Lee

General Electric Company
Aircraft Engine Group
Lynn, Massachusetts/Cincinnati, Ohio

Prepared for
NATIONAL AERONAUTICS AND SPACE ADMINISTRATION

NASA Lewis Research Center

R.J. Denington — Project Manager

CONTRACT NAS 3-14338

FACILITY FORM 802

N72-33743
(ACCESSION NUMBER)

98
(PAGES)

CR 120914
(NASA CR OR TMX OR AD NUMBER)

(THRU)

G-3
(CODE)

28
(CATEGORY)

TABLE OF CONTENTS

	<u>PAGE</u>
ABSTRACT	ii
SUMMARY	1
INTRODUCTION	3
LIST OF SYMBOLS AND ABBREVIATIONS	4
1. CYCLE AND CONFIGURATION SELECTION	5
2. FAN SELECTION AND AERODYNAMIC DESIGN	7
3. ACOUSTICS ANALYSIS AND DESIGN	15
4. FAN TURBINE	42
5. TF34 COMPATIBILITY	47
6. VARIABLE-PITCH FAN MECHANICAL DESIGN	50
7. REDUCTION GEAR	61
8. CONTROL SYSTEM	64
9. ENGINE WEIGHT	74
10. CONCLUSIONS	75
REFERENCE	76
STATION DESIGNATIONS	77
 <u>APPENDICES</u>	
I. ENGINE CYCLE DATA	78
II. DERIVATIVE TABLES FOR DUCT LOSSES	84
III. TIMKEN PHYSICAL LABORATORIES REPORT	87
IV. ENGINE WEIGHT	90
V. ENGINE AND NACELLE DRAWINGS	91

ABSTRACT

A study of high bypass turbofan engines in heavily sound-suppressed nacelles based on the TF34 engine. The four-engine noise objective was 95 PNdB at four locations typical of takeoff and landing. Three engines were studied; these had fan pressure ratios, bypass ratios and fan tip speeds respectively of 1.48/6.5/404 m/s (1327 ft/s), 1.25/13/305 (1000), 1.25/13/366(1200). The bypass 13 engines had a variable pitch fan, direct - and gear-driven. Noise suppressive treatment was identified which met the 95 PNdB objective except for sideline liftoff at 6.5 bypass, full power, which was 2 PNdB noisier; at 90% power, 95 PNdB was achieved.

SUMMARY

This report describes a study of high bypass turbofan engines with noise suppression treatment for use in short-takeoff-and-landing (STOL) commercial aircraft. The noise level objective was 95 PNdB at four points. Full power sea level: (1) static and (2) 50 m/s (100 knots) at 150m (500 ft) sideline; (3) 1850m (1 n. mi) from brake release at 210m (700ft) altitude; (4) 925m (1/2 n. mi) from touchdown at 150m (500 ft) altitude, 50% power.

The study engines were all based on the General Electric TF34-2 turbofan which has a bypass ratio of 6.5 and a maximum thrust of 41000 N (9200 lb). Three engines were selected for investigation: (A) The TF34-2; (B) and (C), bypass 13 derivatives. (B) and (C) used the TF34 core engine, but have a fan pressure ratio of 1.25 instead of 1.45 for the bypass 6.5 standard engine. Engine B has a 1.9:1 reduction gear driving the fan which permits direct use of the TF34 four-stage low-pressure turbine. Fan (B) and (C) are variable pitch with capability to move through zero pitch to negative angles to provide reverse thrust. The fan pressure ratio of 1.25 permits a reduction in tip speed from 404 m/s (1327 ft/sec) for the bypass 6.5 engine to lower values which reduce the variable pitch blade centrifugal loads. Fan C is directly driven by a new, larger four-stage turbine. Engine (A) has a mixed, (B) and (C) a separated, flow exhaust system. Key data for the three engines are as follows:

			A		B		C	
Thrust	SLS	N (lb)	39265	(8909)	45092	(10137)	45336	(10192)
Diameter		m (in.)	1.17	(46)	1.6	(63)	1.57	(62)
Weight		kg (lb)	615	(1358)	1082	(2386)	975	(2150)
Fan Pressure Ratio			1.48		1.25		1.25	
Overall Pressure Ratio			20.0		18		18	
Thrust	} 0.8 M. N. 7620m (25000 ft)	N (lb)	9915	(2230)	9200	(2068)	9275	(2085)
SFC			20.7 μ kg/NS (.73 lb/lb/hr)					
Fan Tip Speed	m/s (ft/sec)		404	(1327)	305	(1000)	366	(1200)
Jet Velocity, Fan	m/s (ft/sec)	}	265	(871)	192	(631)	192	(631)
Jet Velocity Core	m/s (ft/sec)				262	(861)	262	(861)
Fan Blade/Vane Spacing,			.6		1.7		1.5	
Bypass Ratio			6.5		13		13	

The noise suppressive treatment was applied to representative nacelles designed for the engines. The treatment consists of sound-absorbing material applied to the walls of the inlet, fan exhaust and core exhaust ducts. Additional material was also applied to concentric splitter sections in the inlet and fan exhaust ducts, and a series of 16 radial struts in the core exhaust. Estimates of the noise attenuation and pressure loss characteristics of the treatment were made. Calculation of flap impingement noise from 0 to 10 PNdB above the jet noise were made.

It was concluded that the 150m (500 ft)sideline liftoff condition is the critical one for meeting the 95 PNdB noise level objective. Engine(A) had a noise level of 95 PNdB at 90% of maximum takeoff thrust, and would therefore slightly exceed this level (by 2 PNdB) at full thrust. The fan noise suppression of 23.5 PNdB would have to be increased by some 5 - 7 PNdB to reach 95 PNdB overall at full power. This degree of suppression is considered to be excessive. The jet noise is also limiting at full power. These estimates do not include flap impingement noise. Engine (B) and (C) can meet the critical sideline noise objectives because of lower fan source noise (wider blade/vane spacing) and lower jet noise, with less acoustic treatment. Wider spacing on engine (A) would have lowered overall noise by 1.5 PNdB. The noise levels at the other three measurement points varied from 90 to 94 PNdB for all three engines.

Several lower noise sources exist, which while below the level that affects current suppressed engines, may become important or even limiting as greater amounts of suppression for the major sources are provided

The variable pitch fan was designed around solid titanium blades. The resulting centrifugal and blade untwist loads are high and present problems of blade retention and actuation. Although satisfactory solutions to these problems were found, the use of lightweight blades such as composite construction is clearly indicated as a promising direction for further work.

The fan aerodynamic design for variable pitch required only minor compromises. The overall efficiency was estimated at about 2 points lower because of reduction of solidity to 0.95 (to permit travel through zero pitch without blade clashing) relative to a fixed pitch fan. Fan (C) was estimated to be a further 1 point lower in efficiency because of effect of higher tip Mach number at the reduced solidity.

The overall difference between geared and direct drive fans was modest; the main difference is a 107 kg (240 lb) lower weight for the direct drive engine (C).

INTRODUCTION

Current interest in the relief of airport and airspace congestion by the use of smaller existing or additional small airports has led to studies of STOL aircraft and their propulsion systems. An essential element in such studies is clearly the control of noise in the vicinity of such airports. Several current commercial and military aircraft have high bypass ratio engines which provide lower noise levels than previous generations of such aircraft. These lower levels are achieved by attention to source noise such as fan and jet noise and by the use of noise suppressive treatment of nacelles. For STOL aircraft further lowering of the noise level will be required both on the airport and over the nearby community.

The current study was conducted to establish a preliminary design definition of a quiet nacelle for a series of turbofan engines based on the General Electric TF34 turbofan engine. Parallel studies are being sponsored by NASA on experimental STOL aircraft sized for the engines studied herein. Other NASA-sponsored work includes a program to conduct a fullscale ground test of a quiet TF34 nacelle with various suppressive schemes and with flap impingement noise testing. Further NASA exploratory work includes study of a velocity decayer nozzle system for the reduction of flap impingement noise associated with externally blown airfoil flaps.

The scope of the current study included noise treatment definition, noise estimates, engine performance and weight, and preliminary design definition of the associated engine modifications.

The study procedure was analysed based on noise test data of an unsuppressed TF34 engine, on suppressive treatment test data, and on engine performance and weight data available from the TF34 engine development program currently underway.

LIST OF SYMBOLS

C_o	bearing deformation load
F_n	net thrust
H	height
J	mechanical equivalent of heat
K	1000
L	length
M, M. N.	Mach number
N	rotational speed
P/P	pressure ratio
U	linear speed
V	velocity

g	gravitational constant
h	enthalpy drop across turbine
p	pressure
q	dynamic pressure
Δ	change in parameter
η	efficiency

Subscripts

r	relative
g	gas generator
f	fan

Abbreviations

BTU	British Thermal Units
DIA	diameter
FPS	feet/second
FT, ft	feet
Hz	hertz
LP	low pressure
N	newtons
PCL	power control lever
PSI	pounds per square inch
R	Rankine
RPM	revolutions per minute
SEC	sec, seconds
SFC	specific fuel consumption
S. L.	sea level
SLS	sea level static
Ti	titanium
T. O.	takeoff
V. P.	variable pitch

1. CYCLE AND CONFIGURATION SELECTION

Three modified TF34 engines were selected for study within one month after contract initiation. The three engines were recommended to the NASA Lewis Laboratory and approved.

The three engines are all based on the YT34-2 core with identical ratings. This was done to minimize the modifications required to develop an externally blown flap STOL engine for use in experimental flight testing.

The key features of the three modified engines are displayed in Table I.

TABLE I - MODIFIED TF34 ENGINES

<u>Engine</u>	<u>Fan</u>	<u>Fan Turbine</u>	<u>Fan Duct</u>	<u>Exhaust</u>	<u>Core Nozzle</u>	<u>Fan Nozzle</u>
A	YTF34-2	YTF34-2	Long	Mixed	Fixed	-
B	Geared 1.25 pressure ratio variable pitch	YTF34-2	Long	Separate	Fixed	2-Position
C	1.25 pressure ratio variable pitch	4-Stage-new	Long	Separate	Fixed	2-Position
YTF34-2	YTF34-2	YTF34-2	Short	Separate	Fixed	Fixed

Figures 1, 2 and 3 show the uninstalled engine designs. Nacelle outline drawings with these engines installed are shown in Figures 4, 5 and 6. (See Appendix V).

Engine (A)

The mixed flow exhaust was selected to provide primary thrust spoiling during reverse operation. This automatically occurs when the fan flow is diverted through a reverser cascade. Under these conditions the effective primary nozzle area is increased, reducing thrust and more energy is diverted to the fan turbine for greater fan (reverse) thrust. Core exhaust areas and mixer areas were selected to reduce the jet velocity to 274 m/s (900ft/sec), low enough so that in combination with the suppressed fan noise, the objective

of 95PNdB 4 engine 150m (500 ft) sideline noise could be met. Three restrictions on further area increases were: (1), the resultant high swirl and Mach number at fan turbine discharge, (2), minimizing the partial mixer pressure loss and (3), keep the takeoff pressure ratio at 1.5 for good cruise thrust without a variable core nozzle area. The cruise thrust compromise resulting from a constant core nozzle was considered as a good balance for the experimental aircraft missions defined.

The general requirements for acoustic inlet, fan duct and turbomachinery suppression were established and an installation outline is provided with each engine drawing. Bare engine performance is quoted throughout with derivatives furnished for thrust and SFC losses due to various pressure loss decrements. Jet velocities are calculated for the installed engine including approximate pressure losses to provide a consistent noise estimate. Appendices I and II list performance data and pressure loss derivatives respectively.

Engine (B) - Geared Drive

The variable pitch fan is sized on the basis of the maximum usable fan turbine energy extraction. The fan turbine is run at 785 rad/s (7500 RPM), higher than the nominal YTF34-2 takeoff speed 723 rad/s (6900 RPM) to improve fan turbine efficiency at the higher loading condition of Engine B.

A modest boost pressure ratio of 1.14 is estimated for the 1.25 pressure ratio (bypass average) fan. No booster stages are provided. A variable (2 position) fan nozzle is required to optimize cruise thrust without fan overspeed. Table II shows the effect of various nozzle areas.

TABLE II - FAN NOZZLE CRUISE AREA SELECTION

Mach 0.8 at 7620 m (25,000 feet) altitude, max continuous power

Net Thrust,	N (lb)	5013	(1127)	7362	(1655)	8523	(1916)	9194	(2067)
Fan Speed,	%	134.7		111.7		106.7		104.4	
Corrected Fan Speed,	%	139.4		115.5		110.4		104.4	
Fan Pressure Ratio		1.12		1.19		1.23		1.26	
Fan Nozzle Exit Area	m ² (in. ²)	1.044	(1619)	0.940	(1457)	0.888	(1376)	0.835	(1295)
Fan Nozzle Exit Area Reduction from Takeoff,	%	0		10		15		20	

The closed position of the fan nozzle was selected at $.835\text{m}^2$ (1295 in.^2). It is undesirable to run at a high corrected speed with fan efficiency penalties and little acceleration capability due to the proximity of the fan stall line. The same considerations were applied to Engine (C) as in Engine (B) with respect to sizing the nozzle areas at takeoff and determining the fan nozzle cruise setting.

A gear efficiency of .987 was assumed in all cycle calculations for engine (B). The new fan turbine associated with engine (C) required a new exhaust system design. Though the product of gear, fan, and turbine efficiencies for engine (B) exceeds that for (C), the efficiency of the low pressure system for engine (C) yields a higher overall value. Thus engine (B) is 0.9% lower in thrust than the direct drive engine (C).

TABLE III - LOW PRESSURE SPOOL COMPONENT EFFICIENCIES

50 m/s (100 knots) at Sea Level, 288°K (59°F), max power, uninstalled

<u>Engine</u>	<u>(B) Geared</u>	<u>(C) Direct Drive</u>
Gear Efficiency	.987	---
Fan Efficiency	.871	.862
Low Pressure Turbine Efficiency	.907	.896
Tailpipe Efficiency	.982	.994
Product Efficiency	.766	.768

2. FAN SELECTION AND AERODYNAMIC DESIGN

The increased bypass ratio fan engines (B and C) have advantages for an externally blown flap STOL aircraft. In addition to intrinsic advantages of the lower fan and fan jet source and flap impingement noise, the potential capability of obtaining thrust reversal was the key motive for including a variable pitch design study. Although the requirements of this study contract stipulate no thrust reversal capability in the experimental aircraft, it is believed that operational aircraft would require some form of reverse thrust for both landing and rejected takeoff.

Reversal through fine pitch (tangential) was assumed in the aerodynamic design of both fans in engines (B) and (C). Two reasons leading to this decision were:

- (1) less rotation required from nominal to reverse moving through fine pitch $1.22 - 1.57$ radian ($70^\circ - 90^\circ$) compared to 2.62 radian (150°).
- (2) avoids rotating the blade through stall.

Both fans were therefore designed for solidities less than 1 (.95 was used) at all radii to permit non-interfering rotation through reversal. Table IV shows basic aerodynamic data for all three fans.

The key fan aerodynamic design parameters are listed in Tables V and VI. Blading design was carried out in sufficient detail to establish weight and feasibility. Examination of the fan aerodynamic design parameters indicates that only a moderate loss is expected due to variable pitch compromises. A fan stage efficiency decrement was taken from a conventional fixed pitch design based on an estimate of rotor efficiency vs. radial height. The results of this analysis are shown on Figure 7 for both fans. The solidity loss is higher for the higher relative Mach number of the direct drive fan(C). The stage efficiencies at design conditions are referenced in Table IV.

The fan flow annulus area and radius ratios were selected after an investigation of a range from 2.67 to 2.81×10^4 kg/sec/m² (38 to 40 lb/sec/sq ft) for the former and 0.4 to 0.5 for the latter. For the lower tip speed design (B), consideration of hub loading limits, and minimization of hub-to-tip stagger angle change (twist) to .436 radian (25°) resulted in a combination of 2.81×10^4 kg/sec/m² (40 lb/sec/sq ft) and 0.5 for these parameters.

For engine (C) the same range of flow/area and radius was investigated with the additional constraint of a high turbine output speed for direct drive to minimize the number of stages. Selection of the number of stages is discussed in Section 4. After the speed of 4840 RPM was selected, a combination of 2.77×10^4 kg/sec/m² (39.5 lb/sec/sq ft) and 0.45 was chosen. The flow/annulus area was limited to 2.77×10^4 kg/sec/m² (39.5 lb/sec/sq ft) to minimize tip losses with low solidity at a tip relative Mach number in excess of 1.25. The radius ratio is set by the same blade twist as in design (B) and results in a lower hub loading with improved hub efficiency.

The tip rotor/stator spacing ratio was set at a minimum of 1.5 rotor chords for low fan noise. This ratio was 1.7 on the geared fan engine (B) since the minimum distance was controlled by gearbox dimensions.

	<u>Fan Rotor Spacing</u>		<u>Spacing Ratio</u>
	<u>Tip Chord</u>	<u>Spacing</u>	
Geared	.221m (8.7 in.)	.376m (14.8 in.)	1.7
Direct Drive	.272m (10.7 in.)	.409m (16.1 in.)	1.5

TABLE IV - FAN CONFIGURATIONS

Sea level static, maximum thrust, no bleed or accessory power extraction

Configuration	TF34-2	A	B	C
Flow kg/s (lb/sec)	150.1 (331)	153.3 (338)	249.4 (549.8)	251.1 (553.6)
Tip Pressure Ratio	1.47	1.49	1.25	1.25
Hub Pressure Ratio	1.42	1.43	1.14	1.14
Tip Diameter m (in.)	1.11 (43.9)	1.11 (43.9)	1.47 (58.0)	1.44 (56.8)
Speed, rad/s (RPM)	712 (6800)	726 (6929)	414 (3950)	507 (4840)
Tip Speed m/s (ft/sec)	397 (1303)	404 (1327)	305 (1000)	366 (1200)
Tip Efficiency		.902	.878	.867
Hub Efficiency		.832	.793	.824

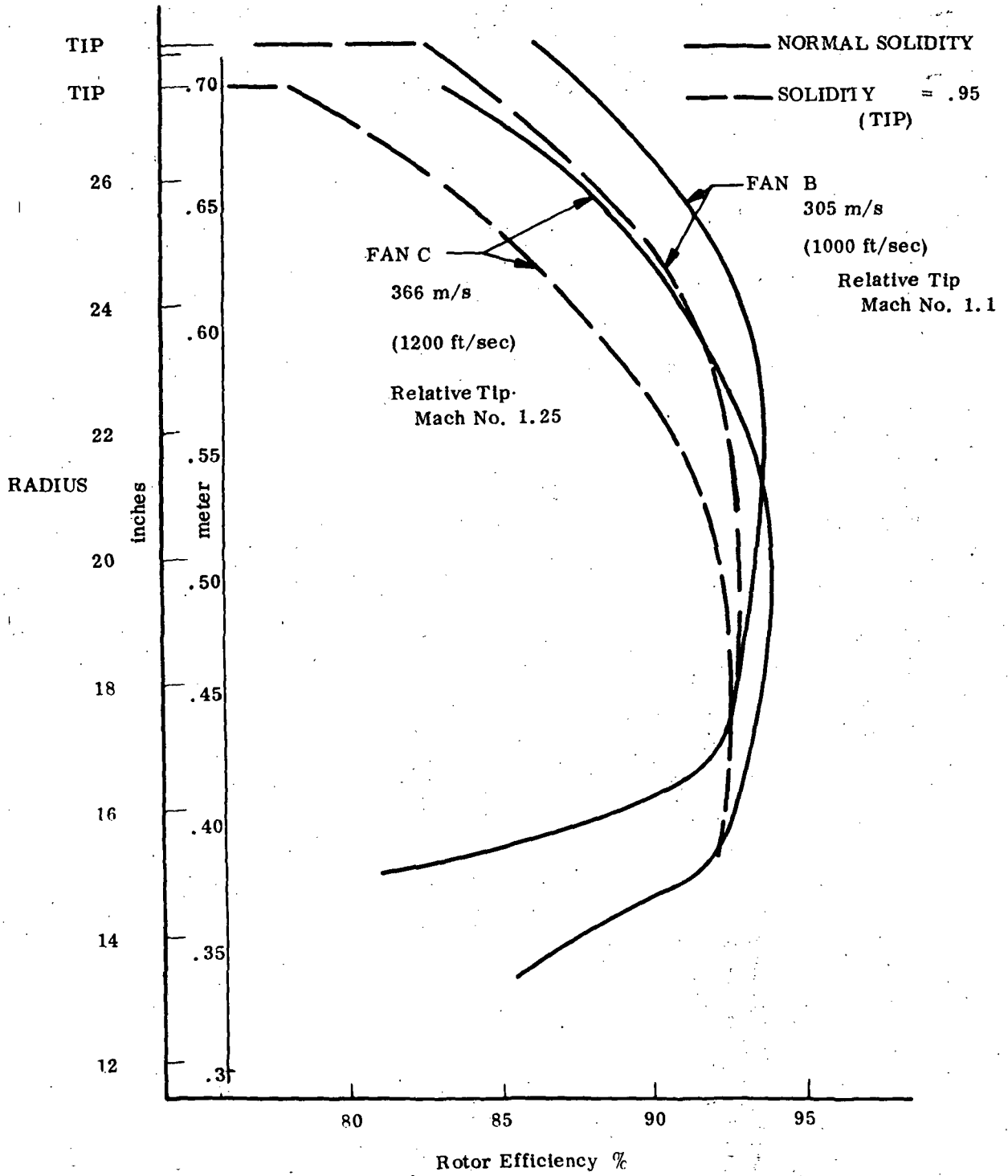


Figure 7 - Effect of Solidity on Fan Rotor Efficiency.

TABLE V - A (S.I. Units) AERODYNAMIC DESIGN DATA FOR FAN (B).

Corrected Airflow	249 kg/s								
Tip Speed	305 m/s								
Corrected Speed	414 rad/s								
Tip Efficiency	.878	Hub Efficiency	.793						
				<u>ROTOR</u>			<u>STATOR</u>		
			Tip	Pitch	Hub	Tip	Pitch	Hub	
Inlet Radius R_{in}	m		.7363	.5847	.3680	.7363	.5842	.2848	
Exit Radius R_{out}	m		.7363	.5982	.3942	.7363	.5725	.3655	
Average Radius \bar{R}	m		.7363	.5913	.3813	.7363	.5781	.3767	
Wheel Speed U	m/s		304.7	241.9	152.3	-	-	-	
Inlet Relative Mach Number			1.104	.943	.736	.495	.567	.524	
Axial Velocity Ratio V_{axout}/V_{axin}			.918	.922	.839	1.156	.917	1.257	
Inlet Relative Air Angle	rad		.9969	.8964	.6852	.4856	.4714	.5384	
Exit Relative Air Angle	rad		.8685	.7168	.3901	0	0	0	
Diffusion Factor *			.361	.395	.520	.172	.330	.048	
Pressure Loss Coefficient	$\frac{\Delta P_T}{q_{in}}$.279	.361	.435	-.083	.265	.860	
Work Coefficient	$\frac{2gJ\Delta h}{U^2}$.599	.744	1.212	-	-	-	
Solidity σ			.95	.95	.95	1.19	1.42	1.89	
Number of Blades				20			46		
Aspect Ratio				2.01			3.38		
Chord	m		.2197	.1765	.1138	.1196	.1123	.0968	
Stagger Angle	rad		.8866	.7540	.4459	.2119	.2014	.2244	
Camber Angle	rad		.1988	.3007	.5428	.7330	.6552	.6767	
Incidence Angle	rad		.0110	-.0079	-.0321	-.0929	-.0576	-.0243	
Deviation Angle	rad		.0812	.1133	.2155	.1546	.1262	.1140	
Max Thickness/Chord			.025	.043	.120	.06	.06	.06	
Axial Chord Projection	m		.1389	.1288	.1026	.1168	.1100	.0945	
Inlet Radius Ratio					.50				

* Defined per NASA SP36

TABLE V-B (F.P.S. Units) AERODYNAMIC DESIGN DATA FOR FAN (B).

Corrected Airflow 550 lb/sec
 Tip Speed 1000 ft/sec
 Corrected Speed 3950 RPM
 Tip Efficiency .878 Hub Efficiency .793

	<u>ROTOR</u>			<u>STATOR</u>			
	Tip	Pitch	Hub	Tip	Pitch	Hub	
Inlet Radius R_{in}	in.	28.99	23.02	14.49	28.99	23.0	15.15
Exit Radius R_{out}	in.	28.99	23.55	15.52	28.99	22.54	14.39
Average Radius \bar{R}	in.	28.99	23.28	15.01	28.99	22.76	14.83
Wheel Speed U	ft/sec	999.8	793.7	499.7	-	-	-
Inlet Relative Mach Number		1.104	.943	.736	.495	.567	.524
Axial Velocity Ratio V_{axout}/V_{axin}		.918	.922	.839	1.156	.917	1.257
Inlet Relative Air Angle	degree	57.12	51.36	39.26	27.82	27.01	30.85
Exit Relative Air Angle	degree	49.76	41.07	22.35	0	0	0
Diffusion Factor *		.361	.395	.520	.172	.330	.048
Pressure Loss Coefficient	$\frac{\Delta P_T}{q_{in}}$.279	.361	.435	-.083	.265	.280
Work Coefficient	$\frac{2gJ\Delta h}{U^2}$.599	.744	1.212	-	-	-
Solidity σ		.95	.95	.95	1.19	1.42	1.89
Number of Blades			20			46	
Aspect Ratio			2.01			3.38	
Chord	in.	8.65	6.95	4.48	4.71	4.42	3.81
Stagger Angle	degree	50.80	43.20	25.55	12.14	11.54	12.86
Camber Angle	degree	11.39	17.23	31.10	42.00	37.54	38.77
Incidence Angle	degree	.63	-.45	-1.84	-5.32	-3.3	-1.39
Deviation Angle	degree	4.65	6.49	12.35	8.86	7.23	6.53
Max Thickness/Chord		.025	.043	.120	.06	.06	.06
Axial Chord Projection	in	5.47	5.07	4.04	4.60	4.33	3.72
Inlet Radius Ratio				.50			

* Defined per NASA SP36

TABLE VI-A (S.I. Units) AERODYNAMIC DESIGN DATA FOR FAN (C).

Corrected Airflow 251 kg/s
 Tip Speed 366 m/s
 Corrected Speed 505 rad/s
 Tip Efficiency .867 Hub Efficiency .827

			<u>ROTOR</u>			<u>STATOR</u>		
			Tip	Pitch	Hub	Tip	Pitch	Hub
Inlet Radius	R_{in}	m	.7198	.5600	.3239	.7198	.5624	.3409
Exit Radius	R_{out}	m	.7249	.5758	.3500	.7198	.5512	.3218
Average Radius	\bar{R}	m	.7198	.5679	.3371	.7198	.5570	.3335
Wheel Speed	U	m/s	365.46	284.07	164.29	-	-	-
Inlet Relative Mach Number			1.253	1.037	.721	.476	.538	.502
Axial Velocity Ratio	V_{axout}/V_{axin}		.929	.919	.902	1.159	.929	1.249
Inlet Relative Air Angle		rad	1.088	.9837	.7615	.4421	.4231	.4815
Exit Relative Air Angle		rad	1.012	.8861	.5332	0	0	0
Diffusion Factor *			.289	.318	.437	.115	.202	.187
Pressure Loss Coefficient	$\frac{\Delta PT}{q_{in}}$.203	.300	.400	-.116	.233	.242
Work Coefficient	$\frac{2gJ \Delta h}{U^2}$.442	.543	.966	-	-	-
Solidity σ			.95	.95	.95	1.18	1.33	2.19
Number of Blades				16			38	
Aspect Ratio				1.81			3.38	
Chord		m	.2687	.2118	.1232	.1405	.1224	.1186
Stagger Angle		rad	1.011	.8866	.5550	.1932	.1817	.1960
Camber Angle		rad	.0820	.1431	.4311	.6672	.6009	.5735
Incidence Angle		rad	.0367	.0244	-.0096	-.0846	-.0592	.0014
Deviation Angle		rad	.0419	.0698	.1037	.1405	.1187	.0881
Max Thickness/Chord			.025	.043	.120	.06	.06	.06
Axial Chord Projection		m	.1425	.1336	.1069	.1379	.1207	.1168

* Defined per NASA SP36

TABLE VI-B (F.P.S. Units) AERODYNAMIC DESIGN DATA FOR FAN (C).

Corrected Airflow 554 lb/sec
 Tip Speed 1200 ft/sec
 Corrected Speed 4840 RPM
 Tip Efficiency .867 Hub Efficiency .827

			<u>ROTOR</u>			<u>STATOR</u>			
			Tip	Pitch	Hub	Tip	Pitch	Hub	
Inlet Radius	R_{in}	in.	28.34	22.85	12.75	28.34	22.14	13.42	
Exit Radius	R_{out}	in.	28.54	22.87	13.78	28.34	21.70	12.69	
Average Radius	\bar{R}	in.	28.34	22.36	13.27	28.34	21.95	13.13	
Wheel Speed	U	ft/sec	1199	932	539	-	-	-	
Inlet Relative Mach Number			1.253	1.037	.721	.476	.538	502	
Axial Velocity Ratio V_{axout}/V_{axin}			.929	.919	.902	1.159	.929	1.249	
Inlet Relative Air Angle			degree	62.32	56.36	43.63	25.33	24.24	27.59
Exit Relative Air Angle			degree	57.98	50.77	30.55	0	0	0
Diffusion Factor*				.289	.318	.437	.115	.202	.187
Pressure Loss Coefficient			$\frac{\Delta P_T}{q_{in}}$.203	.300	.400	-.116	.233	.242
Work Coefficient			$\frac{2gJ\Delta h}{U^2}$.442	.543	.966	-	-	-
Solidity σ				.95	.95	.95	1.18	1.33	2.19
Number of Blades				16			38		
Aspect Ratio				1.81			3.38		
Chord			in.	10.58	8.34	4.95	5.53	4.87	4.67
Stagger Angle			degrees	57.9	50.8	31.8	11.07	10.41	11.23
Camber Angle			degrees	4.7	8.2	24.7	38.23	34.43	32.86
Incidence Angle			degrees	2.1	1.4	-.55	-4.85	-3.39	.082
Deviation Angle			degrees	2.4	4.0	11.1	8.05	6.80	5.05
Max Thickness/Chord				.025	.043	.120	.06	.06	.06
Axial Chord Projection				5.61	5.26	4.27	5.43	9.75	4.60

* Defined per NASA SP36

3. ACOUSTICS ANALYSIS AND DESIGN

Study Objectives, Scope, and Ground Rules

The objective of the acoustics analysis is to define the extent of the engine modification and the associated installation and acoustic suppression features of the nacelle that could result in a significantly quieter engine. The ultimate design goal is a STOL transport powered by four modified TF34s operating at an appropriate thrust level in quiet nacelles to meet 95 PNdB at the 150 meter (500 foot) sideline points and at other measurement reference points specified in Figure 8.

The study is a feasibility investigation, and specifically does not include detailed acoustics design of the quiet nacelle or any external mixer device for controlling the blown flap interaction noise. Estimates are required on the impact of unsuppressed flap interaction noise on the engine systems noise. However, definitions of the nacelle suppression and other engine features toward meeting the 95 PNdB criteria are to be made on the assumption that flap interaction noise can be fully controlled.

Noise calculations are required in PNdB units, for three power settings (100%, 80% and 50% thrust) and at four reference measurement positions. Noise constituent levels for fan, jet, and core sources on the maximum front and maximum aft positions are to be provided. All three engine configurations are to be analyzed.

General Approach to Noise Suppression

Noise reduction for engine (A) is achieved by extensively treating the inlet and aft nacelle which includes three inlet and two long aft splitters. Configurations (B) and (C) are the same from the acoustics viewpoint. The B/C nacelle is more modestly treated, and has one inlet and one aft splitter. The lower fan pressure ratio of these engines also results in considerably lower jet noise than in the baseline engine. For all configurations core noise reduction by acoustically treating the core discharge passage behind the turbine is provided.

Baseline TF34-GE-2 Engine Noise Level

The noise of the baseline TF34-GE-2 engine has been evaluated in detail under static open field conditions at General Electric's Flight Test Center, Edwards Air Force Base, California on two occasions (November, 1970, and March 1971). The second test was sponsored by NASA (Lewis Research Center), and the test results are reported under Reference 1. In general acoustics results from these two tests are consistent with each other.

When operated statically with a reference bellmouth, the 60 meter (200 foot) sideline single engine reference noise level is 122 PNdB at rated thrust, standard day. The perceived noise level is dominated by two strong discrete tones associated with the blade passing frequency (3200 hertz) and its harmonic. The maximum sideline noise is aft controlled, at about 100° from the inlet. Estimated flight noise levels for an airplane equipped with four baseline engines are shown in Figure 9.

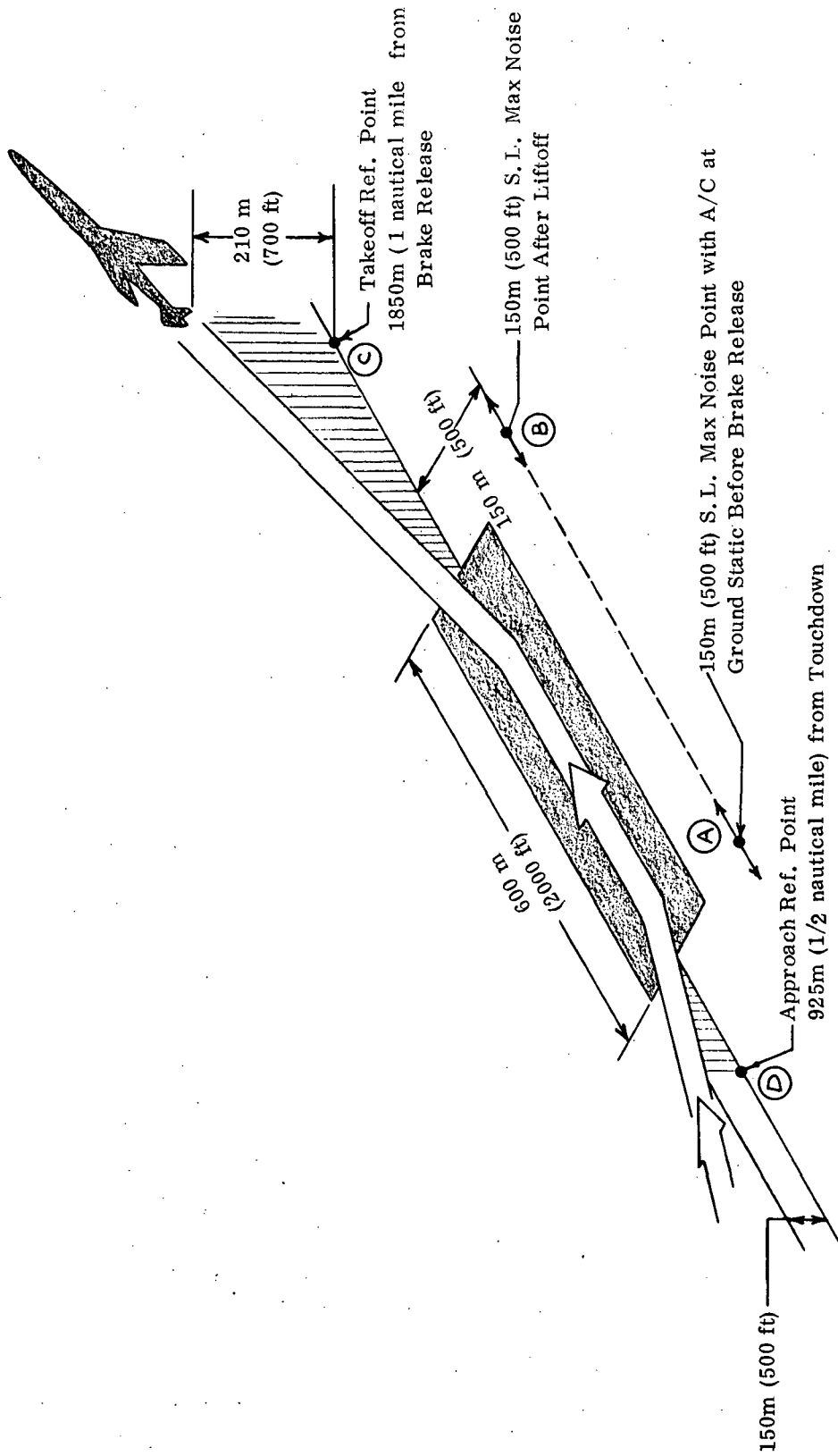


Figure 8 - STOL Aircraft Noise Measurement Reference Locations Used in this Study.

- Bare engine
- Flight effect on jet noise accounted for
- Standard day, 50 m/s (100 knots)
- Max thrust per engine = 41,368 N (9300 lb) sea level static

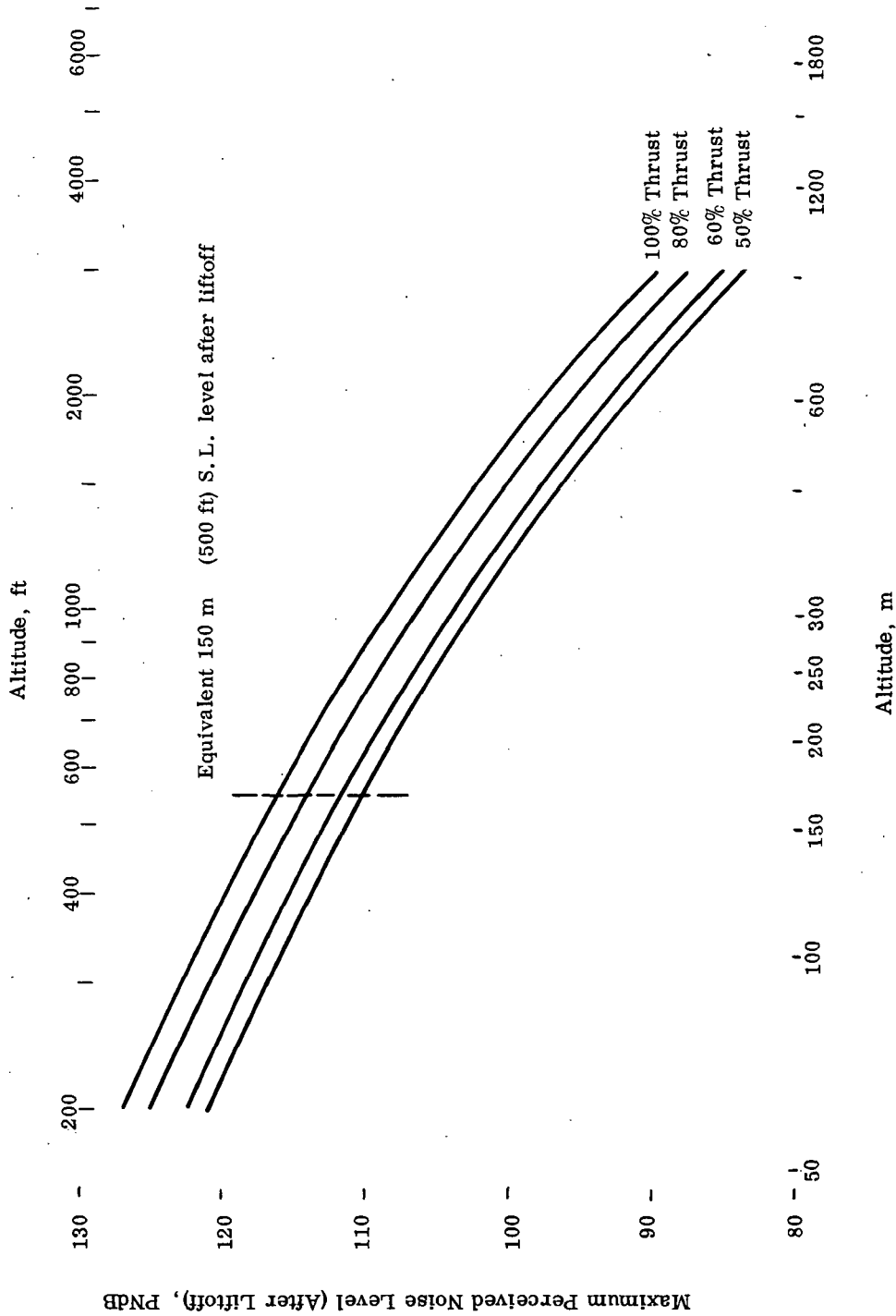


Figure 9 - Estimated TF34-GE-2 Baseline Engine Flight Noise Level, 4 Engines.

The noise level of the baseline TF34-GE-2 engine compares favorably to other in-service low bypass ratio turbofan transport engines - being about 3 to 7 PNdB quieter on a scaled thrust basis. This is due to the single stage IGV-less fan design and the relatively low exhaust velocities on the TF34. The baseline engine, however, is 2 - 3 PNdB noisier than typical in-service high bypass ratio transport engines when compared on an unsuppressed and scaled thrust basis. The relatively close blade-to-vane spacing on the TF34 engine is responsible for this.

It is noted from Figure 9 that the 150 meter (500 foot) sideline noise level after liftoff for four baseline TF34-GE-2 engines is 116 PNdB. The noise constituents are: 115.5 PNdB for the fan, 101 PNdB for the jet, and 98 PNdB for the core which includes the turbine, combustion and other internally generated noises.

In order to meet the nominal STOL objective of 95 PNdB, a systems noise reduction of 21 PNdB is required. The fan noise needs drastic reduction. Attention must also be given to reducing the jet and the core noise.

Configuration (A) - Noise Reduction by Extensively Treating the Nacelle

On Configuration (A), no major modification is made to the baseline TF34 engine. The existing fan and OGV system is retained as well as the core. The baseline engine cycle is rematched for a mixed exhaust system. Noise reduction is achieved mainly by extensively treating a full length engine nacelle. Core engine noise suppression is also provided.

Jet Noise Control

A drawing of the configuration (A) mixed exhaust system is shown in Figure 4. The key exhaust parameters that influence the jet noise are shown in Table VII. The jet noise level for a 4 engine powered STOL at the 150 meter (500 foot) sideline after liftoff is estimated to be about 93.5 PNdB. Losses associated with the nacelle splitter system have been taken into account. The corresponding mixed exhaust velocity is 264 meters (870 foot) per second.

The jet noise estimates provided here are based on scale model test results of mixed exhaust nozzles similar to the proposed system. The predicted levels are approximately 2.5 PNdB lower than predicted by the SAE procedure (with straight line extrapolation for velocity lower than 305 meters/sec (1000 fps)). Evidence is quite strong from scale model results that for low velocity, low temperature jets, the SAE method tends to over-predict the jet noise.

Full relative velocity effect similar to that implicit in the SAE method has been used for in-flight noise estimates. This flight effect is quite strong - amounting to approximately 7 PNdB at 50 meters/sec (100-knots).

For static operation, the 150 meter (500 foot) sideline jet noise at takeoff power is 97 PNdB with extra ground attenuation and shielding effects taken into account. Thus, it is seen that without the benefit of flight effect, the jet noise constituent alone would exceed the nominal 95 PNdB limit. During ground roll, with partial relative velocity influence, the resultant 4 engine jet noise level is on the average about 94 PndB.

TABLE VII - KEY DESIGN PARAMETERS ON ENGINE CONFIGURATIONS (A), (B), AND (C)
FOR NOISE CALCULATIONS.

- Standard day, 50 m/s (100 knots)
- Maximum power
- Installed condition

	Configurations <u>A</u>	<u>B</u>	<u>C</u>
Net thrust, N. (lb)	32,161 (7230)	34,852 (7835)	34,852 (7835)
Fan pressure ratio	1.48	1.24	1.24
Fan tip speed, m/s (ft/sec)	408.9 (1342)	306.3 (1005)	359.7 (1180)
Fan diameter, m (in.)	1.11 (43.9)	1.47 (58.0)	1.44 (56.7)
Blade number	28	20	16
Fan speed, rad/sec (RPM)	733.6 (7005)	431.3 (4119)	518.8 (4954)
Fan blade passing frequency, Hz.	3270	1370	1300
Total flow, kg/sec (lb/sec)	156.0 (344)	255.4 (563)	257.6 (568)
Bypass ratio	6.6	13	13
Exhaust system type	Mixed	Separate	Separate
Primary nozzle area, m ² (in. ²)	.620 (961)	.194 (296)	.194 (296)
Secondary nozzle area, m ² (in. ²)	-	1.045 (1619)	1.045 (1619)
Primary jet velocity*, m/s (ft/sec)	265.5 (871)	262.4 (861)	262.4 (861)
Secondary jet velocity*, m/s (ft/sec)	-	192.3 (631)	192.3 (631)
Primary pressure ratio	1.386	1.155	1.155
Secondary pressure ratio	-	1.234	1.234
Primary total temperature, °K (°R)	400 (720)	829.4 (1493)	829.4 (1493)
Secondary total temperature, °K (°R)	-	310.6 (559)	310.6 (559)
Blade/vane spacing (true chord)	.6	1.7	1.5

* Isentropic

Definition of Quiet Nacelle Suppression Features

To provide adequate room for suppression and to accommodate the mixed exhaust system, a long cowl installation is proposed for configuration (A). All the available inner and outer wall surfaces of the inlet and fan exhaust duct are to be acoustically treated. In addition, three inlet splitters and two aft splitters are provided. Suppression objectives for the inlet and aft fan noise are shown below:

150 meter (500 foot) Sideline Fan PNdB, 4 engines, T.O.

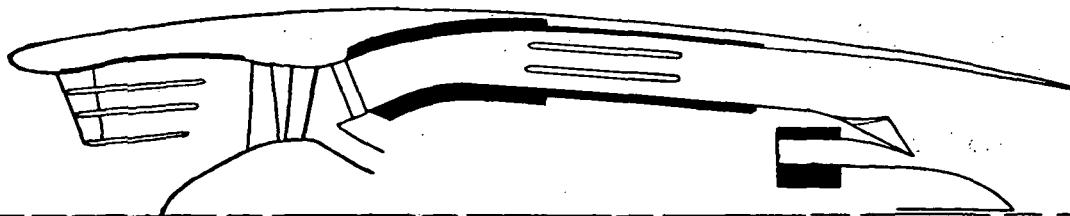
	<u>Inlet</u>	<u>Aft</u>
Unsuppressed level	110	115.5
Objective level	94	92
Suppression Requirement, Δ PNdB	16	23.5

Salient design features and configurations of the wall treatment and splitters necessary to provide the desired suppression are defined in Table VIII. The amounts of suppression expected to be achieved are 14 to 17 PNdB for the inlet, and 20 - 25 PNdB for the exhaust duct. A range of estimated suppression values is shown to reflect the uncertainty and nature of the feasibility design. It should be emphasized that these estimated suppression values refer to only the fan noise.

Note that two stages of aft duct wall treatment of dissimilar suppression designs are provided - one designed for the low frequency broad band fan noise in the frequency range around 800-1000 hertz, extending from the beginning of the treated duct to the splitter region, on both the outer and inner walls; and the other designed for the principal fan frequencies in the neighborhood of 4000 hertz, located opposite to the splitters. The purpose of the two-stage design is, of course, to provide a wide suppression band width.

The preliminary fan exhaust duct suppression design provided in Table VIII calls out the use of single degree of freedom (SDOF) perforated honeycomb lining for both the wall and the two splitters. This is proposed for reasons of economy and earlier availability. An alternate approach may be the use of multiple-degree-of-freedom (MDOF) plastic linings which would provide a wider suppression band width and may net the same amount of total fan noise suppression with less amount of treatment surface. Preliminary estimate shows that about the same amount of fan duct noise suppression can probably be retained if the two SDOF splitters are replaced by a single MDOF splitter of comparable length, and the SDOF wall linings replaced by MDOF linings. A single splitter approach leads to simpler construction and to a lower flow Mach number which is an advantage both from the acoustics and performance loss points of view. Further design study along this line should be explored.

TABLE VIII - TF34 CONFIGURATION (A) - PRELIMINARY DEFINITION OF NACELLE TREATMENT CONFIGURATION.



	Inlet	1st Stage	Aft Duct 2nd Stage
<u>Wall Treatment</u>			
Treated Length, m (in.)	.54 (21)	.62 (24.4)	.99 (39)
Treated Surface Area, m ² (ft ²)	1.8 (19.3)	4.3 (46)	6.5 (70)
Panel Thickness, m (in.)	.013 (.5)	.05 (2) .076 (3)	.025 (1)
Design Frequency, hertz	3 - 4000	800 - 1000	3 - 4000
L/H Effective	-	2.7	-
H/λ	-	0.56	-
Acoustic Material Type	SDOF*	SDOF	SDOF
<u>Splitter System</u>			
Number of Splitters	3		2
Treated Length, m (in.)	.38 (15)	.76 (30)	to 1 (40)
Treated Surface Area, m ² (ft ²)	4.7 (51)	10.5 (109)	to 13.8 (143)
Passage Height, m (in.)	.086 (3.5)	.056 (2.2)	
Splitter Thickness, m (in.)	.025 (1.0)	.025 (1.0)	to .031 (1.25)
Design Frequency, hertz	3000 - 4000	3000 - 4000	
L/H Effective	3.8	11.6 to 15.5	
H/λ	1.0	0.64	
Acoustic Material Type	SDOF	SDOF	
Estimated Total Suppression, Δ PNdB	14-17		20-25

* Single degree of freedom

Inspection of Figure 4 shows that a relatively large center area at the inlet is left unsupported. Selection of the three ring design and the passage height is based on data from another high bypass ratio fan showing the sound intensity near the inlet center to be quite small compared to that near the outer wall. There is some uncertainty as to whether the TF34 engine inlet sound propagation would behave according to that model. Consideration should be given to the possible need for a small fourth splitter near the center, or an extended acoustically treated centerbody.

The proposed aft splitter configuration aimed at achieving a fan-alone noise suppression of upwards of 20 PNdB rests on the design criteria that splitter configurations having progressively large length-to-passage-height ratio and progressively small passage-height-to-design-wavelength ratio yield increasing greater sound attenuation. It is assumed also that splitter thickness and passage height ratio can be optimized in a practical fashion. From the standpoint of past design practices the design selections of about 13 for L/H , and about 0.6 for H/λ for the aft splitter system are fairly extreme choices. While theoretical consideration and design trends tend to support this design approach, it must be clearly recognized that no extensive engine and laboratory test data are available to validate the selected designs as being appropriate. An adequate laboratory program should be conducted on such a design (and its optimization) before commitment is made to full scale engine designs.

The above preliminary splitter and treatment configurations are provided to show design feasibility and general dimension so that performance, weight and cost estimates can be carried out. They are not intended to represent final designs. Specification of exact treatment thickness, length, core cell size, and cover sheet perforation require a detailed mechanical and acoustical design effort which is beyond the scope of the present program.

Core Noise Reduction

Core noise is defined here as consisting of turbine noise, combustion noise and internally generated flow noise, but excluding compressor noise or core jet noise. Four TF34 engines are estimated to have a core noise level of about 98 PNdB for takeoff at the 150 meter (500 foot) sideline point. The estimate is based partly on the microphone array measurement of the turbine noise as described in Reference 1 and partly based on low frequency core engine noise data collected on turboshaft engines of various sizes.

A core noise suppression objective of 12 PNdB with attention given equally to low and high frequencies is established. The region of acoustical treatment will be the flow passage between the low pressure turbine discharge and the internal mixer.

Inner and outer annulus walls in this flow passage of approximately 0.35 meters (14 inches) will be acoustically treated with a relatively thick honeycomb SDOF panel having a design frequency of about 500 hertz. Panel thickness is estimated to be between .05 - .1 meters (2 - 4 inches).

Suppression of high frequency turbine noise will take the form of acoustically treated thin radial splitters of less than .013 meters (1/2 inch) thickness and about 0.35 meters (14 inches) long. The number of radial splitters required is estimated to be between 12 and 16. They will be tuned to about 5000 hertz and of SDOF construction.

The approach of low frequency core noise reduction by use of thick wall treatments indicated above has not been previously proven on full scale engines. Further detail design study supported by laboratory test data should be carried out. Alternate approaches such as the use of a side branch resonator or folded quarter wave tubes also merit exploratory design study.

Summary of Estimated Configuration (A) Noise Levels

Estimated perceived noise levels of a STOL aircraft powered by four TF34 Configuration (A) engines with fully treated nacelles are shown in Table IX for the following four measurements points (see Figure 8.)

- (A) 150 meter (500 foot) sideline noise: ground static; 100%, 80%, 50% thrust.
- (B) 150 meter (500 foot) sideline noise after liftoff 50 m/s (100 knots); 100%, 80%, 50% thrust.
- (C) Community noise: 210 meter (700 foot) altitude; 50 m/s (100 knots); 100%, 80% thrust.
- (D) Approach noise; 150 meter (500 foot) altitude; 35 m/s (70 knots) 50% thrust.

Noise constituents and total levels for both maximum front and maximum aft positions are included. Flap impingement noise adder, however, is not included in Table IX. Figure 10 plots the total noise in PNdB vs percent thrust for the above four measurement points. Figure 11 plots the total noise vs altitude for three levels of thrust.

Figure 10 shows that four TF34 Configuration (A) engines with fully treated nacelles can meet the 95 PNdB criteria at all four reference measurement points when operating at a thrust level of 90% maximum or below. For maximum thrust takeoff, it is about two PNdB above the 150 meter (500 foot) sideline 95 PNdB objective level. At the takeoff community noise point, the airplane noise levels at maximum and at cutback power (80% thrust) are 1 and 4 PNdB respectively below the 95 PNdB objective level. During approach, at the noise measuring point, the airplane noise level is 4 PNdB below the 95 PNdB objective level.

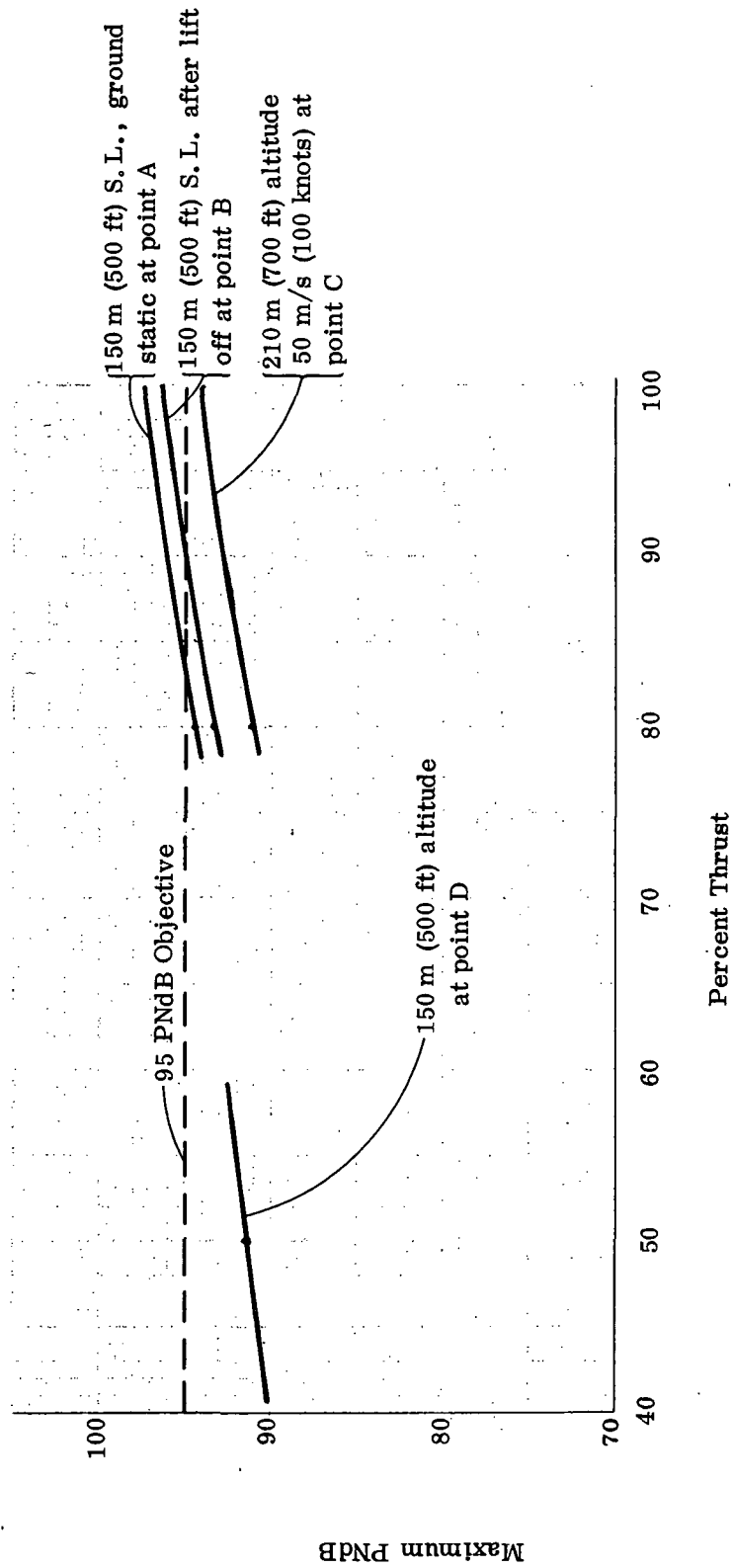
TABLE IX - TF34 CONFIGURATION (A) - ESTIMATED NOISE CONSTITUENT LEVELS - PNdB.

Fully treated nacelle (including 3 inlet and 2 aft splitters)
 Mixed exhaust nozzle
 Core noise suppressed
 4 engines
 Standard day
 Flap impingement noise not considered
 Thrust per engine; installed 38682N (8696 lb) SLS

Measurement Points (A)	% Thrust	Max Front (50°)				Max Aft (100°)			
		Fan	Jet	Core	Total	Fan	Jet	Core	Total
150m (500 ft) Sideline	100	91	89.5	76	94	87	96.5	82	97.5
Ground Static	80	88.5	85	74	91	85.5	93	80	94.5
	50	85.5	78.5	72	87	82	85	78	87.5
(B)									
150m (500 ft) Sideline	100	95	86.5	80	95.5	92	93.5	86	96.5
After Liftoff	80	92.5	82	78	93.5	89.5	89.5	84	93.5
50 m/s	50	89.5	75	76	90.5	86	81	82	89
(C)									
210m (700 ft) Altitude	100	92.5	84	77.5	93	89.5	91	83.5	94
50 m/s	80	90	79.5	75.5	91	87	87	81.5	91
(D)									
Approach, 150 m (500 ft) altitude	50	90.5	76	71	91.5	87	82	83	90

Note: See Figure 8 for reference measurement points - A, B, C and D.

- 4 engines
- Fully treated nacelle (including 3 inlet and 2 aft splitters)
- Mixed exhaust system
- Standard day
- Thrust per engine installed; 100% = 38,700 N (8700 lb) sea level static; 32,160 N (7230 lb) at 50 m/s (100 knots)



NOTE: See Figure 8 for position A, B, C, D

Figure 10 - TF34 Configuration (A) Estimated Noise Level Vs. Thrust at Four Measurement Points.

- Fully treated nacelle (including 3 inlet & 2 aft splitters)
- Mixed exhaust nozzle
- Standard day, 50 m/s (100 knots)
- Maximum thrust per engine, installed: 38,700 N (8700 lb) SLS, 32,160 N (7230 lb) at 50 m/s (100 knots)
- Flap impingement noise not considered

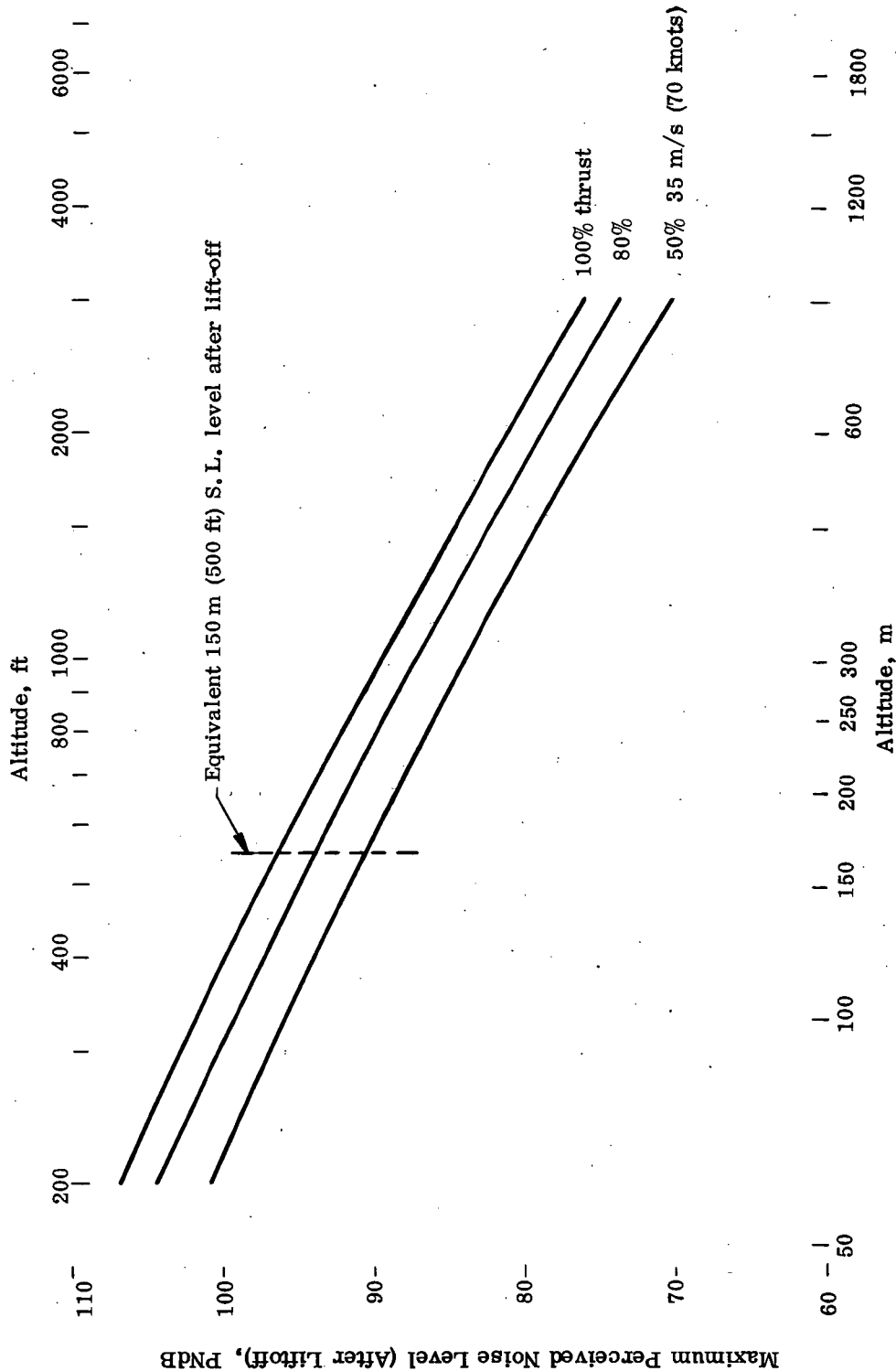


Figure 11 - Estimated TF34 Configuration (A) Flight Noise Level - 4 Engines.

Configurations (B) and (C) - Noise Reduction by Change of Fan System and by Nacelle Treatment

On configurations (B) and (C), a lower speed, low pressure ratio fan with a wider blade-to-vane spacing is provided, thus reducing fan source noise. Further reduction of fan noise is achieved by a modest amount of nacelle treatment, including one inlet and one aft splitter. The core engine will be also suppressed for turbine, combustion and other internally-generated noise.

Fan Source Noise Reduction

The major change from configuration (A) to configuration (B/C) concerns the fan. Listed in Table X are the key fan parameters that have impacts on fan noise:

TABLE X - FAN PARAMETERS
T. O. POWER, 50 m/s (100 KNOTS)

	Configuration (A)		(B)		(C)	
Fan Pressure Ratio	1.48		1.24		1.24	
Fan Tip Speed m/s (ft/sec)	409	1342	305	(1000)	360	(1180)
Fan speed rad/s (RPM)	734	(7005)	431	(4119)	519	(4954)
Fan Diameter, m (in.)	1.11	(43.9)	1.43	(56.3)	1.39	(54.9)
Number of Blades	28		20		16	
Blade-vane spacing (true chords)	0.6		1.7		1.5	
Fan Passing Frequency, Hz	3200		1370		1300	
Airflow kg/s (lb/sec)	156	(344)	255	(563)	257	(567)
60 meter (200ft) noise PNdB (single engine fan only)	121		112.5		112.5	

The noise advantage of about 8 PNdB of configurations (B) and (C) over configuration (A) is due to: Lower fan pressure (-3 PNdB); wider blade/vane spacing (-3.5 PNdB), and blade passing frequency in the less annoying frequency region (-2 PNdB). The method of fan noise prediction adopted for this study makes fan pressure ratio, mass flow, and tone location the controlling parameters affecting noise. Since these parameters are unchanged between (B) and (C), their fan noise levels are estimated to be the same. Exactly how differences in tip speed and other detailed aerodynamic characteristics associated with variable pitch will affect the resultant noise cannot be accurately estimated without experimental data. It is conceivable that improved incidence angles made possible by variable pitch operation at low power settings may result in lower

approach noise. This possible advantage cannot be quantitatively identified at the present time.

Nacelle Treatment for Further Fan Noise Reduction

In spite of the lower fan source noise for configurations (B) and (C), additional reduction by acoustically treating the engine nacelle is necessary to meet the 95 PNdB objective. The amount of fan noise suppression is established below:

4 Engine Fan Noise, 150 meter (500 ft) S. L., after Liftoff, Takeoff Power

		<u>Forward</u>	<u>Aft</u>
Unsuppressed Level	PNdB	105	107
Objective Level	PNdB	<u>94</u>	<u>92</u>
Suppression Required, Δ	PNdB	11	15

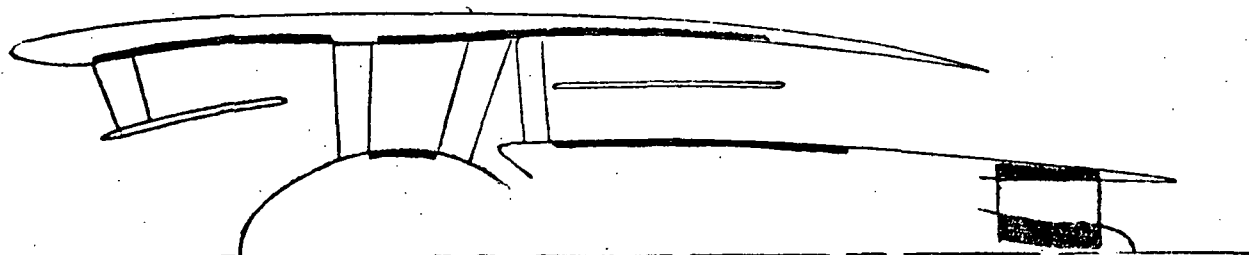
Preliminary design study shows that in addition to having the inlet and aft duct wall surfaces fully treated acoustically, one inlet and one aft splitter are required.

Table XI defines the treatment configuration. For fans with wide blade/vane spacing, the discrete tone noise levels are not as sharp nor as large relative to the broad band noise as in the TF34 baseline engine case. Effective suppression of the fan noise in PNdB requires a wider band width suppression than that associated with single degree of freedom (SDOF) honeycomb panel. Accordingly, a multiple-degree-of-freedom (MDOF) plastic construction panel design similar to that used in the General Electric CF6-6 commercial transport engine nacelle is proposed for both the wall treatment and for the splitters. The estimated inlet and aft duct suppression levels are 10 to 13 PNdB and 14 to 16 PNdB respectively. Again a range of suppression values are shown, reflecting the fact that the design is preliminary. Further analysis and optimization would be required for a detail design.

Higher Bypass Ratio and Jet Noise Advantage

The higher bypass ratios for the Configuration (B) and (C) cycles yield lower jet exhaust velocities, and hence lower exhaust jet noise, when compared to Configuration (A). Comparisons of the exhaust jet parameters between Configuration (A) and (B) and (C) are shown below:

TABLE XI - TF34 CONFIGURATION (B) and (C) - PRELIMINARY
DEFINITION OF NACELLE TREATMENT CONFIGURATION



	Inlet		Aft	
<u>Wall Treatment</u>				
Treated Length, m (in.)	.82	(32)	1.5	(58)
Treated Surface Area, m ² (ft ²)	3.6	(40)	11	(119)
Panel Thickness, m (in.)	.025	(1)	.025	(1)
Design Frequency, hertz	2000		2000	
Acoustic Material Type	MDOF *		MDOF	
<u>Splitter System</u>				
No. of Splitters	1		1	
Treated Length, m (in.)	.54	(21.4)	.83	(33)
Treated Surface Area, m ² (ft ²)	3.42	(36.8)	6.5	(70)
Passage Height, m (in.)	.18	(7.2)	.14	(5.6)
Splitter Thickness, m (in.)	.04	(1.5)	.04	(1.5)
Design Frequency, hertz	2000		2000	
L/H, Effective	2.5		5	
H/λ	1.07		.81	
Acoustic Material Type	MDOF		MDOF	
Estimated Total Suppression, ΔPNdB	10 - 13		14 - 16	

* Multiple degree of freedom

<u>Takeoff, 50 m/s (100 Knots)</u>	<u>Configuration (A)</u>	<u>Configurations (B), (C)</u>
Type of exhaust system	Mixed	Separate
Velocities, V_8/V_{28} m/s (ft/s)	265.5 (871)	262.4/192.3 (861/631)
Nozzle Areas, A_8/A_{28} m ² (in. ²)	.62 (961)	.194/1.045 (296/1619)
Jet Densities, ρ_8/ρ_{28} kg/m ³ (lb/ft ³)	.961 (.06)	.449/1.217 (.028/.076)
Jet Noise, 60 meter (200 ft) altitude PNdB	97.5	90

It is seen that the jet noise advantage of the higher bypass ratio configurations (B) and (C), relative to configuration (A) is only about 7 PNdB.

3.4 Core Engine Noise Reduction

It is assumed that the core engine unsuppressed perceived noise level for Configurations (B) and (C) are about the same as that for Configuration (A), and that the design approach for core noise suppression previously identified for Configuration (A) will also apply for Configuration (B) and (C).

3.5 Summary of Estimated Noise Levels, Configurations (B) and (C)

The unsuppressed noise constituents for Configurations (B) and (C) are shown below for a 4 engine aircraft, 150 meter (500 foot) sideline after liftoff, at maximum power:

Fan	107
Jet	86
Core	<u>98</u>
Total	108.5

Table XII summarizes the suppressed levels of four Configuration (B) or (C) engines at the four reference stations. Figure 12 plots the maximum noise level versus percent thrust at the reference stations. Figure 13 plots the noise level vs altitude for three levels of thrust.

These results indicate that for all the reference stations, operation of the aircraft powered by four configuration (B) or (C) engines will produce noise levels below the 95 PNdB limit.

Consideration of Arbitrary Levels of Flap Impingement Noise

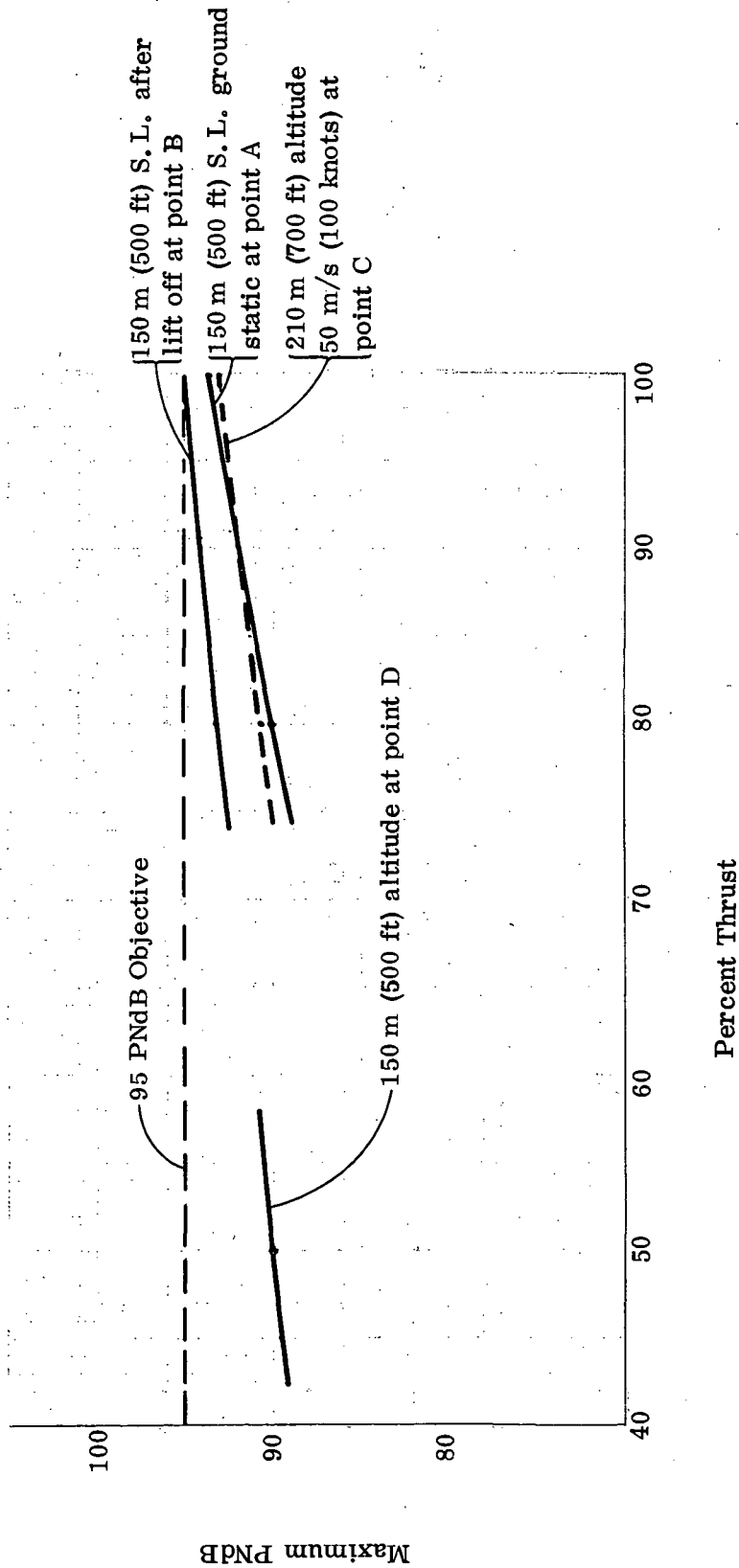
The scope of this study did not include prediction of the flap interaction noise. Similarly no consideration is given to the reduction of flap interaction noise by use of external mixer devices. However, the impact of flap interaction noise where it does exist and cannot be adequately controlled can be assessed by arbitrarily assuming different levels

**TABLE XII - TF34 CONFIGURATIONS (B) & (C) - ESTIMATED
NOISE CONSTITUENT LEVELS - PNdB 4 ENGINES**

Treated nacelle (1 inlet and 1 aft splitter)
 Separate flow exhaust
 Core noise suppressed
 Standard day
 Flap impingement noise not considered
 Thrust per engine; installed 45092N (10137 lb) B 45336N (10192 lb) C SLS

Measurement Points	% Thrust	Max Front (~50°)			Max Aft (~110°)				
		Fan	Jet	Core	Total	Fan	Jet	Core	Total
(A)									
150m (500 ft) Sideline	100	90	84.5	76	92	88	90.5	82	93.5
Ground Static	80	88	79.5	74	89.5	86	85.5	80	90
	50	83	71	72	84	81	76.5	78	84
(B)									
150m (500 ft) Sideline	100	94	80	80	95	92	86	86	94.5
After Liftoff	80	92	74	78	93	90	80	84	92
50 m/s (100 knot)	50	88	65	76	89	85	70	80	86.5
(C)									
210m (700 ft) Altitude	100	91.5	77.5	77.5	93	89.5	83.5	83.5	92
50 m/s (100 knots)	80	89.5	71.5	75.5	90.5	87.5	77.5	81.5	90
(D)									
Approach, 150m (500 ft) Altitude	50	89	66	77	90	86	71	81	87.5

- 4 engines
- Treated nacelle (including 1 inlet & 1 aft splitter)
- Standard day
- Max thrust per engine, installed; 45, 100 N (10, 140 lb) sea level static, 34, 850 N (7835 lb) at 50 m/s (100 knots)



NOTE: See Figure 8 for position A, B, C, D

Figure 12 - TF34 Configuration (B) and (C) Estimated Noise Level Vs. Thrust at Four Measurement Points.

- Nacelle treated (including 1 inlet and 1 aft splitter)
- Separate flow exhaust system
- Standard day, 50 m/s (100 knots)
- Flap impingement noise not considered
- Maximum thrust per engine; installed: 45,100 N (10,140 lb) SLS, 34,850 N (7835 lb) at 50 m/s (100 knots)

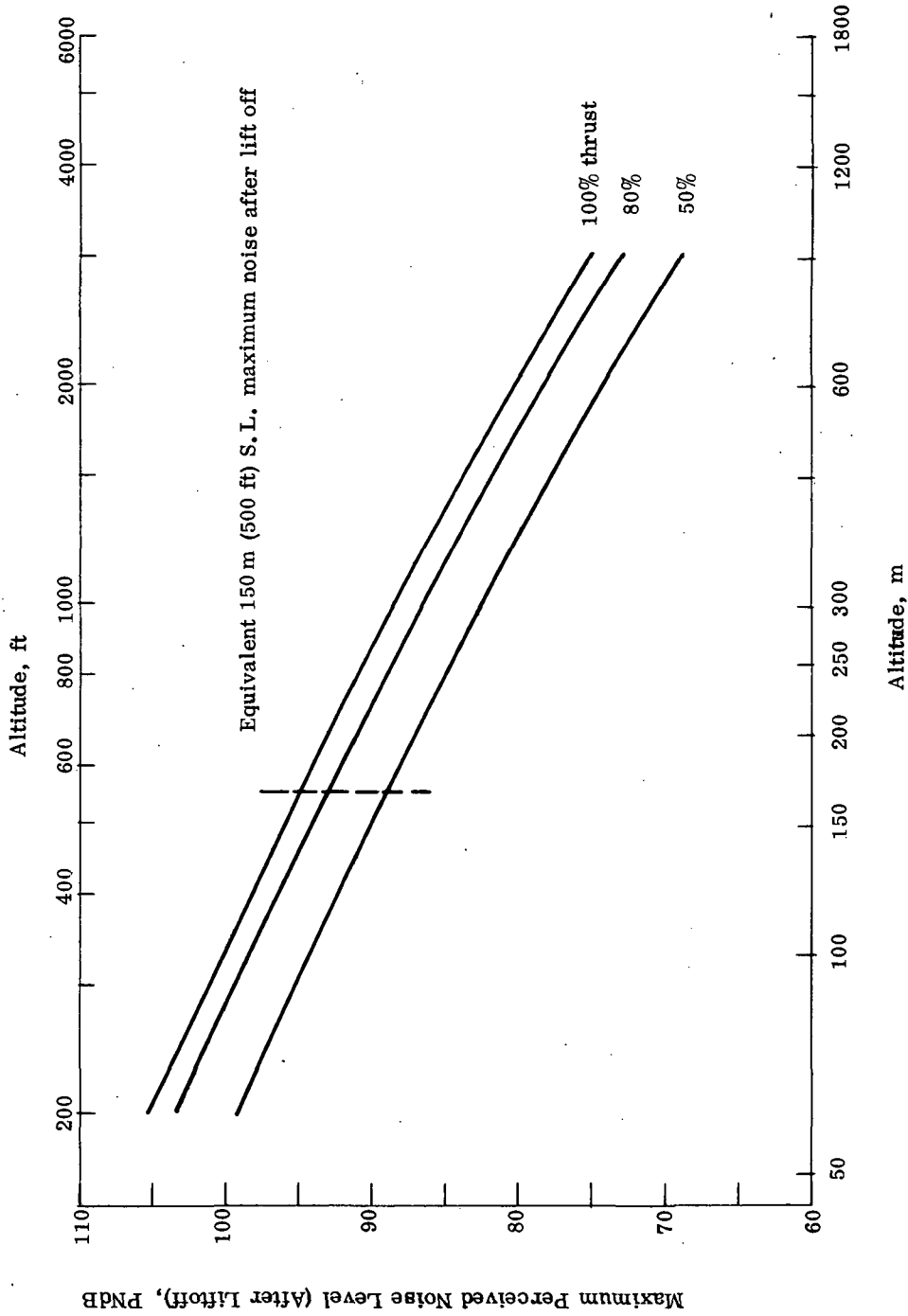


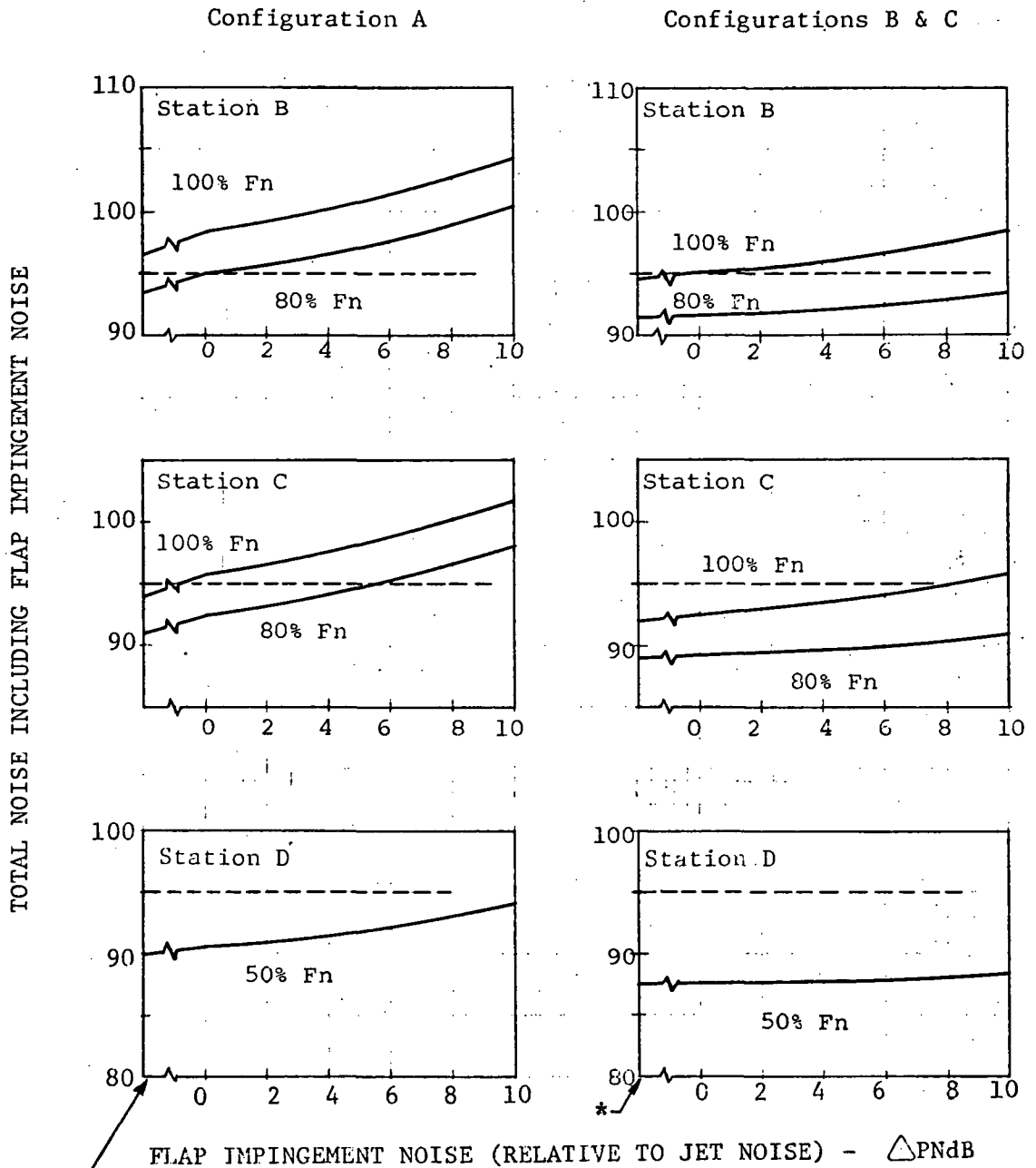
Figure 13 - Estimated TF34 Configuration (B) and (C) Flight Noise Levels - 4 Engines.

of this noise and then adding it to the engine systems noise. The arbitrary levels of flap interaction noise will be defined in terms of delta levels above the jet noise level.

Figure 14 plots the engine system noise plus the flap interaction noise as a function of flap interaction noise that is taken arbitrarily to be varying from 0 to 10 PNdB above the jet noise. This is done for both engine configurations (A) and (B), for 100% and 80% thrust and at three reference measurement stations (B), (C), and (D) of Figure 8. Several observations can be made from inspections of Figure 14:

- On Configuration (A) where jet noise is the dominant noise source at takeoff, effects due to the addition of flap impingement noise is quite strong. A flap interaction noise having an absolute level equal to the jet noise level will add about 2 PNdB to the systems noise, thus bringing the 150 meter (500 foot) sideline maximum noise of 96.5 to about 98.5 PNdB. A flap interaction noise 10 PNdB above the jet noise level would bring the total system noise to about 104 PNdB.
- On Configurations (B) and (C) where the jet noise levels are basically lower, flap interaction noise impact on the systems noise is considerably smaller. Nevertheless a flap interaction noise 10 PNdB above the jet noise would bring the total system noise to about 98.5 PNdB at the 150 meter (500 foot) sideline point at takeoff.
- The above two observations suggest that fairly drastic reduction of the flap impingement noise is mandatory for the 6.5 bypass ratio configuration (A) engine, and a modest reduction is also necessary for the two higher bypass ratio engines.
- At the measurement station (C) which is 700 foot directly beneath the aircraft, a considerable amount of flap impingement noise can be tolerated if the power is cut back to about 80%. Thus, the 95 PNdB limit can still be met for the Configuration (A) engine even if the flap impingement noise level is as high as 6 PNdB above the jet noise level.
- At the measurement station (D) during approach, flap impingement noise does not appear to present a serious problem unless its level exceeds the jet noise by more than 10 PNdB for Configuration (A).
- The impact of flap interaction noise in causing the total systems noise to go over the 95 PNdB limit can be reduced by lowering the engine noise - the payoff being the largest when the major contributing constituent is reduced first. Thus, on Configuration (A), lowering the jet source noise would help the most. On Configuration (B) and (C), lowering the fan noise first would be more beneficial. Of course, the most direct way is to reduce the flap impingement noise itself.

- 4 Engines
- Standard Day



* No flap noise here

FLAP IMPINGEMENT NOISE (RELATIVE TO JET NOISE) - Δ PNdB

Station B - 150m(500 ft) S.L. max PNdB (after liftoff)
 Station C - 210m(700 ft) alt. max FNdB (after liftoff)
 Station D - 150m(500 ft) ait. max PNdB (approach)

Figure 14 - Effect of Flap Impingement Noise Adder to Total System Noise.

GENERAL DISCUSSION

Limitations of the Present Study

The foregoing study and noise estimates have made use of certain assumptions and prediction procedures which are deemed to be appropriate based on today's knowledge, but nevertheless have not been substantiated by actual engine testing. These include:

- Flight effect on jet noise according to the SAE method
- Static jet noise prediction for low velocity jets based on scale model results
- Design method for estimating fan suppression effectiveness for long splitters with small passage height.
- Design method for suppressing low frequency core engine noise
- Prediction method for low frequency core engine noise level
- Fan noise prediction for low pressure ratio low tip speed variable pitch fans

The probable accuracy for noise or noise suppression prediction on each of the above items is believed to be not better than ± 3 PNdB. While the possible errors introduced on different noise components may not necessarily be cumulative on the total engine noise estimate, it is easy to see that there is a great deal of room for possible significant discrepancies between predicted systems noise and actual levels.

There are several possible noise sources which are not taken into consideration in the present study but which may surface into prominence when the major noise sources as we understand them now are drastically suppressed or reduced. These are:

- Casing radiation of the fan or core engine noise through the nacelle and core engine walls.
- Flow noise in the fan duct associated with support struts, surface discontinuities, and possibly with minor flow separations.
- Flanking path transmission of fan noise along the casing wall and splitter structure, thus negating the full suppression effects of the treatment.
- Engine control and accessory noise including pumps, gears and other mechanical vibration-related noise radiation.

These secondary sources of noise are known to exist. Data and state-of-the-art knowledge in quantifying their levels are limited. It is anticipated that they may become limiting items as the "major" noise sources are reduced. Adequate and special design and testing attention must be given to these secondary noises if the extremely challenging 95 PNdB objective is to be met.

STOL Operations Aspects on Noise

Table XIII quickly summarizes the four-engine noise levels of the two TF34 configurations:

TABLE XIII - SUMMARY OF ESTIMATED NOISE LEVELS FOR BYPASS 6.5 AND
13 ENGINES

<u>Position *</u>	<u>Configuration (A), PNdB 100%/90% Thrust</u>	<u>Configurations (B) and (C), PNdB 100% Thrust</u>	<u>Objective, PNdB</u>
A	97.5/96	93.5	95
B	96.5/95	95	95
C	94/	93	95
D	91 (50% Thrust)	90 (50% Thrust)	95

The above Table shows that Configuration (B) and (C) will have maximum noise levels equal to or significantly lower than the 95 PNdB limits at the four reference positions. Configuration (A) maximum noise levels at maximum takeoff power, however, exceeded the 95 PNdB limit at the two sideline positions. The slight excess at the sideline points may in reality be less critical from several points of view described below:

- Station A refers to the sideline point receiving the maximum noise when the airplane is static on the ground just before brake release. The maximum noise impact area is relatively small since the sideline noise level will drop as soon as the aircraft accelerates down the runway and enjoys the relative velocity effect on the jet noise. Thus, when the aircraft is say 1/3 down the runway the projected 150 meter (500 foot) sideline noise is only about 94 PNdB. This can be indirectly seen from the noise contour plots shown in Figure 15.
- The problem associated with static and early ground roll operation can be solved by other means. For example, erection of barriers or locating airport buildings on the sides of the runway can effectively attenuate the noise propagation.
- Since sound attenuates faster when propagating over ground (so-called extra ground attenuation), noise levels at distances beyond the 150 meter (500 foot) sideline points during static and ground roll operation become less intensive at a faster rate as compared to the situation where a problem exists after the aircraft is in the air. Calculations on Configuration (A) show that had the reference sideline been taken at say 300 meters (1000 foot) sideline, the maximum noise level during static operation would have been 3 PNdB less than that associated with after-lift-off operation; instead of being 1 PNdB higher when using the 150 meter sideline reference.

* See Figure 8

- STOL airplanes will takeoff with considerable thrust margin and climb at a faster rate than conventional aircraft. With automated equipment, it is not unreasonable to consider that early power cutback may be feasible. Because of partial extra ground attenuation and engine shielding effect, the maximum after-lift-off sideline noise does not occur until the aircraft has achieved an altitude higher than about 75 meters (250 feet). Therefore, early power cutback operation, if it can be performed, will tend to lower the after-lift-off maximum noise level.

The above discussions indirectly point out that sideline noise criteria, by themselves, are probably not the most meaningful index for measuring STOL aircraft noise intrusion. An alternative method may be the use of the noise exposure area concept where the area within which noise exceeds a certain prescribed level, say 95 PNdB, is to be limited to certain specified values, say X units of area, during takeoff and approach operation of the aircraft. Estimations of the PNdB noise contours and the enclosed areas are relatively simple once the engine noise levels and the aircraft operational characteristics are defined.

Figure 15a shows the 90, 95, and 100 PNdB noise contours for Configurations (A) and (B) with the STOL aircraft takeoff and landing characteristics conforming to that specified in Figure 8. No power cutback is used during takeoff operation. However, realistic STOL takeoff and landing characteristics are believed to be somewhat different from that of Figure 8 (takeoff climb angle being steeper and the approach angle less sharp). Figure 15b, including a sketch of the new takeoff and landing profiles, shows the resulting noise contours. Again, no power cutbacks are used. The Table below summarizes the noise exposure areas for 90, 95 and 100 PNdB contours for Configuration (A) and (B) engines operating under two sets of takeoff and approach profiles described above. Calculation was also made of the 95 PNdB contour area assuming that the aircraft exactly meets the 95 PNdB noise limits at the four reference measurement points. This equivalent "noise limit area" is included in the Table also. It is seen that both configurations (A) and (B) have noise exposure areas (at 95 PNdB) considerably less than that associated with the 95-PNdB-at-four-points criteria.

TF34 CONFIGURATIONS (A) (B) & (C) - ESTIMATED TF34 NOISE EXPOSURE AREA *

Flight Paths	Config-uration	PNdB	T.O.		Approach		Total		Engine Requirement		
			$m^2 \times 10^{-3}$	(acres)	$m^2 \times 10^3$	(acres)	$m^2 \times 10^{-3}$	(acres)	$m^2 \times 10^{-3}$	(acres)	
See	A	90	1150	(284)	295	(73)	1445	(357)	-	-	-
Figure	A	95	542	(134)	113	(28)	656	(162)	750	-	(185)
15a	A	100	267	(66)	40	(10)	308	(76)	-	-	-
	B/C	90	955	(236)	219	(54)	1174	(290)	-	-	-
		95	425	(105)	81	(20)	506	(125)	750	-	(185)
		100	194	(48)	32	(8)	219	(54)	-	-	-
See	A	90	664	(164)	403	(99.5)	1068	(264)	-	-	-
Figure	A	95	340	(84)	154	(38)	494	(122)	750	-	(185)
15b	A	100	186	(46)	57	(14)	243	(60)	-	-	-
	B/C	90	550	(136)	300	(74)	850	(210)	-	-	-
	B/C	95	267	(66)	113	(28)	380	(94)	750	-	(185)
	B/C	100	134	(33)	40	(10)	174	(43)	-	-	-

* Equivalent to area enclosed by 95 PNdB at 1.52 meter (500 foot) sideline, 910 meter (.5 N. mile) from landing threshold; 1850 meter (1 N. mile) from brake release.

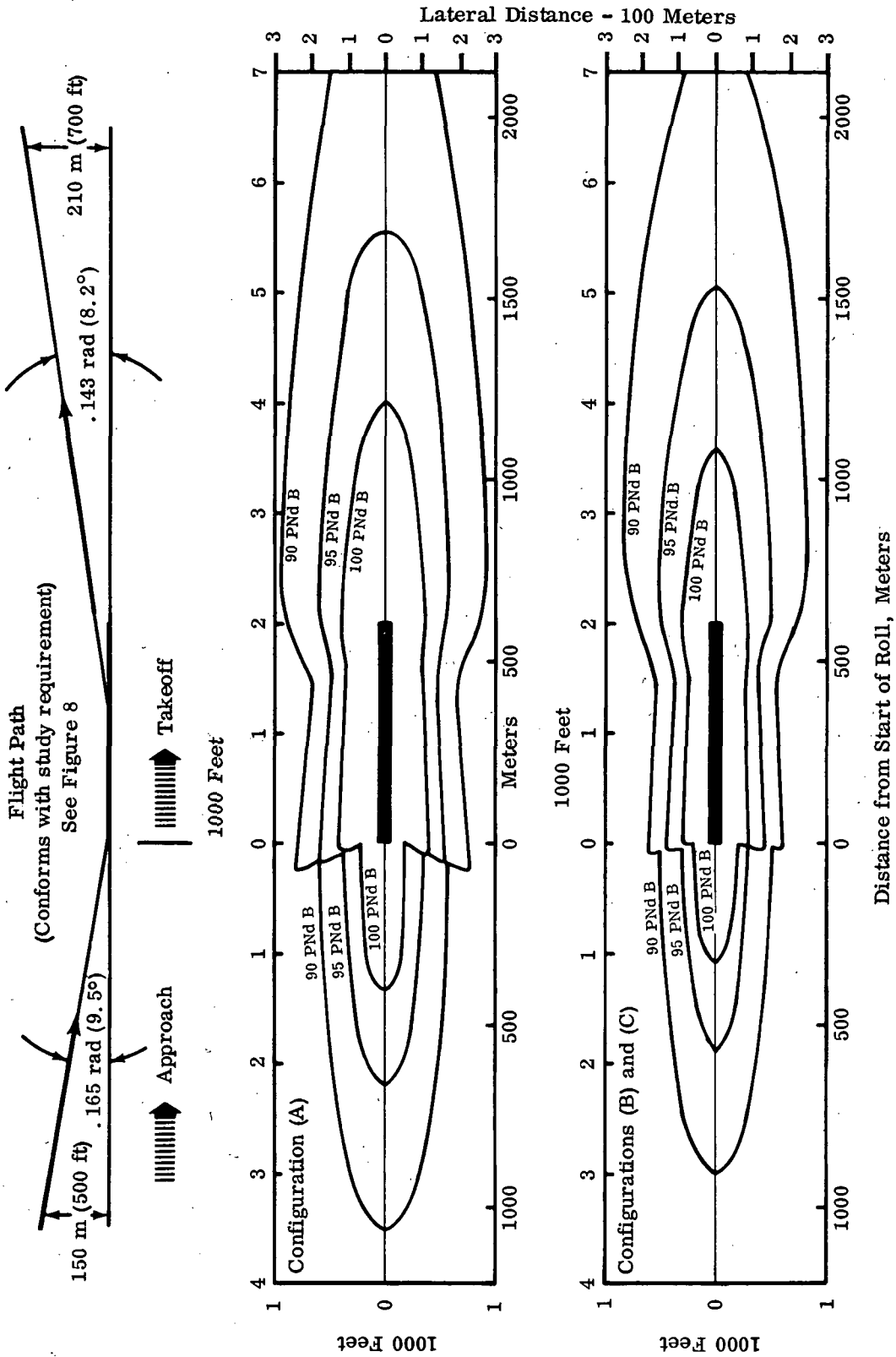


Figure 15a - Estimated STOL Noise Contours Using Four TF34 Configuration (A), (B), and (C) Engines, Standard Day.

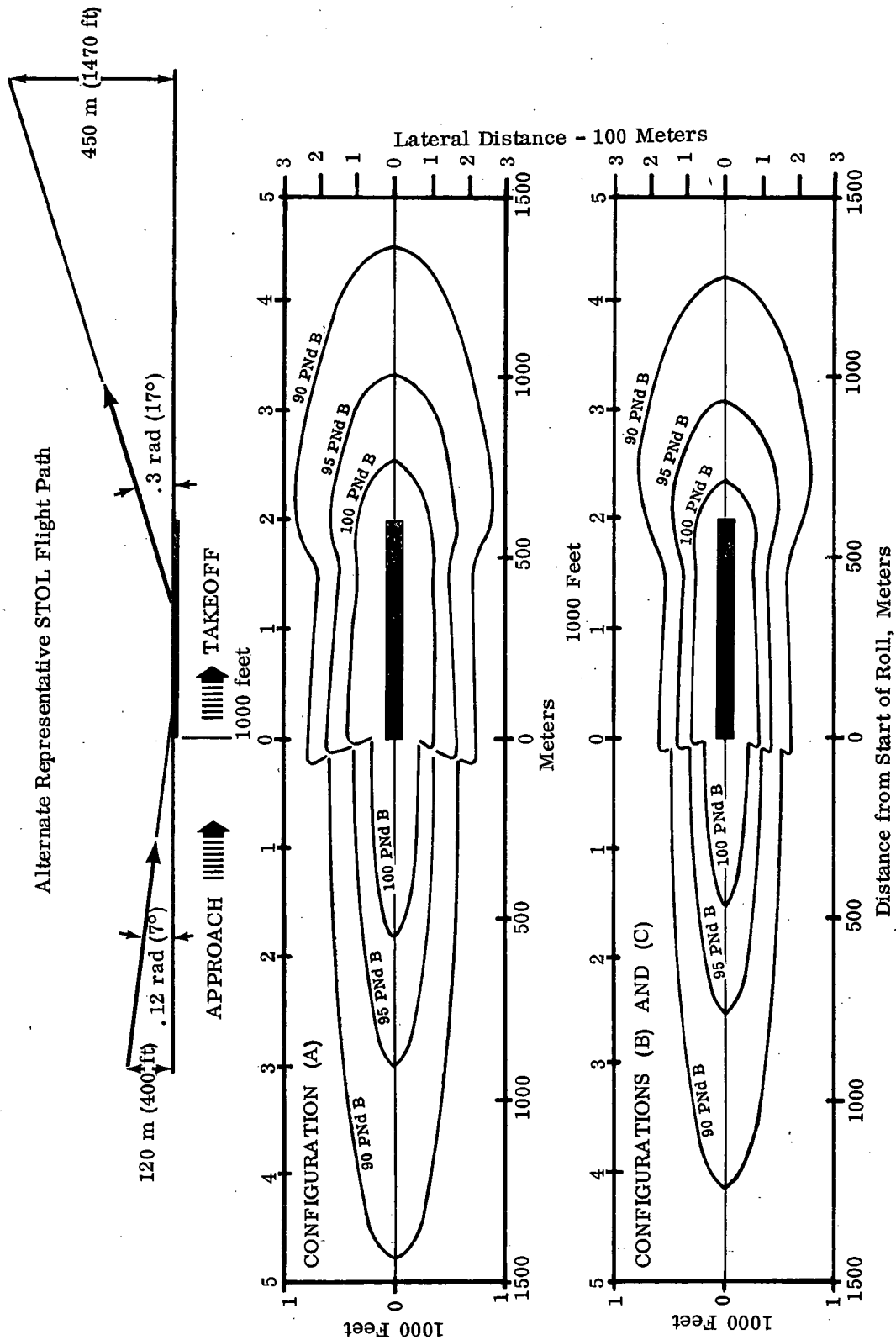


Figure 15b - Estimated STOL Noise Contours Using Four TF34 Configuration (A), (B), and (C) Engines, Standard Day.

Prospects for Further Noise Reduction

Depending on the magnitude of the flap impingement noise and the degree to which it can be practically reduced, and depending on the accuracy of the noise estimates, the amount of additional noise reduction required for configurations (A) and (B/C) relative to the ultimate objective will obviously vary. For configuration (A) which starts with the noisier and unmodified engine/fan system, and where the jet noise is marginal, prospects for further significant noise reduction are relatively limited. Four possibilities, however, do exist: (1) The engine cycle may be further rematched and the exhaust system resized (possibly with some cruise performance decrement) to drop the exhaust velocity and the jet noise by a small amount. (2) A larger amount of engine air bleed and/or horsepower extraction required for certain external blown flap STOL systems than that considered in the present study may also drive the exhaust velocity and the jet noise lower. A 1 - 1.5 PNdB drop in jet noise may be envisioned. (3) Additional fan noise suppression (say 3 PNdB more) may be obtained by using full MDOF linings and longer splitter lengths. (4) The external mixer device necessary for controlling flap interaction noise may have some small benefit on the exhaust jet noise level providing that special care is given to its design from the viewpoint of low velocity jet operation.

It should be mentioned that a 3 to 4 PNdB reduction in fan noise may be achieved through a modest modification of configuration (A) engine; namely opening the spacing between the rotor and the outlet guide vanes. The basic engine cycle is retained. The net effect on the systems noise is, however, only about 1.5 PNdB.

The prospects for further noise reduction are significantly greater on configurations (B) and (C) for two primary reasons: (1) the jet noise and flap interaction noise levels are less limiting because of the higher bypass ratio cycle, and (2) additional nacelle treatments can be provided since the current design has only one inlet and one aft splitter, just sufficient to meet the objective. It should be pointed out, however, that installation of additional splitters on the very high bypass ratio configuration (B) or (C) cycle will have a stronger adverse effect on the performance, as will be seen from the thrust and sfc influence factors of duct pressure loss given in Appendix II.

4. FAN TURBINE - ENGINE (A) AND (B)

The TF34-2 four-stage fan turbine is utilized in both Engines (A) and (B). Somewhat different operating conditions were selected for the two engines. Engine (A) is a mixed flow cycle with a partial mixer. Matching of static pressures at the mixer was one of the factors determining the fan turbine operating point, while reducing exhaust velocities as low as possible for minimum jet noise. Table XIV shows the sea level takeoff operating point compared to the YTF34-2 engine. The 7620m (25,000 ft) Mach .8 cruise operating point is also shown. Since cruise performance is not emphasized for the projected experimental aircraft, a two-position jet nozzle is not recommended despite the lower fan turbine efficiency.

Engine (B) fan turbine operating conditions are also shown on Table XIV both at takeoff and cruise conditions. A higher turbine speed was selected for Engine (B) to permit operation of the turbine at higher efficiency, a flexibility made possible by the geared design. The fan turbine energy extraction was set by the objective of reducing core noise to the fan jet noise level. The maximum fan turbine speed within the experimental aircraft cruise operation envelope is 785 rad/s (7500 RPM).

Table XIV indicates that no area adjustment to the low pressure turbine will be required for either modified Engines (A) or (B).

Fan Turbine - Engine (C)

A newly designed fan turbine was required for Engine (C) since this 1.25 pressure ratio fan is driven at 513 rad/s (4900 RPM), whereas the YTF34-2 turbine is designed to run at 733 rad/s (7000 RPM). By increasing the turbine loading and also increasing turbine diameter to a maximum of .737 m (29 inches) it was possible to retain four stages.

The alternative of five stages with its greater complexity was not considered attractive since the combination of loading and diameter change provides an acceptable flowpath from the high to the low pressure turbine while keeping the aerodynamic design within proven state of the art. The selection of four stages is also consistent with the results of numerous optimization studies made on low pressure turbines for other similar turbofans.

The design employs high swirl in the first three stages and low swirl, low energy extraction in the last stage. The efficiency assumed is consistent with performance levels demonstrated on an air turbine of similar loadings designed and tested under NASA Contract NAS 3-14304.

Several key parameters are tabulated in Tables XV and XVI.

A weight breakdown is shown in Table XVII.

TABLE XIV - LOW PRESSURE TURBINE AEROTHERMODYNAMIC DATA.

Engine	TF34-2		A		B	
	I	II	I	II	I	II
Flight Condition *						
Inlet Flow Function	.00151	.00150	.00151	.00150	.00150	.00150
$\frac{W\sqrt{T}}{P}$	$\frac{\text{kg/s} \sqrt{\text{OK}}}{\text{N/m}^2}$					
	(30.86)	(30.59)	(30.86)	(30.59)	(30.68)	(30.65)
	$\left(\frac{\text{lb/sec} \sqrt{\text{OR}}}{\text{lb/in.}^2}\right)$					
Energy Function	261	269	263	269	272	304
$\frac{\Delta h}{T}$	(.0624)	(.0624)	(.0628)	(.0642)	(.0649)	(.0726)
Corrected Speed	62.90	71.2	68.12	71.2	73.85	76.37
$\frac{N}{\sqrt{T}}$	(156.4)	(164)	(156.9)	(164)	(170.1)	(175.9)
Efficiency η	.904	.896	.904	.896	.906	.896

* I is sea level static, max power

II is 7620m (25,000 ft) max continuous power, Mach number .8.

TABLE XV -- FAN TURBINE -- ENGINE (C).

	1	2	3	4
Blade Exit	.559	.608	.658	.562
Diameter	(22.0	23.95	25.90)	(22.14
Stage Energy	82,983	(35.7)	82,518	(35.5)
J/kg	(BTU/lb)	83,587	(35.96)	46,140
Reaction	Δh_{stg}	.05	.052	.048
Swirl Γ	rad (degree)	.646	(37)	.698
Turning Angle, rad	(degree)	1.899	(108.8)	1.929
Root Relative	Mach Number	.569	.564	.600
Stage Work	$\psi = \frac{gJ\Delta h}{2U_p^2}$	1.66	1.57	1.47
Coefficient	Absolute Average	.319	.287	.333
Mach Number	No. Vanes	54	128	118
No. Vanes	No. Blades	152	152	114

TABLE XVI - COMPARISON: NASA 3-STAGE FAN DRIVE TURBINE AIR TEST VEHICLE
AND PROPOSED 4-STAGE TF34 STOL CONFIGURATION.

<u>OVERALL PARAMETERS, DESIGN POINT</u>		TF34 STOL		NASA Fan Turbine, Air Test Vehicle				
		4		3				
Number Stages								
Corrected Speed $\frac{N}{\sqrt{T}}$	rad/s//°K (RPM//°R)	48.8	(112.5)	28.1	(87.7)			
Energy Function $\frac{\Delta h}{T}$	J/kg °K (BTU/lb °R)	270	(.0645)	266	(.0635)			
Flow Function $\frac{W\sqrt{T}}{P}$	$\frac{\text{kg/s/°K}}{\text{N/m}^2}$ ($\frac{\text{lb/sec/°R}}{\text{lb/in.}^2}$)	.00142	(28.99)	.00532	(108.4)			
Pressure Ratio		3.33		3.4				
Loading $\psi = \frac{gJ\Delta h}{2U_p^2}$		1.38		1.50				
Tip Diameter, Max	m (in.)	.737	(29.0)	.726	(28.6)			
Objective Efficiency		89.0		89.0				
Test Efficiency		-		89.3				
 <u>STAGE PARAMETERS</u>								
STAGE		1	2	3	4	1	2	3
Loading $\psi = \frac{gJ\Delta h}{2U_p^2}$		1.66	1.57	1.47	.81	2.07	1.76	.85
Pitch Swirl Γ	rad	.646	.698	.628	.087	.775	.703	.052
	(degree)	(37)	(40)	(36)	(5)	(44.4)	(40.3)	(3.0)
Work Split $\Delta h_{stg}/\Delta h_{total}$.281	.279	.283	.156	.409	.384	.207
Root Reaction		.0505	.052	.048	.057	.05	.14	-.19
Root Inlet Relative Mach Number		.569	.564	.600	.447	.80	.78	.63
Root Turning, Rotor, rad		1.902	1.920	1.867	1.222	1.972	1.937	1.414
	(degree)	(109)	(110)	(107)	(70)	(113)	(111)	(81)

TABLE XVII - FAN TURBINE MASS - ENGINE (C)

		TF34-2		ENGINE (C)	
		4 Stage 712 rad/s (6800RPM)		4 Stage (Long Chord .737m (29 in.) Dia.)	
		kg	lb	kg	lb
Stator		30	67	44.5	98
Rotor		44	97	46	101
Transition		15	33	20.0	44
Exhaust Frame		15.4	34	17.2	38
Total		105	231	127	281
				Margin 12.7	28
Total No. Vanes			450	140	309
Total No. Blades			605		418
					550

5. TF34 COMPATIBILITY

Engine (A)

All operating conditions are within the YTF34-2 specification flight envelope. All speeds and engine temperatures fall well within demonstrated limits. The only significant modifications requiring proper design and evaluation result from the change from a separate to a mixed flow exhaust. A fan duct transition must be provided as part of the nacelle design to ensure that no local flow separation occurs which could result in forward distortion into the fan and compressor as well as reduced effectiveness of the fan duct acoustic treatment.

The core exhaust duct will require the addition of a longer plug to support combustor/turbine noise suppression devices. Methods of mounting this extended core duct from existing aft flanges within specification load limits would have to be reviewed at a time when installation details are defined. These interface areas are being reviewed for the NASA TF34 ground test nacelle. A more complete design analysis would be required for the eventual experimental flight application targeted in this study.

Engine (B)

All operating conditions are within the demonstrated capability of the core engine, which performs nearly like an unboosted core. Unboosted cores have been run frequently during the course of the YTF34-2 development, and the performance simulation includes all effects, such as Reynolds Number and lower absolute fuel flows, which have been measured.

The effect of a new fan and compressor transition on the core compressor must of course be calculated. The severity of the inlet gooseneck has not increased from the YTF34-2. The ratio between the fan discharge hub radius and the compressor inlet hub radius has been maintained equal to that of the YTF34-2.

A gear ratio was chosen to run the low pressure turbine at 790 rads/sec (7500 RPM), higher than in the YTF34-2 (723 rads/sec at takeoff power). Unless high altitude operating conditions are required, this is compatible with the life capability of the fan turbine. This can also be considered in the selection of the cruise fan nozzle area.

Compatibility of the engine to the shaft dynamics of a shorter low pressure shaft driving into the gearbox must be evaluated during the design and development of this engine. Well-established analytical tools which correlate accurately with test data are available for shaft dynamic behavior prediction.

Similarly, the compatibility of the core to the distorted reverse inlet flow during thrust reversal is an essential part of this development. The basic YTF34-2 fuel control is compatible with the variable pitch fan with the addition of suitable functions described in the control portion of this report.

Engine (C)

Most of the statements relative to Engine (B) apply also to Engine (C). In addition, the new low pressure turbine and shaft system require a new turbine casing and a new turbine rear frame. The compatibility of these parts needs to be established with respect to mounting loads and the overall engine dynamic system. No problems are anticipated. They were not considered in detail since the nacelle design was not within the scope of this study.

ENGINE LIFE ESTIMATES

The Work Statement of the study contract did not provide an experimental aircraft mission as a basis for life estimates but typical research and ferry missions were established after consultation with NASA personnel. Figure 15 shows the mission profiles used for ferry and research missions. A total of 300 experimental flights and 10 ferry flights was used. The duty cycle used is shown in Table XVIII.

TABLE XVIII - MISSION DUTY CYCLE

<u>Power Setting and Flight Condition</u>	<u>Time Per Flight Research Mission</u>		<u>Time Per Flight Ferry Mission</u>		<u>Cumulative Time</u>	
	Sec.	(Hrs)	Sec.	(Hrs)	Sec. x 10 ⁻³	(Hrs)
Idle	680	(.188)	680	(.188)	218	(60.5)
50-70% Max Continuous	300	(.083)	300	(.083)	100	(27.6)
Max Continuous, .8 Mach No. 7620m (25000 ft)	900	(.250)	2500	(.700)	295	(82.0)
Max, Sea Level 50 m/s (100 knots)	270	(.075)	270	(.075)	90	(24.8)
Total	2150	(.596)	3750	(1.046)	700	(194.8)

All mechanical design calculations were made using this mission profile, based on YTF34-2 temperature ratings.

Recent information indicates that maximum power will not be used during takeoff or landing except in the case of an engine-out emergency. To this extent the life estimates are conservative.

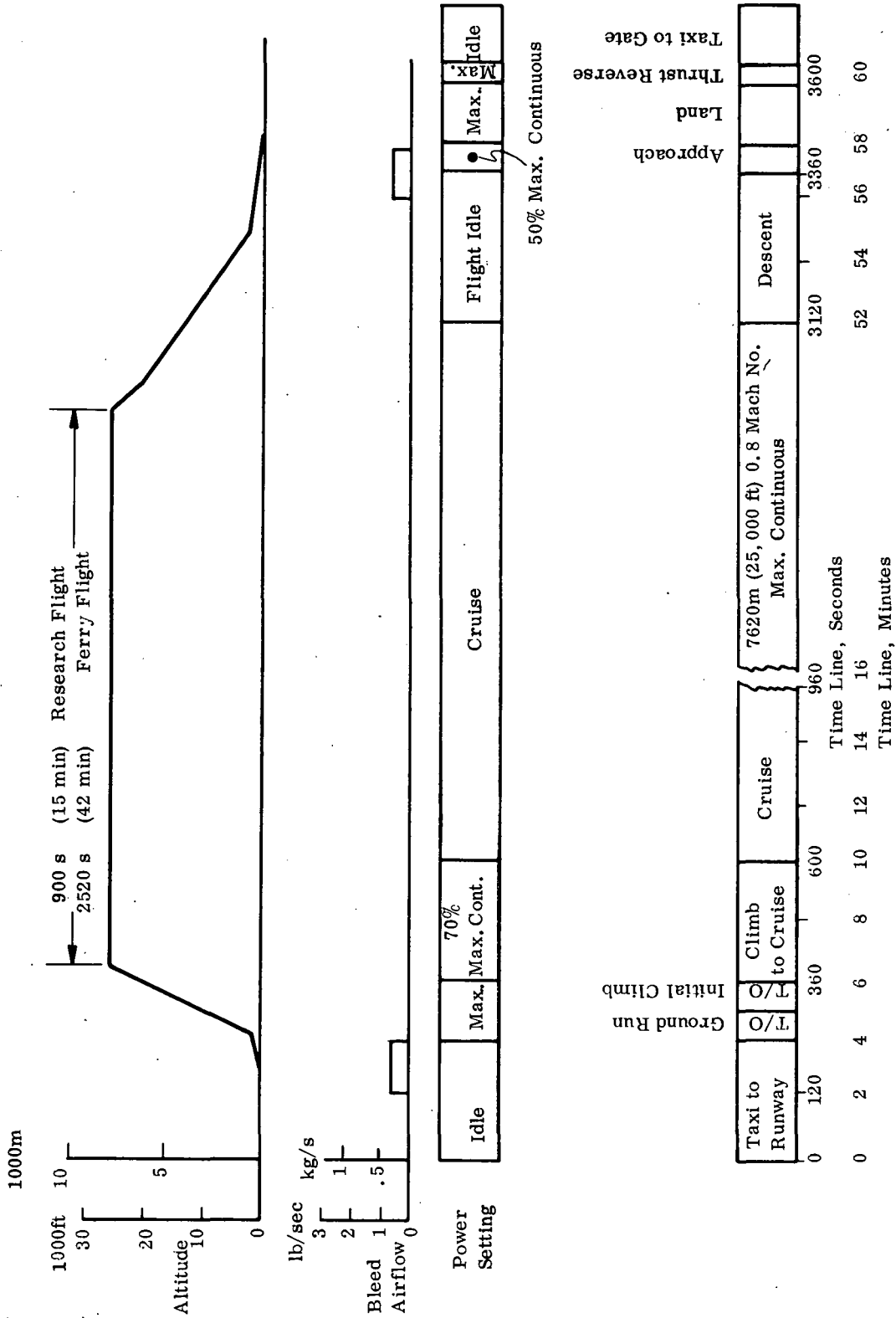


Figure 15 - NASA Experimental STOL Aircraft Mission.

6. VARIABLE-PITCH FAN MECHANICAL DESIGN

Variable Pitch Fan Blade Description

The configuration (B) and (C) fan blades are similar in all mechanical respects. The major difference between the two is that, due to blade reduced velocity torsional stability criteria requirements, fan (C) has 16 blades rather than 20 and the blade chord is increased correspondingly. A summary of the major aerodynamic and physical characteristics of both fans is given in Tables IV, V, and VI.

The attempt to maintain a very conservative blade torsional frequency margin coupled with the low solidity design produced fans with a low number of blades. The blades are forged and machined out of titanium 8-1-1. This was consistent with the near-term technology period when this design could be utilized. However, the conventional material and construction did produce high blade bearing loads. It also led to very high centrifugal blade couples that always tend to drive the blade toward the flat pitch (or closed) position.

Since it was felt that blade torsional stability would be most important in this application, the General Electric Twisted Blade Analysis program was used to obtain the expected vibrational response of the blade. Campbell diagram plots of the results are given in Figures 16 and 17. The first four modes of vibration as a function of fan speed are shown. For both blade designs, the third mode of response was the first torsional response mode.

Boundary conditions were applied at the blade stem root at the bevel gear that led to a more accurate torsional response model. The blade trunnion was only assumed as being fixed against movement at the midpoint at the sector gear, to let the blade model reflect the full torsional softness of the response. The model was softer in flexural response than is actually the case. The restraint of the thrust bearing against the blade trunnion was not completely applied. Thus, the flexural response acted as though the blade extended down to the sector gear when, in actuality, the blade flexural restraint extends only down to the thrust bearing resulting in a shorter blade beam than modeled. Therefore, the flexural responses, as shown, are lowered. This would especially be true for the first flexural response mode. However, the Campbell diagram plot is reasonably representative of the variable pitch blade response and indicates that both the (B) and (C) blade designs are feasible.

When the number of blades for both fans was picked, a very conservative reduced velocity parameter V_r^* was applied. V_r was chosen to be 1.18 for the (B) and 1.27 for the (C) configuration fan. These values were based on initially predicted torsional response frequencies of 410 Hz and 386 Hz for the (B) and (C) fan blade respectively. However the Twisted Blade Analysis indicated that the maximum speed blade torsional response frequencies would be approximately 325 Hz and 290 Hz, increasing the V_r values to 1.49 and 1.69. These are less conservative designs, but still reasonable based on existing GE fan blade experience. The drop in calculated torsional frequencies was due to three factors, two of which were because the blade aerodynamic designs were biased toward better reverse pitch performance: The first two factors relate to blade camber, and blade twist.

$$* \quad V_r = \frac{\text{Air Velocity relative to Airfoil (5/6 span)}}{\text{chord (5/6 span)}} \cdot \frac{\text{Blade Torsional Frequency (rad/s)}}{2}$$

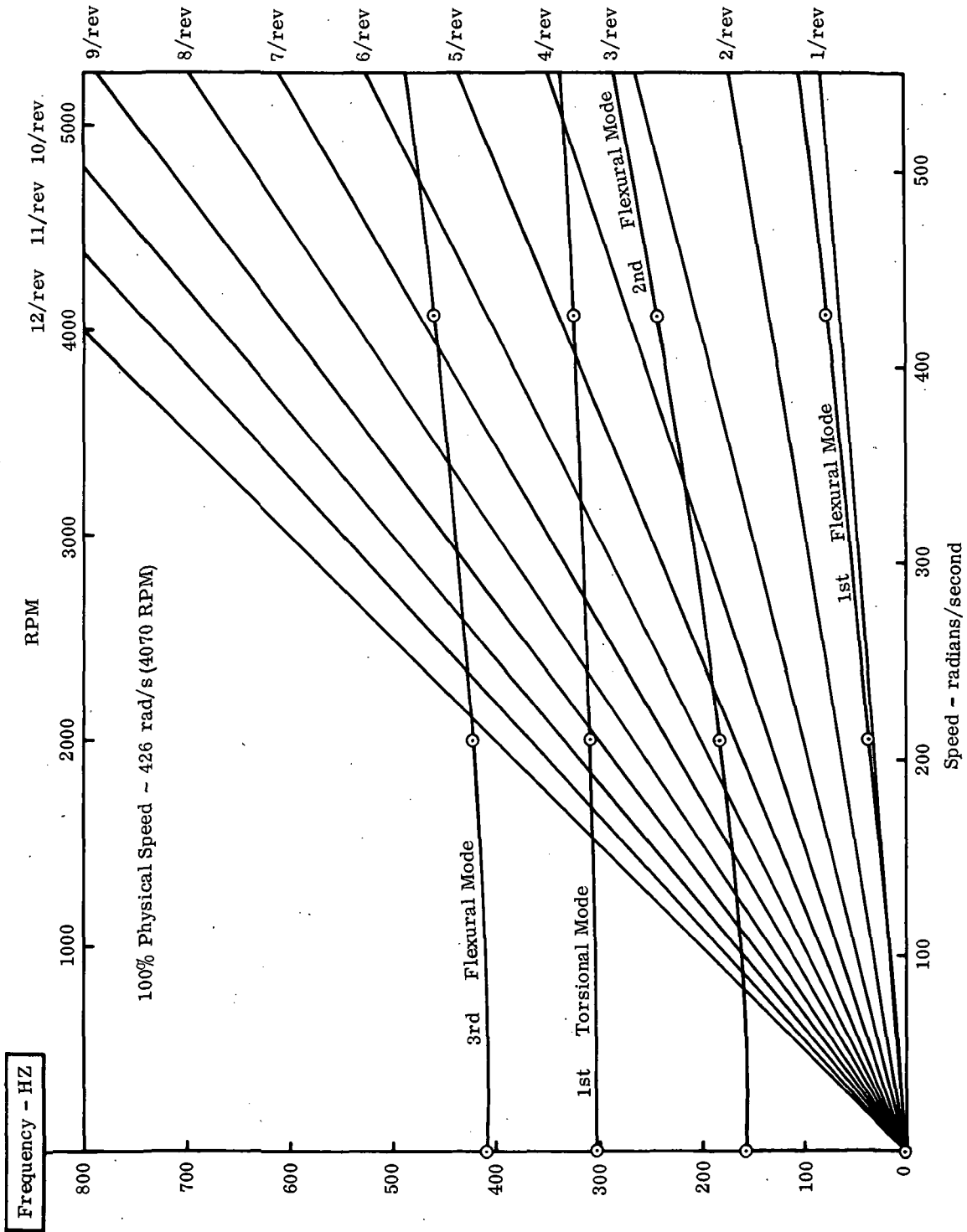


Figure 16 - Campbell Diagram.- Fan B.

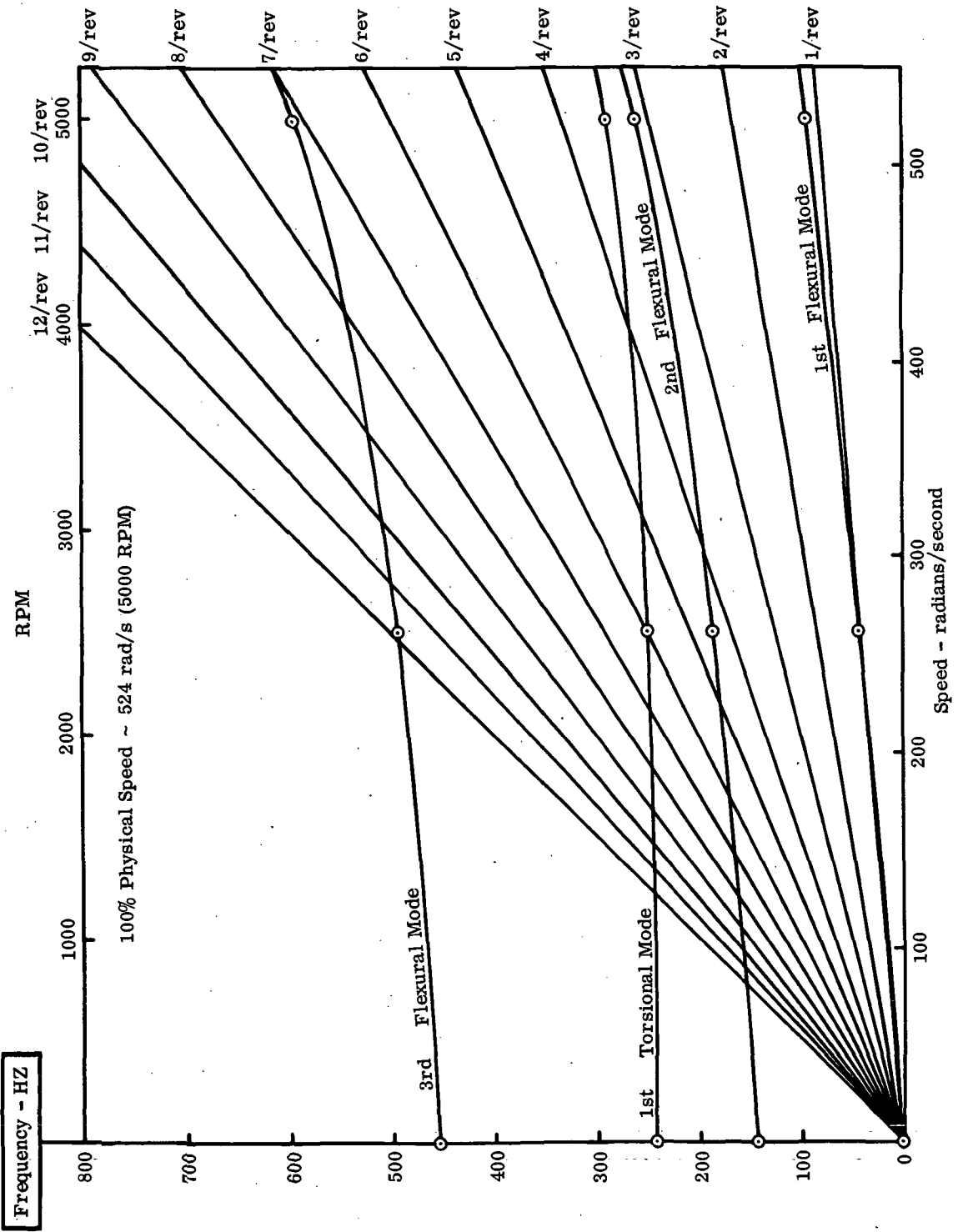


Figure 17 - Campbell Diagram - Fan C.

Both blades were designed to have a lower camber and a smaller twist than where no reverse mode is needed. Thus, much of the usual induced blade torsional stiffness was lost. The third factor was the effect of having the blade suspended on a stem (or trunnion) rather than on an axial dovetail all along the root chord, which also tended to drop the blade torsional stiffness. This has been anticipated to some extent and chords were made long enough to give reasonable V_r values, but the increase in V_r was more than expected.

A steady state stress analysis of both blade designs was also made using estimated aerodynamic loads. Plots of the centrifugal and Von Mises-Hencky stresses along the blade span from the thrust bearing retainer area to the tip are shown in Figure 18 through 21. No unusually high stresses were found and it is believed that the design is feasible from a stress standpoint.

The blade centrifugal loading is applied to the disk through a tapered roller thrust bearing and a steel retainer nut that is threaded onto the blade stem. Although the stress levels in the threaded blade stem area are not exceptionally high, a thread relief is required to prevent a low cycle fatigue problem. The thread and retainer system should be more than adequate to retain the blade.

The blade platform is circular and fits into the counterbored disk. Due to the flowpath taper in the blade root area, the platform and disk surface will be exactly flush at only one blade orientation. However, for small changes in orientation angle from the design value, say $\pm .175$ radians (10°), the misalignment of the blade platform edge and the disk surface will be very small and the chamfered edges will minimize aerodynamic interference. At the reverse pitch orientation, the platform-to-disk misalignment will be much greater, but since no useful aerodynamic work will be done in the root area, this is not considered significant. The circular platform was considered to be the best solution to excessive fan blade leakage in the root area.

Variable Pitch Actuation System and Blade Suspension

The blade variable pitch actuation system is basically the conversion of a fore and aft axial motion of a hydraulically actuated piston-cylinder assembly to circumferential motion through a pitched spline and a bevel ring gear. As shown in the engine cross-sections, Figures 2 and 3, the hydraulic control function is transmitted to the piston-cylinder assembly through a rotating seal and then through drilled holes in the piston rod.

As the cylinder wall moves axially, a spline drum attached to the cylinder moves through two sets of spline followers. The aft set of splines on the drum is pitched and thereby imparts a rotary motion to the spline drum as it moves fore and aft. The forward set of splines is straight so that the spline follower-ring gear rotates with the drum as the drum moves fore and aft.

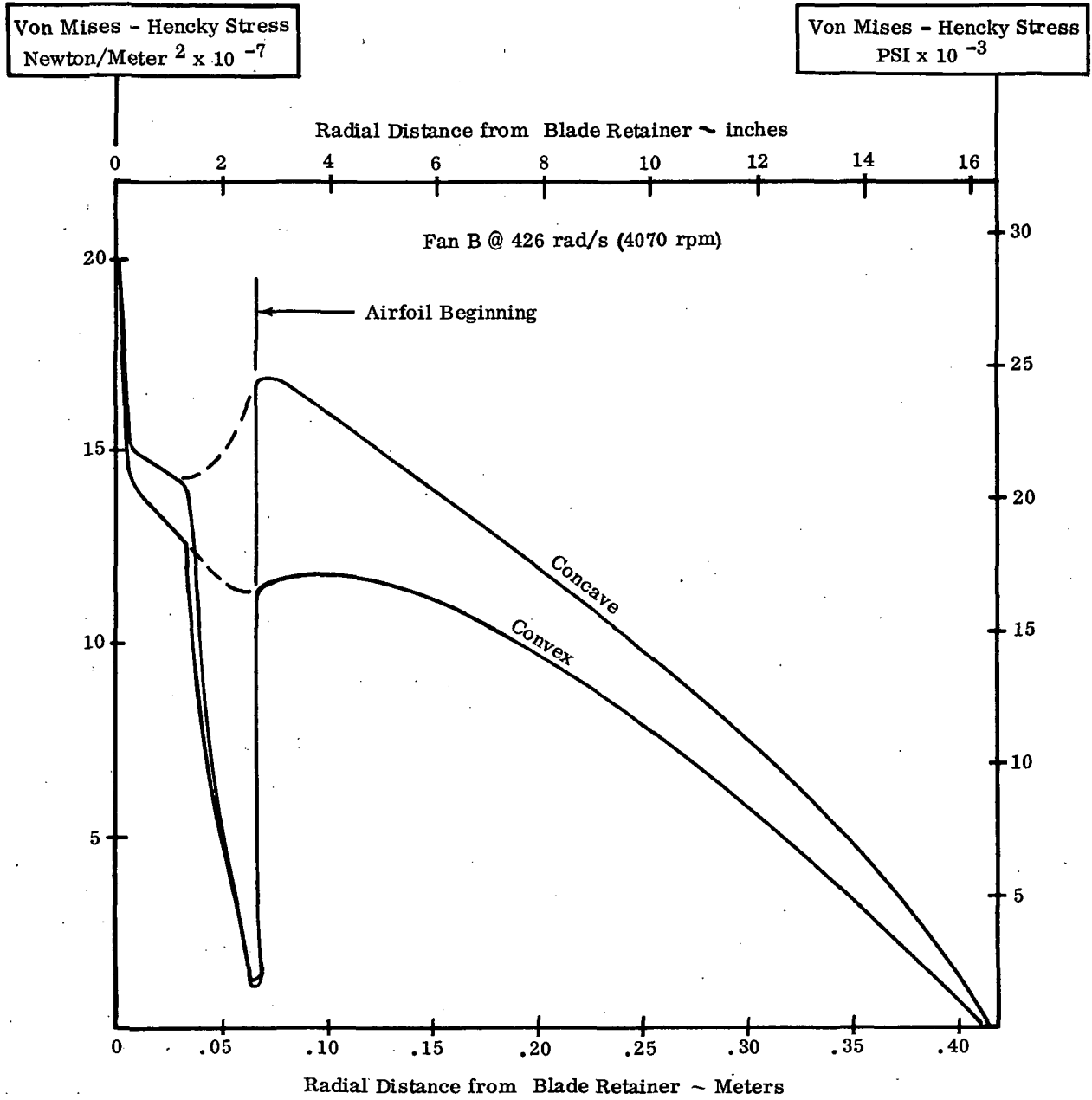


Figure 18. Von Mises-Hencky Stresses from Blade Tip to Retainer.

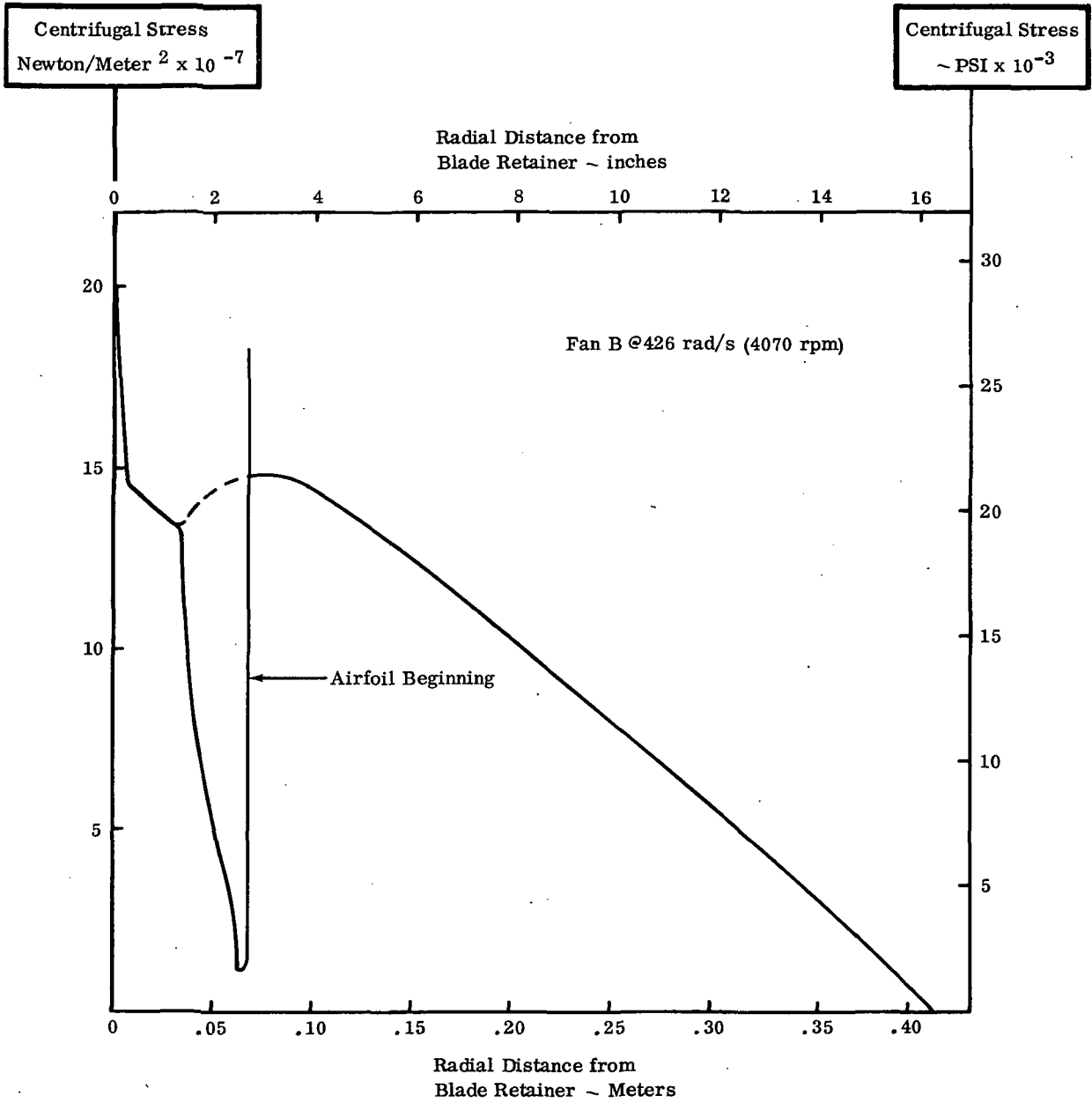


Figure 19 - Centrifugal Stresses from Blade Tip to Retainer.

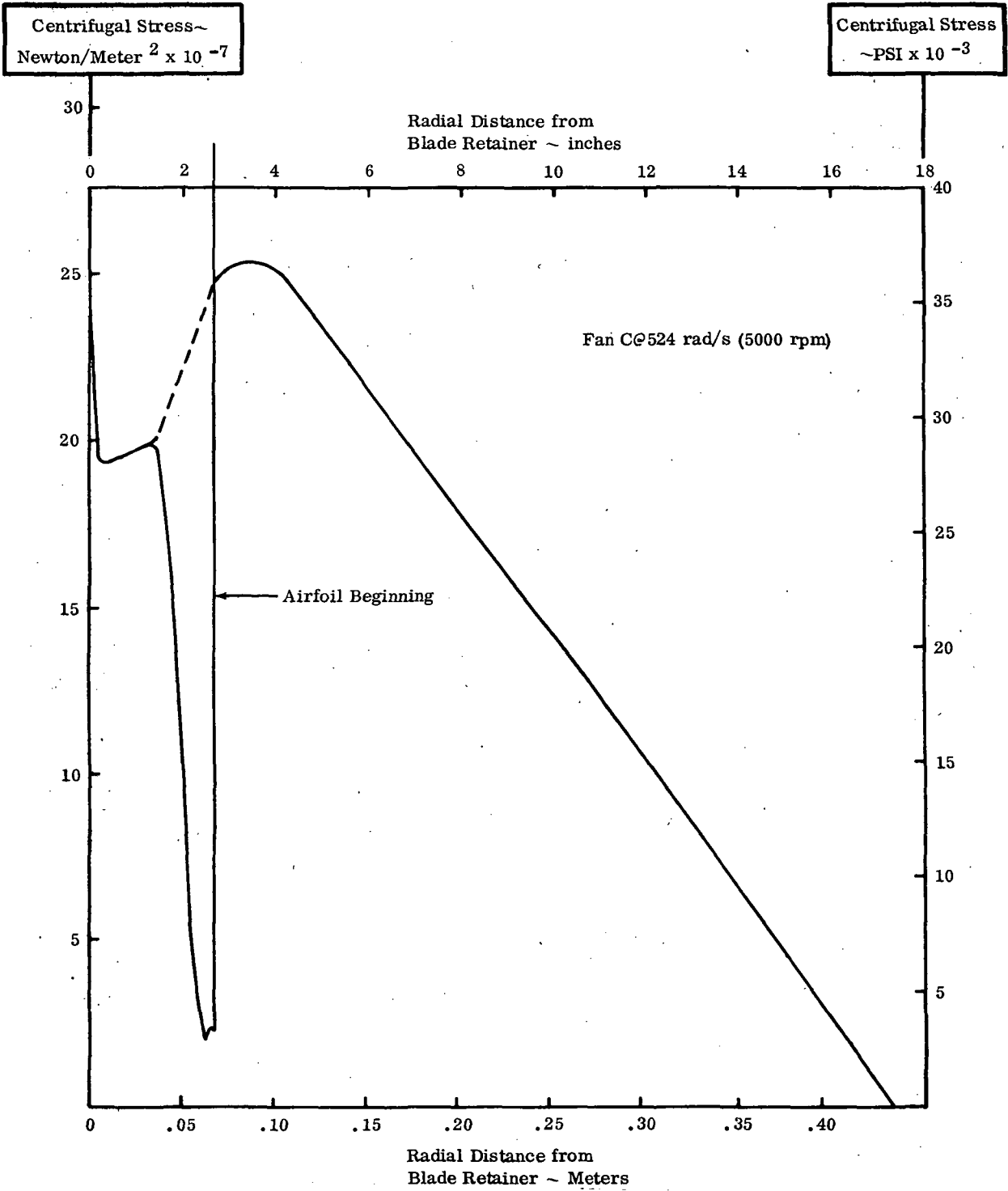


Figure 20 - Centrifugal Stresses from Blade Tip to Retainer.

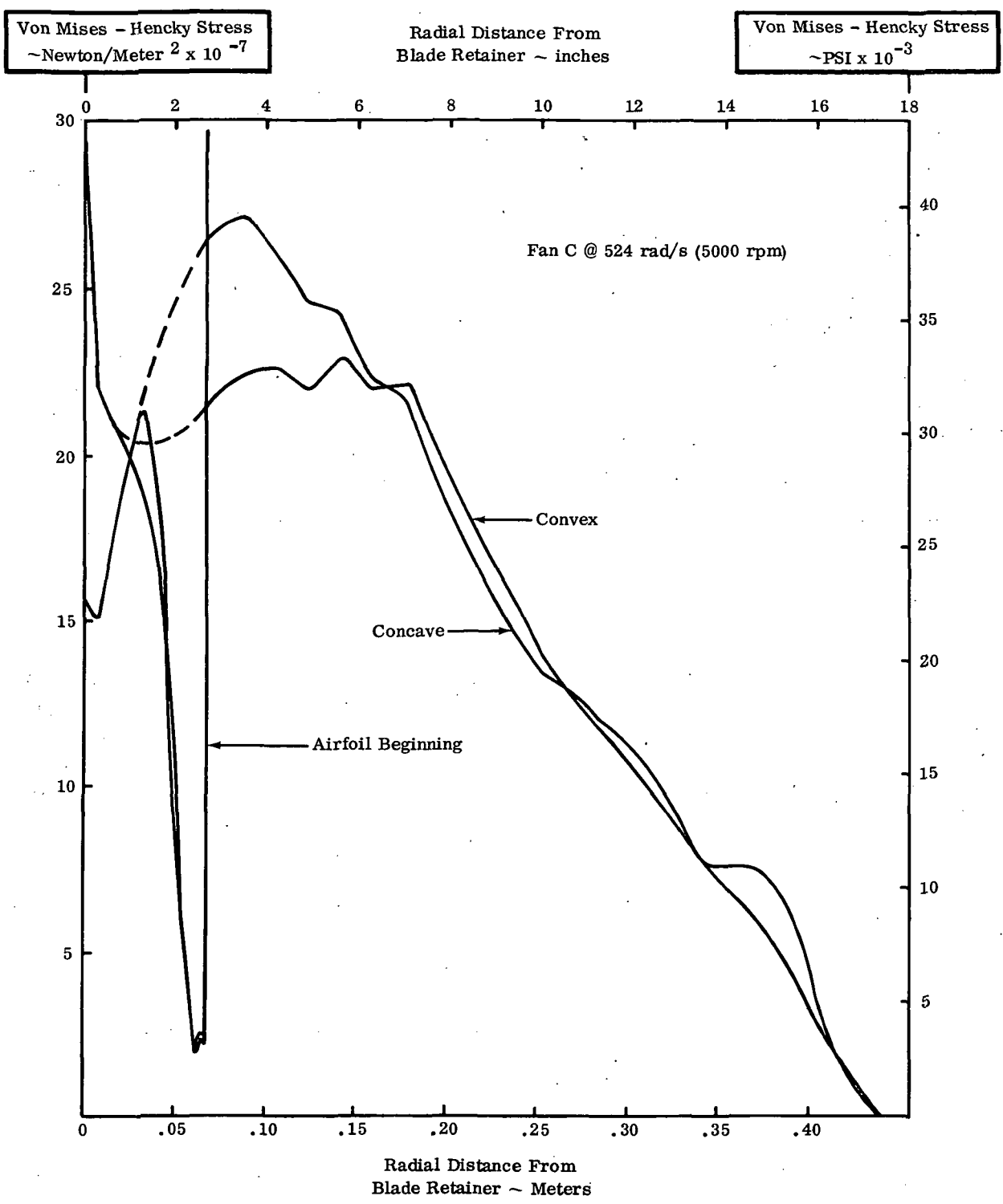


Figure 21 - Von Mises-Hencky Stresses from Blade Tip to Retainer.

The master ring gear is held in place axially by the large thrust bearing mounted in the fan disk but can still rotate freely. This ring gear motion is translated into blade orientation changes by individual sector bevel gears mounted on each blade.

In Table XIX, some actuation loads and blade pitch change design data are presented. All loads are those that result when the blade orientation is moved toward the engine centerline (open) position from the nominal design orientation. As can be seen, the largest actuation loads result from the centrifugal couples tending to drive the blade toward flat pitch (closed).

The actuation control system, as now envisioned, would be an active one, in that a constant hydraulic pressure would have to be maintained to keep any desired blade orientation. Expected maximum hydraulic actuation pressures are given in Table XIX and should be well within the capability of an engine-driven pump. However, the pressures required to hold the blade in a given orientation will be much lower than (perhaps half) the maximum pressures given in Table XIX.

Attention was given to the gear tooth stresses in this application and very conservative gear design practices were applied. It is anticipated that gear and bearing lubrication for the actuation system will be grease and dry lubricants. An oil mist or direct oil spray system would be complex if it were to avoid large overboard oil losses.

The bearing system is composed of a heavy duty cageless tapered roller thrust bearing and a radial roller bearing. As can be seen in Table XIX, the blade dead loads taken through the thrust bearing are very high and the bearing must be considered to be the highest risk part in the system. No experience in bearings loaded this heavily has been accumulated in aircraft gas turbines, but talks with various bearing companies indicate these loadings are common in large, heavy machinery when loading is smoothly applied and well known.

A series of tests was run by the Timken Bearing Company on a smaller bearing of the series used in this design loaded at a value of approximately $1 C_0$ (where C_0 is defined as the load that causes a permanent deformation of .1% of the rolling element diameter in the roller-race system).

The testing indicated that the bearing would survive a load of $1 C_0$ under an oscillating condition of as little as $\pm .175$ radian (10°). In Table XIX, it can be seen that the configuration (B) maximum loading is 78% of C_0 and the configuration (C) maximum loading is 97% C_0 . The test report on the smaller bearing and the load application method is included in this report, Appendix III. On the basis of the testing and industry-wide experience, it is felt that both the configuration (B) and (C) thrust retention systems are feasible. Since the bearings tested employed coined races and non-selective roller fits, additional bearing strength margins could be achieved with ground races and selectively-fitted rollers.

Since it can be expected that the thrust bearing mount would deflect significantly under these loads, the problem of maintaining square bearing surfaces must be solved. An approximate analysis of the configuration (C) mount showed that under the maximum loads, deflection would be at least .01 mm (.0004 inches) at the inner diameter of the bearing mount relative to the outer diameter. This could be compensated for by grinding the top

TABLE XIX - (S.I. Units) VARIABLE PITCH ACTUATION DATA AT MAXIMUM SPEED.

	<u>Fan B (Gear Drive)</u>	<u>Fan C (Direct Drive)</u>
Maximum Rotation	~ 2.44 rad	~ 2.44 rad
Design Rotation	~ 1.57 rad	~ 1.40 rad
Actuation Torques		
Centrifugal Couple/Blade	253 N-m (closed)	732 N-m (closed)
Aero Couple/Blade	62.1 N-m (open)	65.5 N-m (open)
Thrust Bearing Strut Torque	~76 N-m (opp. rotation)	~124 N-m (opp. rotation)
Max. Resultant/Blade	267 N-m (to open)	791 N-m (To open)
Stage Actuation Torque	5333 N-m	12654 N-m
Assumed Piston Stroke	.10 m	.10 m
Design Actuation Piston Force	171 kN	265 kN
Max. Design Pressure	20.7 MN/m ²	20.7 MN/m ²
Working Pressure	9.4 MN/m ² (.15m Piston)	10.7 MN/m ²
Max Bevel Gear Stresses	217 MN/m ² bending	238 MN/m ² bending
Bevel Gear Tooth	10 pitch	10 pitch
Actuation Efficiency (excluding Blade Bearing)	88%	88%
Blade Bearing Load	294 kN	489 kN
Bearing Approximate C _o Rating	378 kN	503 kN

TABLE XIX - (F.P.S. Units) VARIABLE PITCH ACTUATION DATA AT MAXIMUM SPEED.

	<u>Fan B (Gear Drive)</u>	<u>Fan C (Direct Drive)</u>
Maximum Rotation	~ 140°	~ 140°
Design Rotation	~ 90°	~ 80°
Actuation Torques		
Centrifugal Couple/blade	2240 in-lb (closed)	6480 in-lb (closed)
Aero Couple/blade	550 in-lb (open)	580 in-lb (open)
Thrust Bearing Strut Torque	~ 670 in-lb (opp. rotation)	~ 1100 in-lb (opp. rotation)
Max Resultant/blade	2360 in-lb (to open)	7000 in-lb (to open)
Stage Actuation Torque	47200 in-lb	112000 in-lb
Assumed Piston Stroke	4 inches	4 inches
Design Actuation Piston Force	38500 lb	59500 lb
Max Design Pressure	3000 psi	3000 psi
Working Pressure	1370 psi (6" piston)	1550 psi (7" piston)
Max Bevel Gear Stresses	31500 psi bending	34500 psi bending
Bevel Gear Tooth	10 pitch	10 pitch
Actuation Efficiency (excluding Blade Bearing)	88%	88%
Blade Bearing Load	66000 lb	110000 lb
Bearing Approximate C ₀ Rating	85000 lb	113000 lb

and bottom surfaces of the bearing out of square or grinding the outer bearing mount surface of the disk out of square so that everything squares up at the maximum load condition. This is a detail that cannot be neglected in heavily-loaded bearings such as these.

The radial bearing located just above the blade bevel section gear serves two purposes. First, it helps take out expected blade overturning moments and second, it resists the gear thrust loads. For instance, at maximum speed, it is expected that the configuration (C) blade sector gear would feel a 6230 N (1400 lb) thrust due to gear loads only. However, the radial bearing has an excess load capacity and should pose a very small risk to the blade suspension system.

As shown, the roller bearing is prevented from contacting either the titanium blade or the titanium disk by the blade retainer, and a bearing spacer. This was done to forestall any fretting problems in high stress areas.

The threaded blade retainer is steel and should have an adequate capacity for the blade dead loads. Careful stress relieving must be done, however, to keep the retainer stress largely compressive and to prevent the typical first thread failure mode.

The sector gear is shown as being retained by a washer-nut system. Since the thrust loading on the gear is aft and upward, tensile loading should be negligible on the nut due to actuation loads. As designed, it was anticipated that the gear would be broached with a square hole for a close fit with a square blade stem seat. This would ease assembly and provide the torque capability required with the cheapest manufacturing methods. Sector gears were chosen so that the largest gear radius possible could be used to reduce tooth loads and crushing pressures. As designed, a 2.44 radian (140°) sector gear is used. This is the only item that prevents a larger blade rotation than the planned 1.40 to 1.57 radian (80 to 90°) for this system.

It may be concluded from the above discussion of the various design features required to cope with the large centrifugal and untwist loads that a much improved and lighter design would result by using some form of lightweight blade construction instead of solid titanium. High strength fiber plus plastic matrix composite construction is a typical example of a lightweight technique. Another construction is the use of a metal spar with a composite plastic airfoil fairing. The weight saving resulting from such blade constructions would be in the attachment, disks, pitch actuation and hydraulic system, as well as in the blades themselves, and thus would be greater in a variable- than in a fixed-pitch fan.

7. REDUCTION GEAR

A 1.9:1 speed reduction gearbox is used in the TF34 with the fan configuration (B) to transmit low pressure turbine power to the fan rotor. A five-branch, double helical star gear was chosen, which results in a compact, lightweight gearbox while minimizing gear noise.

The gearset is positioned inside the fan rotor stub shaft to decrease engine length. This is possible due to the compactness of the gear designed for the short life mission requirement. The large bore roller and thrust bearings are from GE TF39 and CF6 engines respectively, simplifying procurement.

The gearset is made up of a sun gear, five star gears and a split ring gear. These are of the double-helical type with the helix angle selected so that the split ring gear halves are clamped together by the resultant axial forces during the drive mode.

The input power is extracted at 780 rad/s (7500 RPM) from the power turbine shaft through an adapter shaft which is integral with the low pressure turbine thrust bearing adapter. On the aft end, the adapter supports the thrust bearing, and on the front end it supports and drives the .152m (6 inch) pitch diameter sun gear. This feature allows the use of the present turbine shaft.

The sun gear drives five .0635 m (2.5 inch) pitch diameter star gears which are mounted to a ribbed stator cantilevered from an internal sump flange. Each star gear is supported in the stator by a set of flanged M50 roller bearings. The star gears in turn drive a flexibly-mounted .279m (11 inch) pitch diameter ring gear.

Power is transmitted at 415 rad/s (3950 RPM) from the ring gear to the fan rotor through a flexible, splined shaft.

The sun, ring and star gears will be made of AISI 9310 CLVM (AMS 6365), and the gear teeth, splines and bearing journals will be case-carburized and ground. Star gear bearings will have locked inner and outer races. A minimum journal radial wall thickness of 1.5 times bearing inner race thickness will be provided on the star gear stub shafts. The driving ring will be made from nitralloy nickel forging with its internal splines nitrided. This will result in hard cases with low friction coefficients and excellent wear characteristics.

The gear teeth have been conservatively designed for the application life (see Table XX). Tooth root bending and compressive stresses are well within acceptable design limits under the load conditions imposed and the scoring indices are below general practice limits. Low oil inlet temperatures coupled with good tooth flank finishes will assure elasto-hydrodynamic lubrication.

All cylindrical roller bearings are of CEVM M50 tool steel with silverplated steel cages. The bearing life has been calculated to be in excess of 1000 hours B1 life for each bearing.

Generally, all bearings will be oil jet lubricated. Oil entry into the bearings will be between the outer diameter of the inner race and the inner diameter of the cage. Star gears will be spray jet lubricated coming out of the sun-star and star-ring meshes. Estimated oil flow rate required is 2.95 m³/s (13 GPM). Maximum heat rejection of the gearbox is 62,980W (3584 BTU/min.).

TABLE XX - GEARBOX DESIGN LIFE REQUIREMENTS

Flight Condition	Time		Input Speed		Input Torque		Output Speed		Shaft Power	
	ks	(hrs)	rad/s (RPM)	(RPM)	N-m (lb-ft)	(lb-ft)	rad/s (RPM)	(RPM)	kW (hp)	(hp)
SLS Idle	218	(60.5)	205	(1960)	529	(390)	115	(1100)	108	(145)
SL 50 m/s (100 knots) Max. Power	89.3	(24.8)	785	(7500)	6535	(4820)	414	(3950)	5108	(6850)
SL 50 m/s (100kts) 50-70% Max. Continuous	99.4	(27.6)	547	(5220)	2793	(2060)	288	(2750)	1521	(2040)
7620 m (25000 ft) .8 Mach No. Max. Continuous	346	(96.0)	752	(7180)	3633	(2680)	396	(3780)	2729	(3660)

GEARING LOAD DATA MAXIMUM CONDITIONS

Root Stress	400 MN/m ²	58,000 lb/in. ²
K Factor	900	(.35 rad (20°) pressure angle)
Pitch Line Velocity	119 m/s	(23,500 ft/min)

8. CONTROL SYSTEM

Summary

The control system for the variable pitch fan/TF34, engines (B) and (C), will meet the following requirements:

Permit rapid power changes, safely, under all aircraft operating conditions.

Permit fan speeds and blade angles to be achieved in a controlled manner over the full range of experimental interest for low noise, efficiency and reverse thrust performance.

Utilize the present TF34 control as the "power control" modified as required to adapt to reverse thrust operation.

Be compatible with current commercial aircraft propulsion controls for operational safety and full experimental capability.

The key modification to the present TF34 control is to separate the fuel stopcock and incorporate a heart-shaped power input cam. The separate stopcock will be connected to the main fuel control to continue the capability of an "automatic starting control". It will also be used to shut down the engine and to switch control of the engine to the power control lever. This will leave the pilot free to use the power control lever, (PCL) for all power changes including single line movement (backward) into reverse thrust and return (advance PCL) to forward thrust. Movement into reverse thrust and back again to forward thrust is preceded by automatic switching of fan blade angle and a variable area system which opens up the flow area to the fan "inlet" in reverse. While the fan blades are reversing through fine pitch, the power control is calling for the safe minimum power schedule to prevent fan overspeed.

While the power control setting determines the power delivered to the fan rotor, a second control sets the fan condition of speed and blade angle. This is a simple speed governor that calls for that blade angle required to achieve and maintain the speed setting. To operate at a particular fan blade angle and speed, the PCL may need to be adjusted to change the blade angle while the fan governor holds the speed.

To protect against failure in any part of the fan governor-blade actuation system, mechanical stops limit the range of blade angle and an emergency fan overspeed governor will cut back engine power. The mechanical stops permit operation over the useful range of blade angle with safety to avoid fan stall or excessive speed decrease due to overload at the high end and an acceptable and safe minimum blade angle on the low end. The fan overspeed governor is for emergencies only and will automatically cut back fuel flow to the gas generator to prevent excessive overspeed.

For the engine with a fixed blade position fan, the control will be only slightly changed from the present TF34 configuration. These changes, like inactivating the automatic gun gas ingestion control, will be done in the simplest, lowest cost, manner.

The use of the variable pitch fan to obtain reverse thrust requires a small actuator to remove the low pitch stop and a set of actuators to increase the airflow area behind the fan. The removable low pitch stop is similar to those used on reversible propellers. The additional area at the fan "inlet" during reverse can be provided by opening up the fan nozzle area or by deploying auxiliary scoops which could take advantage of ram air.

Pilot's Control Levers - Operation

The control of each engine will be through three separate levers. For the most part, operation will be in a hands off, automatic fashion, and only one lever need be moved at a time. The schedule for each lever is shown in Figure 22.

To start, the starter button is depressed and the "condition lever" is moved from OFF to the START position. Ignition comes on and will be turned off automatically after the engine reaches an appropriate speed. The control will automatically supply fuel through both primer and main fuel nozzles to quickly and safely bring the engine to idle speed. By advancing the lever to RUN, control of the engine is switched to the PCL. By retarding the condition lever to OFF, the engine can be shut down, manually, at any time from any operating condition.

The PCL can be moved between Idle and Maximum at any rate or movement pattern. This is the same linear power schedule used for the TF34. Movement into the reverse thrust region will require manual movement of a lock to prevent inadvertent action. Releasing the PCL lock will (a) trigger the removal of the minimum flight pitch stop on the fan blades, allowing them to move to reverse and (b) deploy the increased area system behind the fan. After the fan blades pass a predetermined position, the PCL is released and may be moved from idle power into the increasing (reverse thrust) power region. Appropriately designed pilot's quadrants will permit an operator to make these motions fast enough to change the gas generator and fan output from maximum forward thrust (takeoff) or normal landing condition thrust to maximum reverse thrust in less than two seconds.

There will be no restrictions in advancing the PCL from reverse thrust to forward thrust. At the end of a landing run with fan braking, the pilot's manual movement will be expected to be at moderate speed to a low power setting. The fan blades will be triggered to move to forward thrust angle. Taxiing power can be adjusted with the PCL near idle. By setting the fan speed governor to a low value, the blades will move into the normal operating region and the minimum fan blade angle stop will lock into place.

In the case of a landing abort, the PCL can be burst to maximum forward thrust position. The time to 90% of maximum forward thrust will be roughly two seconds or less, depending on the initial position of the fan blades, their rate of change and the specific characteristics of the fan overspeed governor.

The fan speed control lever will permit the achievement of a wide range of fan speeds and fan blade angles for normal flight and experimental purposes. These functions can be adjusted for optimization during takeoff, climb, cruise, landing approach and landing. By using the speed governor approach, the pilot is prevented from inadvertently establishing conditions which may result in fan overspeed.

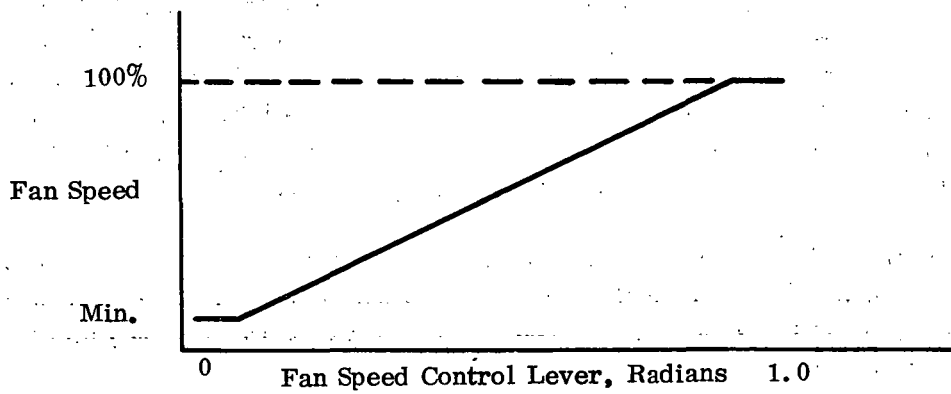
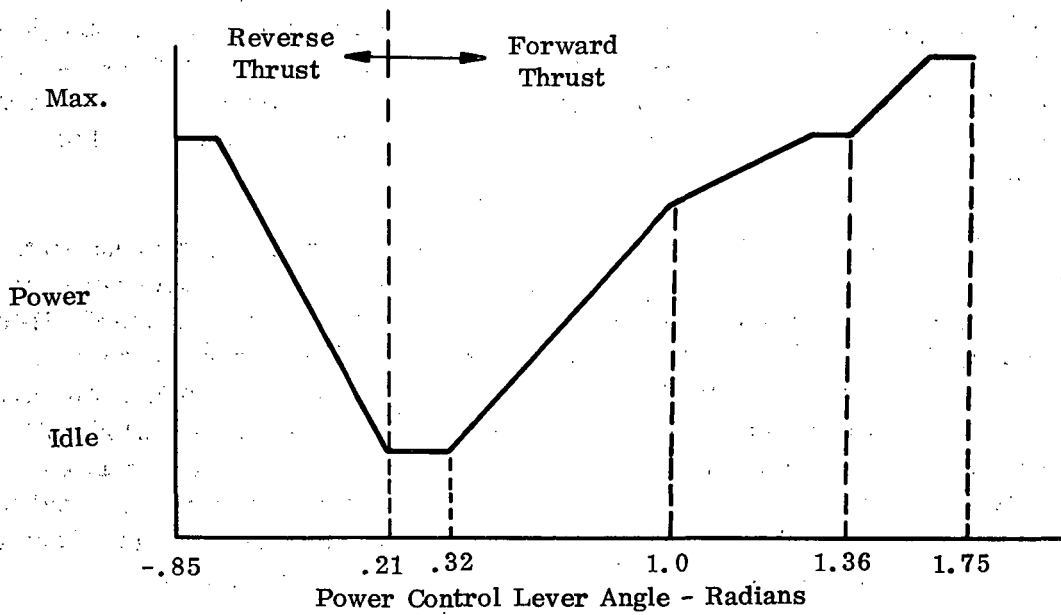
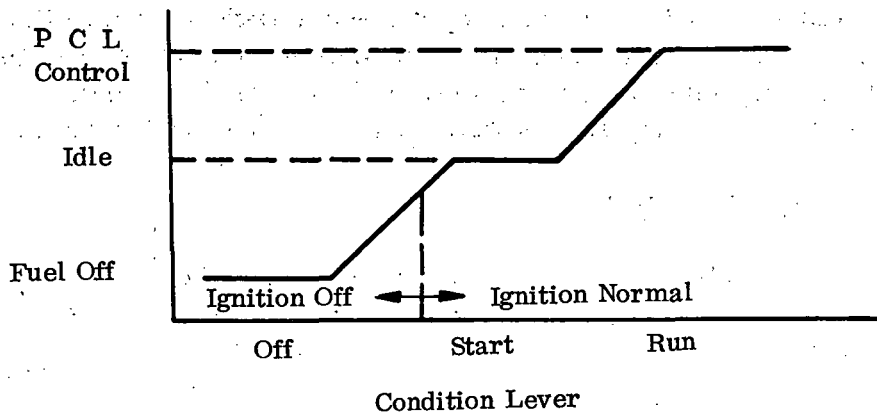


Figure 22 -- VP Fan Cockpit Control Levers.

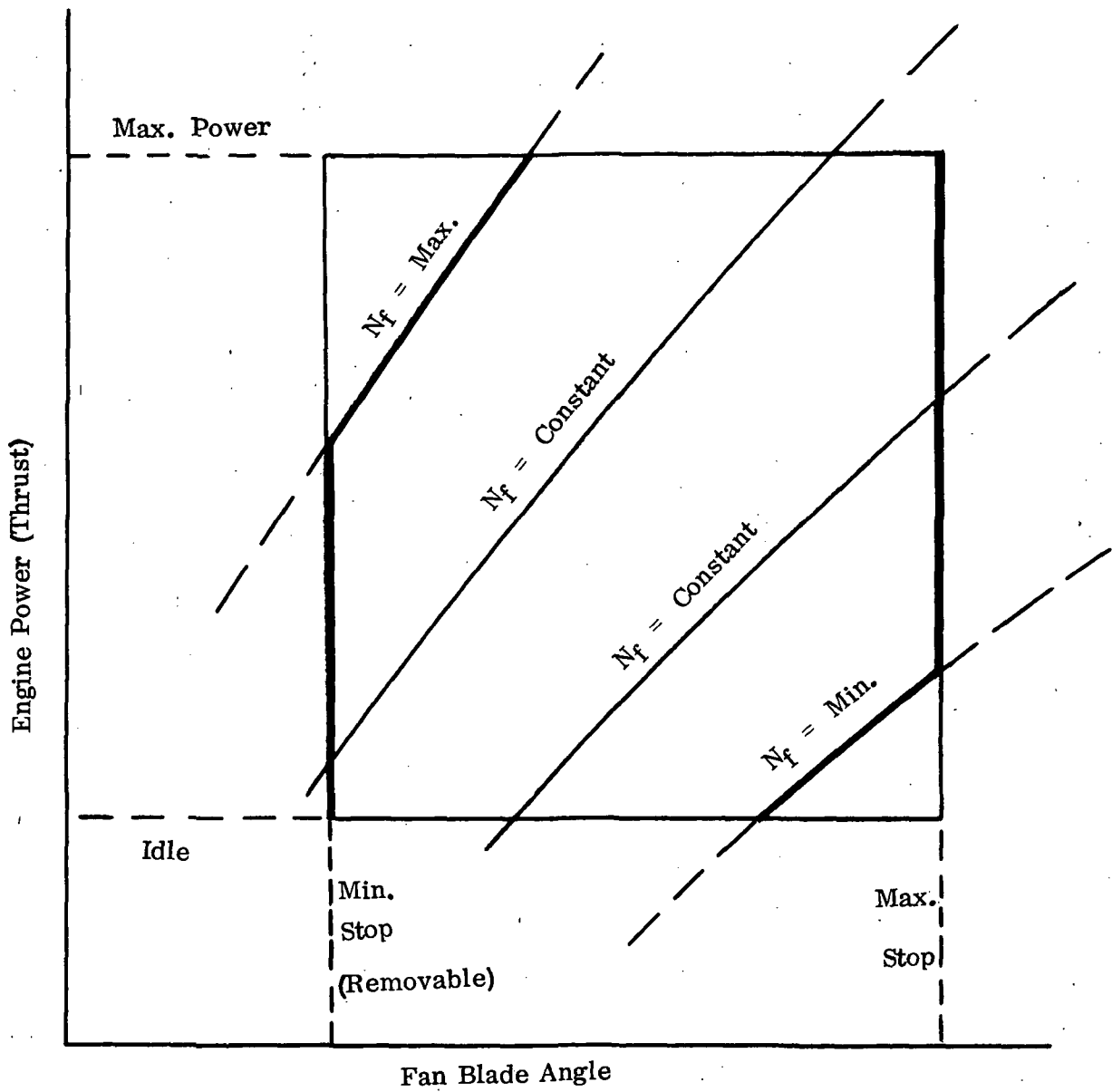


Figure 23 - Normal Range of Fan Operation (Excluding Reverse Thrust).

Fan speed is controlled via blade angle change. Should the pilot call for less power than required to maintain fan speed, the blades will move toward the minimum blade angle stop. Further reduction in power will result in a fan speed fall-off with the blades against the stop. Conversely, if the fan speed setting is too low for the power generated, the fan speed will increase (safely below 100%) with the blades against the high blade angle stop. The interrelated parameters are shown in Figure 23.

POWER CONTROL

Starting/Shut Down

A separate package containing a stopcock, receives the pilots input commands to "start" and "shut down" the engine. The modified main fuel control continues to provide all automatic control functions. The new input device permits a single, linear PCL for all other operations. A schematic of the major control elements is shown in Figure 24.

Forward/Reverse Thrust Schedule

The present TF34 main fuel control input cam has a linear schedule of power from idle to maximum, controlling both gas generator speed and turbine gas temperature. This will be retained. The balance of the heart-shaped input cam will call for an increase in power to a maximum predetermined value for reverse thrust. The cam can be moved continuously between extreme positions except for an external lock and switch arrangement. This mechanism assembly will prevent movement to "reverse" until the pilot's quadrant signals a removal of its lock and the fan blades are moving beyond a predetermined position. Removal of the pilot's quadrant lock will also signal the opening of the fan as reverse inlet area. The PCL will have adjustable stops at either end.

FAN SPEED BLADE ANGLE CONTROL

The typical turboprop approach of governor control of propeller-fan speed via actuation of blade angle will be used. A shaft-mounted electric alternator will provide both the speed signal and electric power for the governor. The electro-hydraulic governor will be mounted forward of the engine accessories.

Two major differences from turboprops are evident. (1) The higher fan speeds result in much higher blade twisting moments due to centrifugal forces. The counteracting aerodynamic loads are, proportionately, very much smaller. This results in relatively large friction forces, load gradients and the need for large actuators. (2) The blade angle/torque relationship is much lower than for a propeller, requiring higher rates of change for desired response and stability. A dynamic response and stability study as performed for the GE-T64 and other turboprops will be an important part of the control design activity.

High rates of blade angle change are also required for thrust reversal. Based on studies described below, a rate of 0.7 radians per second or more may be desired. This corresponds to oil flow rates to the actuator of 950 cm³ per second (15 gpm). An established aircraft hydraulic pump of 4.2 kilograms is available to meet a 0.7 radian per second requirement. The hydraulic system is shown in Figure 25. This system shows a hydraulic pump as the primary flow supply. A small accumulator may be needed to smooth out the pressure characteristic of the system.

A study was made of a system using a large accumulator with a small charging pump. The charging pump must be sized after detail study of normal operation consumption, emergency requirements and leakage. A prime advantage of this system is that it would reverse the fan blades in a calculated time of 0.6 seconds. A prime disadvantage is the large size. A two-charge accumulator (reverse and forward) requires a 11,500 cm³ (700 in.³) internal (oil and nitrogen) volume.

All stops of blade angle travel are adjusted into the actuator assembly. Normal operation for forward thrust is between a removable low blade angle stop and a fixed high blade angle stop. The reverse blade angle stop is also fixed.

The removable stop is cylindrical in shape and is located between the actuation cylinder and the fan disk. The cylindrical structure consists of a rigid cylinder attached to the actuator cylinder butting a deeply serrated or finger-like unit. The fingers are held tightly in a slightly tapered, cylindrical shape surrounded by a locking device. By hydraulic force, the locking device is moved out of position to allow the fingers to spread open, releasing the rigid cylinder to move within the spread fingers. By appropriate choice of configuration, the hydraulic force for opening and relocking can be kept very small.

The position sensor for fan blade angle will be a linear variable differential transformer (LVDT) located at the rear of the hydraulic transfer sleeve in the gear reduction configuration as shown on Figure 26. The armature will be at the end of a long thin rod located on the engine centerline and rotating with the fan assembly. The stator will be mounted on the stationary portion of the hydraulic transfer sleeve. The stator will contain graphite bushings to act as bearings for the armature.

When no gear reduction is used, the configuration requires the position sensor to be in a rotating location. The most probable location is between the actuator and fan disk, just outside of the minimum blade angle stop. The signal transmission will be via slip rings mounted next to the hydraulic transfer sleeve.

The operating characteristic of the LVDT will be a combination of five linear schedules. These will emphasize maximum accuracy in the normal forward thrust blade angle region, the switching point in the flat pitch region and the end of travel in the reverse thrust region. The two long regions between these will be with lower gradients.

REVERSE THRUST

An approximate picture of the transition to reverse thrust can be obtained by combining TF34 transient performance data and assumed characteristics for a variable blade angle fan. Such explorations indicate that the TF34 gas generator responds very rapidly to its power lever input. Also, the response of the variable blade angle fan will be even faster than the fixed fan. In going from forward to reverse thrust, the rate of blade angle change is the dominant factor in determining the elapsed time. These ballpark studies also indicate that, assuming reasonably rapid PCL movement and fan blades moving 0.7 radian per second and 1.05 radian per second respectively, the reverse thrust will begin in about 1.0 and 0.8 seconds respectively and reach 95% of full value in about 1.8 and .33 seconds respectively, after initiation. Although the gas generator power can be "chopped" very rapidly to the

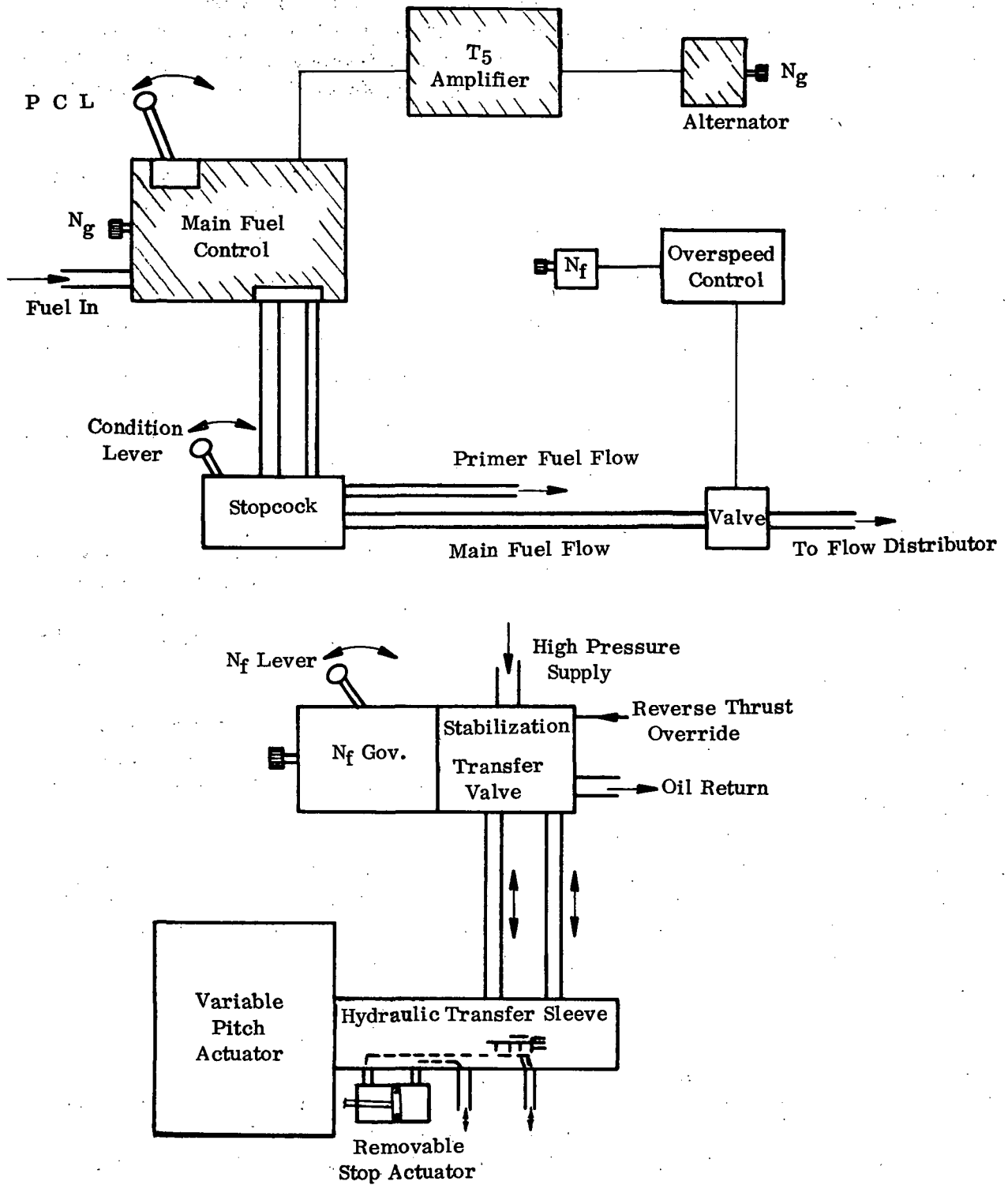


Figure 24 - Variable Pitch Fan Control Including Modified TF34 Control.

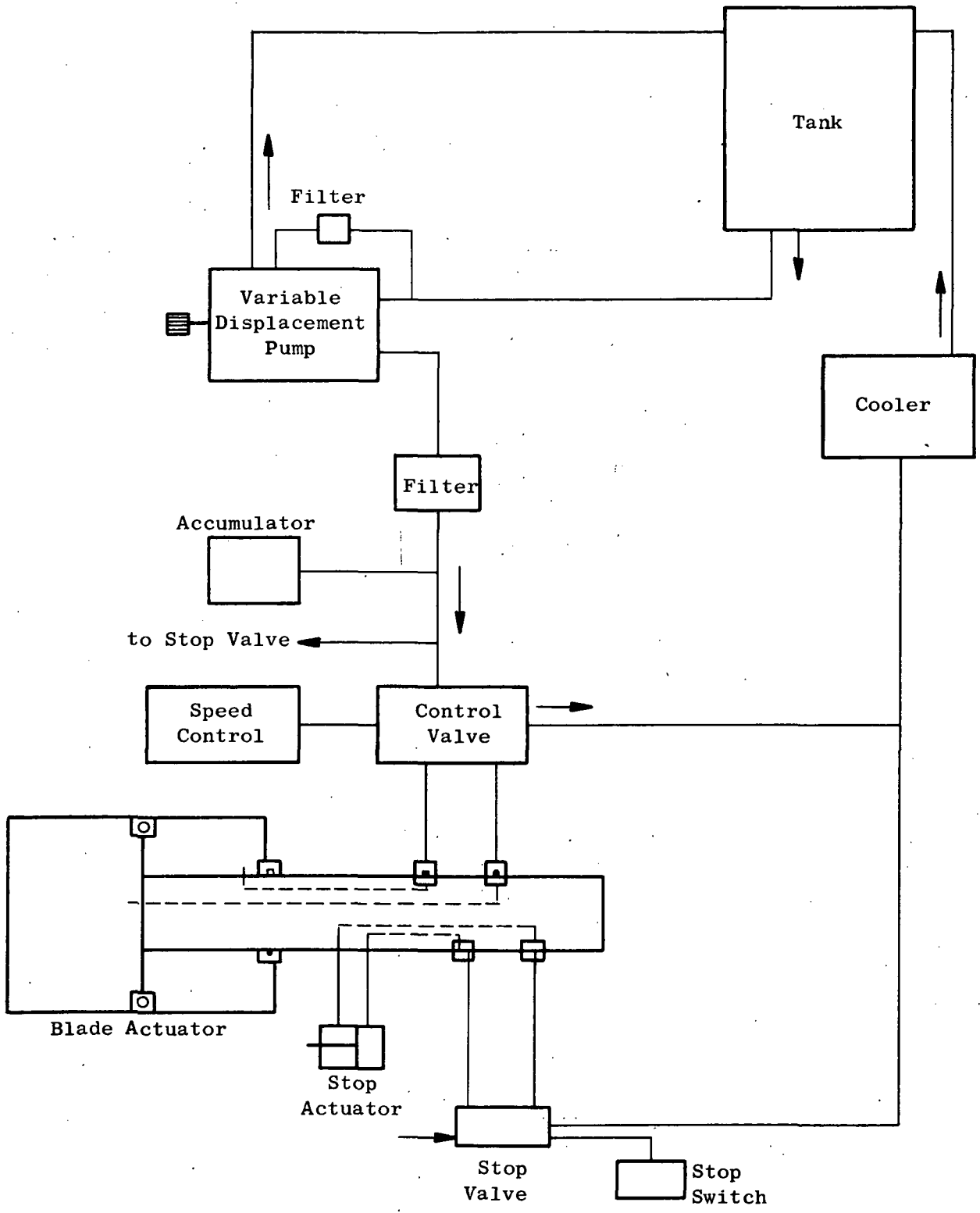


Figure 25 - Hydraulic System Schematic.

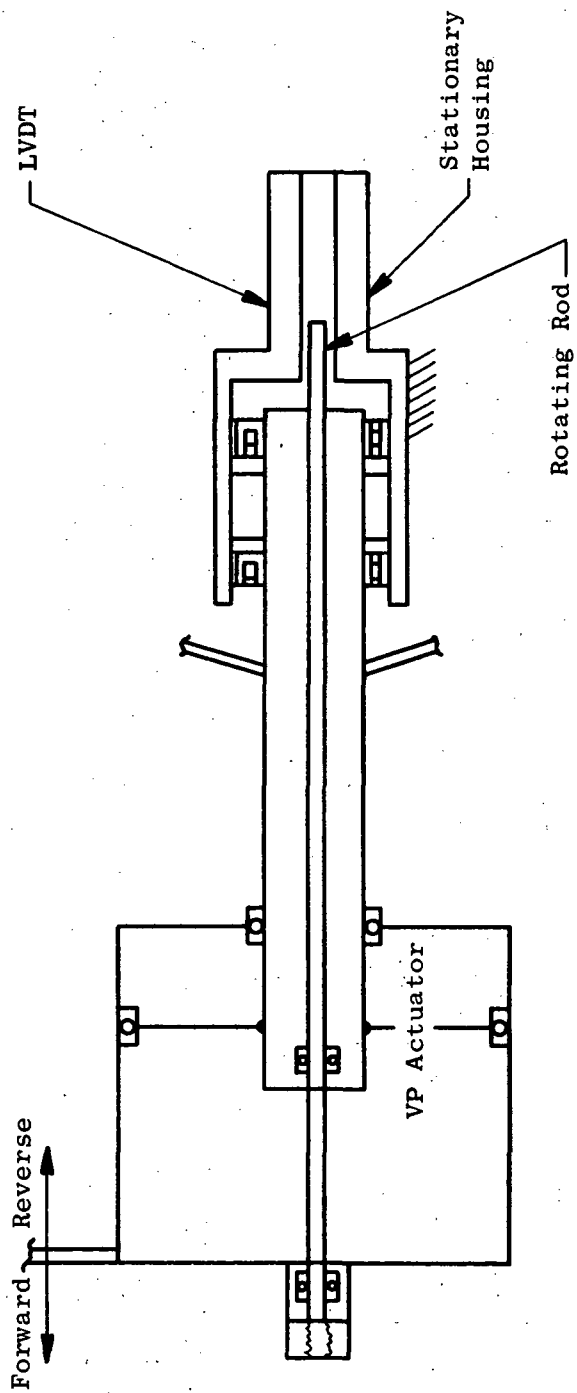


Figure 26 - Variable Pitch (VP) Fan Blade Angle Measurement (Based on Linear Position of Actuator).

minimum fuel schedule and "burst" very rapidly to maximum power, the fan remains the dominant thrust producer through most of this cycle as its speed decays only about 10% to 15% before rising again.

In the process of landing, the fan governor should be set at 100% speed. This will permit flight maneuvering and landing at appropriate power settings and allow full power potential immediately in case of wave-off, and all controlled by the PCL alone. After touchdown, to reverse thrust, the PCL is rapidly retarded to cut power. Automatically, the fan blades will move toward flat pitch to try to maintain the high fan speed setting. The low blade angle stop must then be removed and the actuator call for full reverse blade position. Simultaneously, the fan reverse "inlet" area should be increased. These three actions are triggered by the pilot's manual removal of a "reverse" lock on the PCL. A second "reverse" lock on the PCL is released when the fan blades pass a predetermined angle near flat pitch. This latter action allows the PCL to be burst to maximum reverse thrust without the fan experiencing undesirable overspeed or correction by the overspeed governor.

Overspeed Emergency Control

Safety during potential failure conditions require the addition of a fan overspeed emergency control which will reduce engine fuel flow. Preliminary work on such a control indicates that it may be able to hold a safe, high, fan speed allowing the pilot to take corrective action. The prominent potential failures are:

- a. Any part of the fan governor or hydraulic system which will drop the hydraulic pressure in the actuator. The fan blade twisting moment will turn the blades against the minimum blade angle stops and if the PCL is calling for maximum power, the fan speed will exceed 100% by an amount dependent on the minimum stop setting. Either PCL position or minimum stop setting, or both, may prevent destructive overspeed without the overspeed governor.
- b. Waveoff after starting reverse thrust operation. In this "landing failure", the pilot is required to regain maximum forward thrust as fast as possible. A PCL "burst" from reverse will bring the fan into overspeed as it moves through fine pitch. The overspeed governor will limit the rate of acceleration of the gas generator as the fan blades move to absorb the load and reduce speed below the "overspeed" setting. The time to maximum forward thrust will depend primarily on rate of blade angle movement. If the PCL "burst" is replaced by a more restrained movement of the PCL, the overspeed governor may not be activated, the result being a slight increase in time to maximum thrust.
- c. Aerodynamic or mechanical unloading of the fan without corresponding unloading of the gas generator. This may take the form of partial inlet blockage.

9. ENGINE WEIGHT

A complete weight breakdown of engines (B) and (C) is given in Appendix IV. The total weights are -

<u>Engine</u>	<u>kg</u>	<u>lb</u>
A	615.5	1358
B	1082	2386
C	975	2150

These weights are for the engines without suppression.

10. CONCLUSIONS

1. Of the noise measurement locations defined, which represent typical takeoff, approach and landing situations, the sideline noise after liftoff is the most critical. Inasmuch as the noise levels at the other locations were only slightly below the sideline noise level, all locations should continue to be used for assessment since such items as actual flight operational procedures (for example, power cutback) and airplane characteristics (for example drag as affecting approach power level) can vary from those assumed in this study. Also, the positions of the measuring points themselves are arbitrary and subject to modification.
2. For the standard 6.5 bypass TF34 engine, extensive suppressive treatment is required: in the inlet, 3 splitters plus wall treatment; in the fan exhaust, 2 splitters plus wall treatment of several different thicknesses for attenuation at different frequencies; in the core exhaust, thick wall treatment for combustor noise plus thinner treatment on multiple radial struts for turbine noise. With this treatment the sideline noise is slightly above (2 PNdB) the objective of 95 PNdB at 100% power and meets the objective at 90% power. Reducing the noise to 95 PNdB would require increasing the fan noise suppression about 5-7 PNdB, an amount which is considered excessive relative to the state-of-the-art. The jet noise would also be limiting if fan noise were to be suppressed further. A wider blade/vane spacing of 1.5 - 2.0 instead of 0.6 chords would reduce the overall noise 1.5 PNdB.
3. For the bypass 13 engines, noise treatment was selected to just meet the 95 PNdB objective. It consists of: in the inlet and fan ducts, a single splitter plus wall treatment; in the core exhaust, similar treatment as in the bypass 6.5 engine. There was no difference between the geared and direct drive engines as regards noise or treatment, on the assumption that gear noise was not an additive element, and that turbine noise was the same for both engines.
4. Noise levels were in the range 90-94 PNdB for all three engines except for the sideline noise for engine A, as noted above, using full power for the takeoff measurement point. These values do not, however, include flap impingement noise.
5. Several additional sources of noise are known, such as casing radiation, splitter supports, direct transmission along casings, and accessories. These may well become important and possibly limiting as the major sources are increasingly suppressed. Some unknown sources may also exist, with similar results. Such sources could be primary and fan exhaust noise caused by upstream turbulence.
6. The variable pitch fan was designed around solid titanium blades. The resulting centrifugal and untwist loads on these blades are high. The use of lighter weight blade construction such as plastic composite or combined metal and plastic composite is clearly indicated as a promising direction for further work.
7. The variable fan pitch feature resulted in some compromises to the aerodynamic design. These were: a reduction in solidity to 0.95 to permit the blades to pass through zero pitch without clashing, and a reduced amount of camber and twist to make the blades more suitable for reverse pitch operation. The reduced solidity resulted in a 2 point reduction in fan (B) efficiency and a further loss of about 1 point in fan (C) efficiency

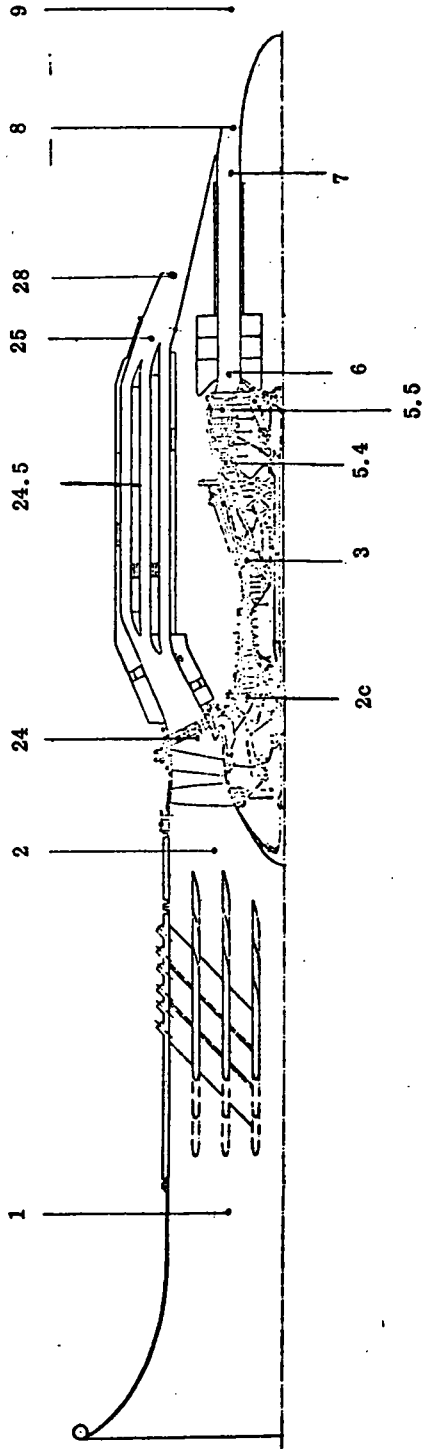
resulting from its higher tip relative Mach number. The absolute levels of efficiency were still quite acceptable, however, at 87 and 86% respectively. The camber and twist resulted in some loss of induced blade torsional stiffness. However the overall stiffness was considered satisfactory.

8. A comparison of the geared and direct drive fan systems showed that the main difference was a weight reduction of 107 kg (240 lb) for the direct drive system.

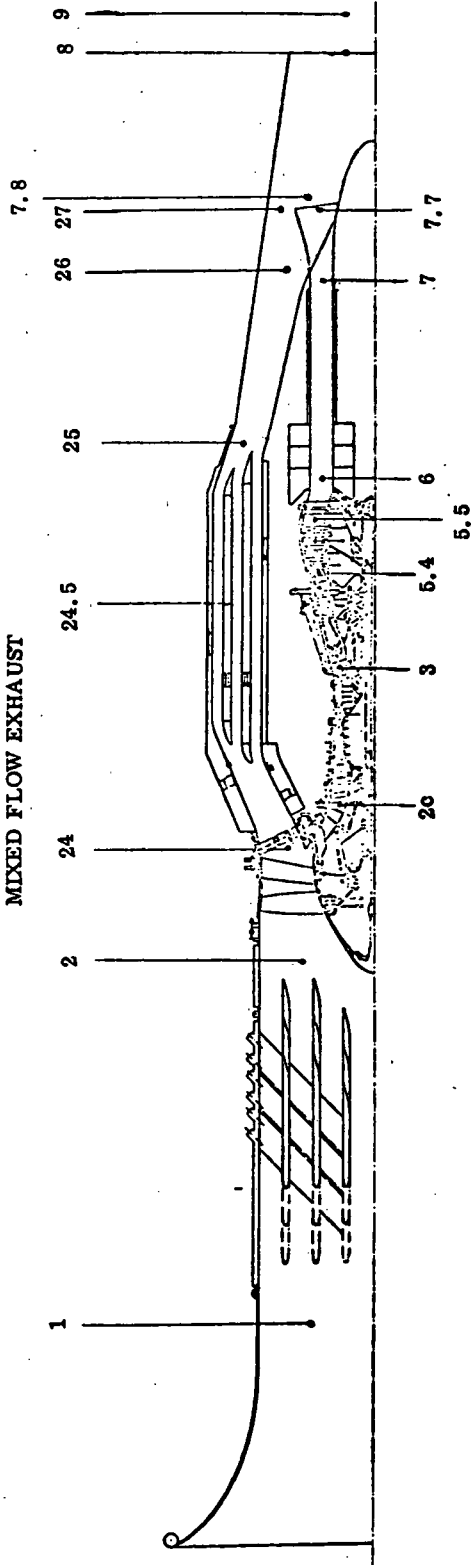
Reference 1

Latham, D; McCann, E. O. , et al "TF34 Engine Detail Noise Data and Analysis", Report prepared by General Electric Company for NASA (Lewis) under contract No. NAS 3-15545, July 8, 1971.

SEPARATE FLOW EXHAUST



MIXED FLOW EXHAUST



ENGINE STATION DESIGNATION

APPENDIX I - ENGINE CYCLE DATA

ENGINE (A) (S. I. Units)

100% Inlet Recovery
Heating Value of Fuel 42.8 MJ/kg

Altitude	m	0	0	7620
Ambient Temperature	°K	288.15	288.15	-
Flight Velocity		0	36 m/s	.8 Mach
Power Extraction	W	18,640	18,640	18,640
Bleed Flow, Stage 10	kg/s	.226	.226	0
Net Thrust	N	39624	34914	9915
Specific Fuel Consumption SFC	μkg/Ns	10.43	11.88	20.75
Total Engine Airflow	kg/s	151.9	153.1	92.9
Fan Speed	%	98.10	98.25	98.25
Fan Tip Pressure Ratio		1.477	1.474	1.414
Fan Hub Pressure Ratio		1.425	1.423	1.394
Engine Core Airflow	kg/s	20.29	20.37	11.25
Gas Generator Speed	%	108.52	108.55	103.58
Pressure Ratio		14.293	14.250	13.854
Turbine Rotor Inlet Temperature	°K	1487	1487	1365
High Pressure Turbine Pressure Ratio		4.38	4.38	4.36
Fan Turbine Inlet Temperature	°K	1081	1082	988
Low Pressure Turbine Pressure Ratio		3.16	3.17	3.34
Fully Expanded Jet Velocity	m/s	287.5	289.5	380.7
Exhaust Exit Area	m ²	.5868	.5868	.5868
Exhaust Flow Coefficient		.9731	.9733	.9823
Fan Exit Velocity				
Fan Exit Area				
Fan Flow Coefficient				

APPENDIX I

ENGINE (B) (S. I. Units)

Altitude	m	0	0	7620
Ambient Temperature	°K	288.15	288.15	-
Flight Velocity		0	36 m/s	.8 Mach
Power Extraction	W	18640	18640	18640
Bleed Flow, Stage 10	kg/s	.226	.226	0
Net Thrust	N	45092	37552	9199
Specific Fuel Consumption SFC	μkg/Ns	8.26	9.96	20.75
Total Engine Airflow	kg/s	247.2	250.2	148.7
Fan Speed	%	101.1	101.7	100.9
Fan Tip Pressure Ratio		1.245	1.242	1.256
Fan Hub Pressure Ratio		1.138	1.137	1.142
Engine Core Airflow	kg/s	17.85	17.93	10.20
Gas Generator Speed	%	107.62	107.65	103.1
Pressure Ratio		15.762	15.716	15.371
Turbine Rotor Inlet Temperature	°K	1487	1487	1365
High Pressure Turbine Pressure Ratio		4.358	4.357	4.38
Fan Turbine Inlet Temperature	°K	1080	1080	985
Low Pressure Turbine Pressure Ratio		3.291	3.302	4.05
Fully Expanded Jet Velocity	m/s	255.8	257.2	355.7
Exhaust Exit Area	m ²	.1909	.1909	.1909
Exhaust Flow Coefficient		.9588	.9589	.9622
Fan Exit Velocity	m/s	184.3	186.8	307.8
Fan Exit Area	m ²	1.045	1.045	.836
Fan Flow Coefficient		.9916	.9917	.9896

APPENDIX I

ENGINE (C) (S.I. Units)

Altitude	m	0	0	7620
Ambient Temperature	°K	288.15	288.15	-
Flight Velocity		0	36 m/s	.8 Mach
Power Extraction	W	18640	18640	18640
Bleed Flow, Stage 10	kg/s	.226	.226	0
Net Thrust	N	45336	37809	9274
Specific Fuel Consumption SFC	μkg/Ns	8.24	9.92	20.65
Total Engine Airflow	kg/s	248.6	251.9	149.7
Fan Speed	%	99.26	99.83	98.95
Fan Tip Pressure Ratio		1.2448	1.2422	1.2566
Fan Hub Pressure Ratio		1.1385	1.1384	1.1437
Engine Core Airflow	kg/s	17.89	17.98	10.24
Gas Generator Speed	%	107.61	107.64	103.13
Pressure Ratio		15.799	15.75	15.416
Turbine Rotor Inlet Temperature	°K	1488	1488	1365
High Pressure Turbine Pressure Ratio		4.345	4.344	4.373
Fan Turbine Inlet Temperature	°K	1079	1079	984
Low Pressure Turbine Pressure Ratio		3.348	3.36	4.127
Fully Expanded Jet Velocity	m/s	256.1	257.5	356.3
Exhaust Exit Area	m ²	.1908	.1908	.1908
Exhaust Flow Coefficient		.9589	.9589	.9623
Fan Exit Velocity	m/s	184.2	186.8	308.0
Fan Exit Area	m ²	1.052	1.052	0.842
Fan Flow Coefficient		.9775	.9778	.9896

APPENDIX I

ENGINE (A) (FPS Units)

100% Inlet Recovery
Heating Value of Fuel 18400 BTU/lb

Altitude	ft	0	0	25K
Ambient Temperature	°F	59	59	
Flight Velocity		0	70 kts	.8 Mach
Power Extraction	hp	25	25	25
Bleed Flow, Stage 10	lb/sec	0.5	0.5	0
Net Thrust	lbf	8908	7849	2229
Specific Fuel Consumption SFC	lbm/lbf hr	.3683	.4194	.7324
Total Engine Airflow	lb/sec	325.0	337.7	204.8
Fan Speed	%	98.10	98.25	98.85
Fan Tip Pressure Ratio		1.4779	1.4745	1.4145
Fan Hub Pressure Ratio		1.4251	1.4239	1.3940
Engine Core Airflow	lb/sec	44.74	44.92	24.81
Gas Generator Speed	%	108.52	108.55	103.58
Pressure Ratio		14.293	14.250	13.854
Turbine Rotor Inlet Temperature	°R	2678	2678	2458
High Pressure Turbine Pressure Ratio		4.38	4.38	4.36
Fan Turbine Inlet Temperature	°R	1947	1947	1778
Low Pressure Turbine Pressure Ratio		3.16	3.17	3.34
Fully Expanded Jet Velocity	ft/sec	943.4	949.8	1249.2
Exhaust Exit Area	in ²	909.5	909.5	909.5
Exhaust Flow Coefficient		.9731	.9733	.9823
Fan Exit Velocity				
Fan Exit Area				
Fan Flow Coefficient				

APPENDIX I

ENGINE (B) (FPS Units)

Altitude	ft	0	0	25K
Ambient Temperature	°F	59	59	
Flight Velocity		0	70 kts	.8 Mach
Power Extraction	hp	25	25	25
Bleed Flow, Stage 10	lb/sec	0.5	0.5	0
Net Thrust	lbf	10137	8442	2068
Specific Fuel Consumption SFC	lbm/lbf hr	.2917	.3517	.7327
Total Engine Airflow	lb/sec	545.0	551.8	327.9
Fan Speed	%	101.1	101.7	100.9
Fan Tip Pressure Ratio		1.245	1.242	1.256
Fan Hub Pressure Ratio		1.138	1.137	1.142
Engine Core Airflow	lb/sec	39.35	39.54	22.48
Gas Generator Speed	%	107.62	107.65	103.1
Pressure Ratio		15.762	15.716	15.371
Turbine Rotor Inlet Temperature	°R	2678	2678	2458
High Pressure Turbine Pressure Ratio		4.358	4.357	4.38
Fan Turbine Inlet Temperature	°R	1944	1944	1773
Low Pressure Turbine Pressure Ratio		3.297	3.302	4.05
Fully Expanded Jet Velocity	ft/sec	839.4	843.9	1167.1
Exhaust Exit Area	in ²	295.9	295.9	295.9
Exhaust Flow Coefficient		.9588	.9589	.9622
Fan Exit Velocity	ft/sec	604.7	612.9	1010.0
Fan Exit Area	in. ²	1619.1	1619.1	1295.3
Fan Flow Coefficient		.9916	.9917	.9896

APPENDIX I

ENGINE (C) (FPS Units)

Altitude	ft	0	0	25K
Ambient Temperature	°F	59	59	
Flight Velocity		0	70 kts	.8 Mach
Power Extraction	hp	25	25	25
Bleed Flow, Stage 10	lb/sec	0.5	0.5	0
Net Thrust	lbf	10192	8500	2085
Specific Fuel Consumption SFC	lbm/lbf hr	.291	.3503	.7292
Total Engine Airflow	lb/sec	548.2	555.5	330.2
Fan Speed	%	99.26	99.83	98.95
Fan Tip Pressure Ratio		1.2448	1.2422	1.2566
Fan Hub Pressure Ratio		1.1385	1.1384	1.1437
Engine Core Airflow	lb/sec	39.45	39.64	22.57
Gas Generator Speed	%	107.61	107.64	103.13
Pressure Ratio		15.799	15.75	15.416
Turbine Rotor Inlet Temperature	°R	2678	2678	2458
High Pressure Turbine Pressure Ratio		4.345	4.344	4.373
Fan Turbine Inlet Temperature	°R	1944	1944	1772
Low Pressure Turbine Pressure Ratio		3.348	3.36	4.127
Fully Expanded Jet Velocity	ft/sec	840.4	844.8	1169
Exhaust Exit Area	in ²	295.7	295.7	295.7
Exhaust Flow Coefficient		.9589	.9589	.9623
Fan Exit Velocity	ft/sec	604.4	612.8	1010.4
Fan Exit Area	in ²	1631.5	1631.5	1305.2
Fan Flow Coefficient		.9775	.9778	.9896

APPENDIX II

Derivative Table - Inlet Losses

Exhaust Areas Resized

Thrust vs. Pressure Loss Derivative	$\frac{\Delta F_N}{F_N}$ $\Delta \left[\frac{P}{P} \right]$	SFC vs. Pressure Loss Derivative	$\frac{\Delta SFC}{SFC}$ $\Delta \left[\frac{P}{P} \right]$
---	---	---	---

Sea level, 288 °K (59 °F), maximum power
no bleed, no power extraction

Engine A	- 2.42		1.47
B	- 3.92		3.12
C	- 3.93		3.11

Mach 0.8
7620 m (25,000 ft), no bleed, no power extraction

Engine A	- 3.52		2.49
B	- 5.97		5.33
C	- 6.00		5.36

APPENDIX II

Derivative Table - Fan Duct Pressure Losses
Exhaust Areas Resized

Thrust vs. Pressure Loss Derivative	$\frac{\Delta F_N}{F_N}$ $\Delta \left[\frac{\Delta P}{P} \right]$	SFC vs. Pressure Loss Derivative	$\frac{\Delta SFC}{F_N}$ $\Delta \left[\frac{P}{P} \right]$
---	--	--	---

Sea level, 288 °K (59 °F), maximum power
no bleed, no power extraction

Engine A	- .95	.98
B	- 2.38	2.54
C	- 2.38	2.54

Mach 0.8
7620 m (25,000 ft), no bleed, no power extraction

Engine A	- 2.10	2.17
B	- 4.32	4.80
C	- 4.33	4.82

APPENDIX II

Derivative Table - Core Duct Pressure Losses

Exhaust Areas Resized

Thrust vs. Pressure Loss Derivative	$\frac{\Delta F_N}{F_N}$ $\Delta [P/P]$	SFC vs. Pressure Loss Derivative	$\frac{\Delta SFC}{SFC}$ $\Delta [P/P]$
---	--	--	--

Sea level, 288 °K (59 °F), maximum power
no bleed, no power extraction

Engine A	- .60		.63
B	- .67		.66
C	- .67		.67

Mach 0.8
7620 m (25,000 ft), no bleed, no power extraction

Engine A			
B	- .48		.49
C	- .55		.50

APPENDIX III

Timken Physical Laboratories Report - Test No. 266.3-H

Torque and High Load Characteristics of the T-127 Thrust Bearing

Test Objective

The objective of this test was to determine if the T-127 thrust bearing would be capable of withstanding extremely high loads (249 kN (56,000 lb) thrust) without severe damage to the rollers or races. Ten T-127 series thrust bearings were tested with the retainers removed.

Conclusion

When the full test load of 249 kN (56,000 lb) - approximately 7 1/2 times the Basic Thrust Rating of the bearing was applied to these bearings statically, there was slight brinelling of the races. This resulted in erratic torque readings. However, when the bearings were being oscillated while the load was being applied, there was uniform deformation over the races. One set of bearings was subjected to 445 kN (100,000 lb) thrust load which is 13 times the Basic Thrust Rating. This load resulted in severe plastic deformation of the races; however, there were no cracked races or rollers from this load. The one broken roller in the tests with 249 kN (56,000 lb) load was apparently caused by not having the bearing properly assembled.

It is felt that the T-127 thrust bearing is capable of withstanding the excessive loads for short periods of time without severe bearing damage. A short period of running-in the bearings at maximum load would probably result in lower bearing torque, by causing uniform plastic deformation of the races.

Method of Testing

The metal bearing retainers were removed from the T-127 thrust bearings. The thrust bearings were then lubricated with Sinclair L-300 grease and installed in the test set-up. A Baldwin Press was used for applying thrust load to the bearing test set-up.

The loading procedure consisted of the following method:

1. Apply 26.7 kN (6000 lb) load and record torque.
2. Increase load statically to 249 kN (56,000 lb) and record torque.
3. Reduce load to 26.7 kN (6000 lb) and record torque.
4. Increase load to 249 kN (56,000 lb), oscillate the bearings for 600 s (10 minutes) and record torque.
5. Reduce load to 26.7 kN (6000 lb) and record torque.

This procedure was used for the first eight bearings with four being oscillated 1.57 rad (90°) and four being oscillated 0.17 rad (10°). The final two bearings were installed in the rig and oscillated approximately 0.17 rad (10°) while the load was increased to 445 kN (100,000 lb) in an attempt to determine the bearings ultimate strength.

Test Results

The following Table lists the torque values for each load applied and appropriate comments for the condition of each set of thrust bearings tested:

Bearing Number	Thrust Load		Bearing Torque		Remarks
	kN	lb	N-m	lb-ft	
1 & 2	26.7	6,000	7	5	This set of bearings was oscillated approximately .17 rad (10°) resulting in slight plastic disformation
	249	56,000	87-141	64-104	
	26.7	6,000	7-14	5-10	
	249	56,000	71-119	52-88	
	26.7	6,000	4-7	3-5	
3 & 4	26.7	6,000	9	7	This set of bearings was oscillated approximately .17 rad (10°) resulting in slight plastic deformation.
	249	56,000	136	100	
	26.7	6,000	5-10	4-8	
	249	56,000	81-136	60-100	
	26.7	6,000	4-8	3-6	
5 & 6	26.7	6,000	8	6	This set of bearings was oscillated approximately 1.57 rad (90°). Note: Roll overlap eliminate erratic torque.
	249	56,000	87-141	64-104	
	26.7	6,000	5	4	
	249	56,000	125	92	
	26.7	6,000	8	6	
7 & 8	26.7	6,000	5	4	This set of bearings was oscillated approximately 1.57 rad (90°) and also oscillated while applying load. One roller was broken result in higher final torque.
	249	56,000	81	60	
	26.7	6,000	5	4	
	249	56,000	125	92	
	26.7	6,000	6	5	

APPENDIX IV - ENGINE (B) AND (C) WEIGHT.

		FAN "B"		FAN "C"				
	Item		Total		Item		Total	
	kg	(lb)	kg	(lb)	kg	(lb)	kg	(lb)
Fan Rotor			147.6	(325.3)	153.5	(338.4)		
Blades	54.4	(120)			63.6	(140.3)		
Disk and Shaft	50.7	(111.8)			55.3	(121.9)		
Bearings	11.8	(26)			10.2	(22.4)		
Gears	12.7	(28)			10.2	(22.4)		
Nose Cone	5.6	(12.3)			4.0	(8.8)		
Miscellaneous	12.3	(27.2)			10.3	(22.6)		
Variable Pitch			58.0	(127.9)	46.7	(102.9)		
Bearings and Gear	25.	(55)			21.0	(46.3)		
Spline Followers								
Spline Drum	15.6	(34.5)			12.5	(27.5)		
Miscellaneous	17.4	(38.4)			13.2	(29.1)		
Forward Fan Shaft			7.0	(15.5)	5.1	(11.2)		
Gearbox			64.0	(141)	0			
(includes sun gear)								
Fan Shaft			12.4	(27.4)	14.7	(32.3)		
Shaft	10.8	(23.7)			13.0	(28.6)		
Miscellaneous	1.7	(3.7)			1.7	(3.7)		
Rear Fan Shaft			4.9	(10.9)	6.4	(14)		
Fan Stator			102.8	(226.6)	108.2	(238.5)		
Vaness	38.9	(85.8)			432.8	(97.3)		
Vane Support Hub	4.2	(9.3)			34.3	(7.7)		
Vane Spacers	4.1	(9.0)			36.5	(8.2)		
Fan Case	9.8	(21.7)			93	(21)		
Stator Case	23.7	(52.3)			22.2	(50)		
Flowpath Sound Suppression	18.6	(41.1)			208.6	(46.9)		
Miscellaneous	3.4	(7.4)			32.9	(7.4)		

APPENDIX IV - ENGINE (B) AND (C) WEIGHT (Concluded).

	FAN "B"				FAN "C"			
	Item		Total		Item		Total	
	kg	(lb)	kg	(lb)	kg	(lb)	kg	(lb)
Front Frame			65.	(143.2)			65.	(143.3)
Frame	22.8	(50.2)			22.8	(50.2)		
Splitter Nose	5.4	(12)			5.4	(12)		
Tie Rods	12	(26)			12.	(26)		
Miscellaneous	.91	(2)			.91	(2)		
Tie Rod Hub	24	(53)			24.	(53)		
Core			191.1	(421.4)			191.1	(421.4)
Low Pressure Turbine Rotor			39.1	(86.3)			39.4	(86.8)
Low Pressure Turbine Stator			45.7	(100.7)			64.5	(142.3)
Exhaust Frame			15.6	(34.4)			17.1	(37.7)
"A" Sump			91.6	(201.9)			20.6	(45.5)
"C" Sump			7.9	(17.5)			8.3	(18.2)
Accessories & Controls			107.8	(237.7)			107.8	(237.7)
Miscellaneous			42.8	(94.4)			42.8	(94.4)
Fan Actuation Hydraulics			27.	(59)			28.	(62)
10% Margin on Calculated Mass			51.9	(114.5)			56.1	(123.6)
Total Mass			1082	(2386)			975	(2150)

FOLDOUT FRAME 1

FOLDOUT FRAME 2

APPENDIX V

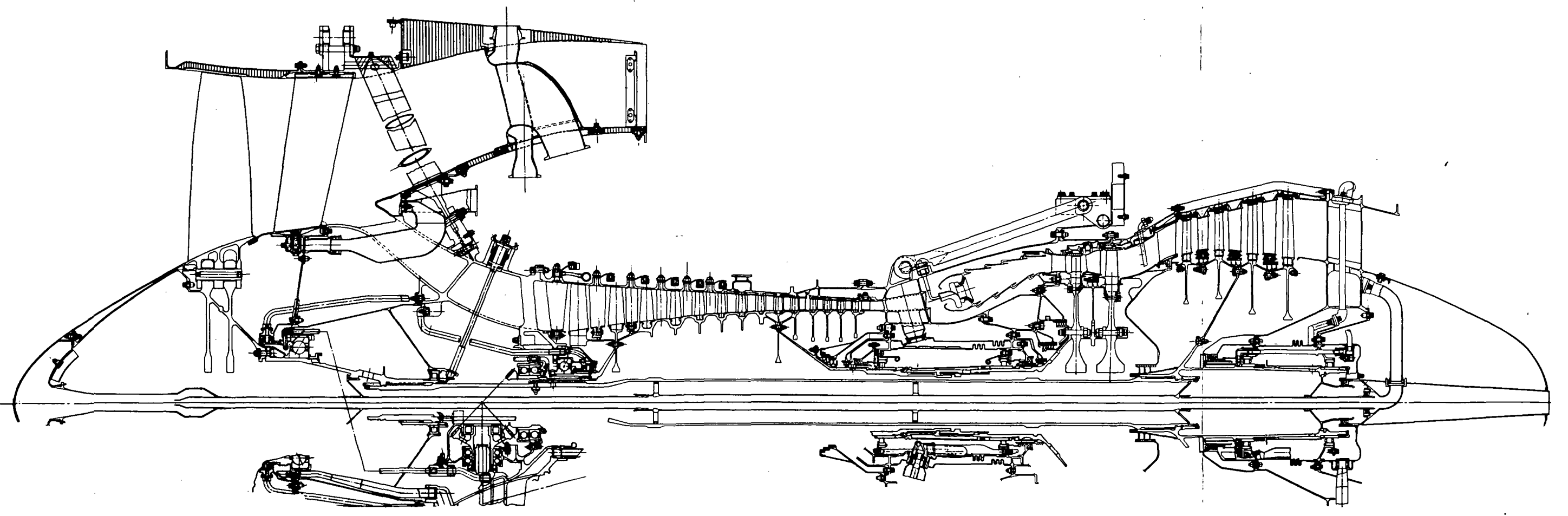


Figure 1 - Engine A, YTF34-2.

ε

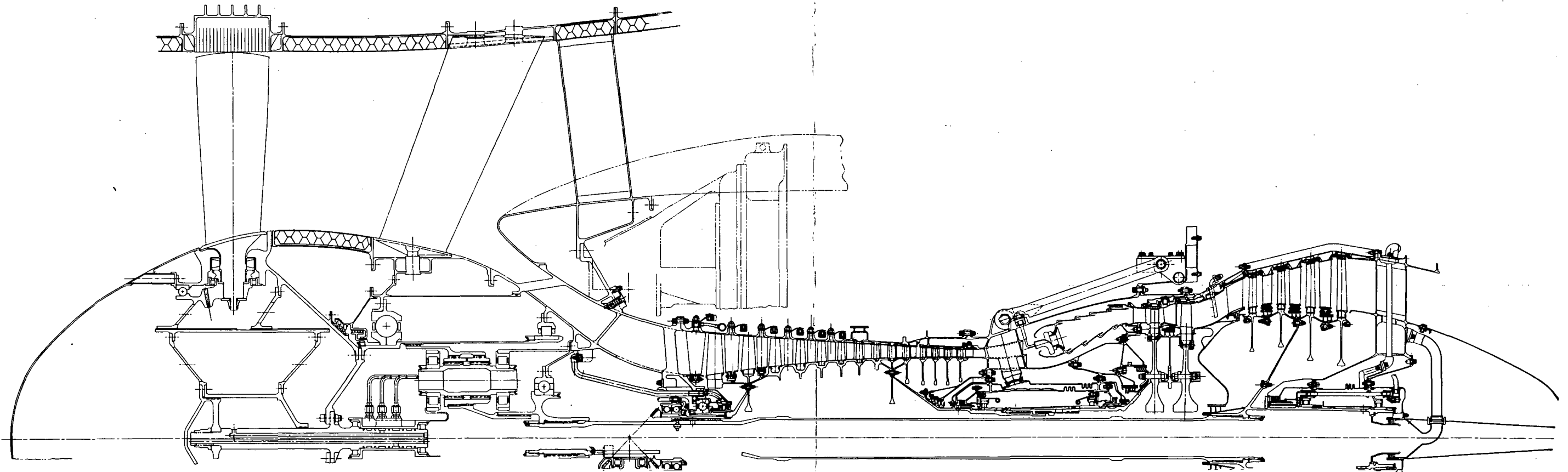


Figure 2 - Engine B, TF34 Core and LP Turbine with Geared Variable Pitch Fan.

FOLDOUT FRAME 1

FOLDOUT FRAME 2

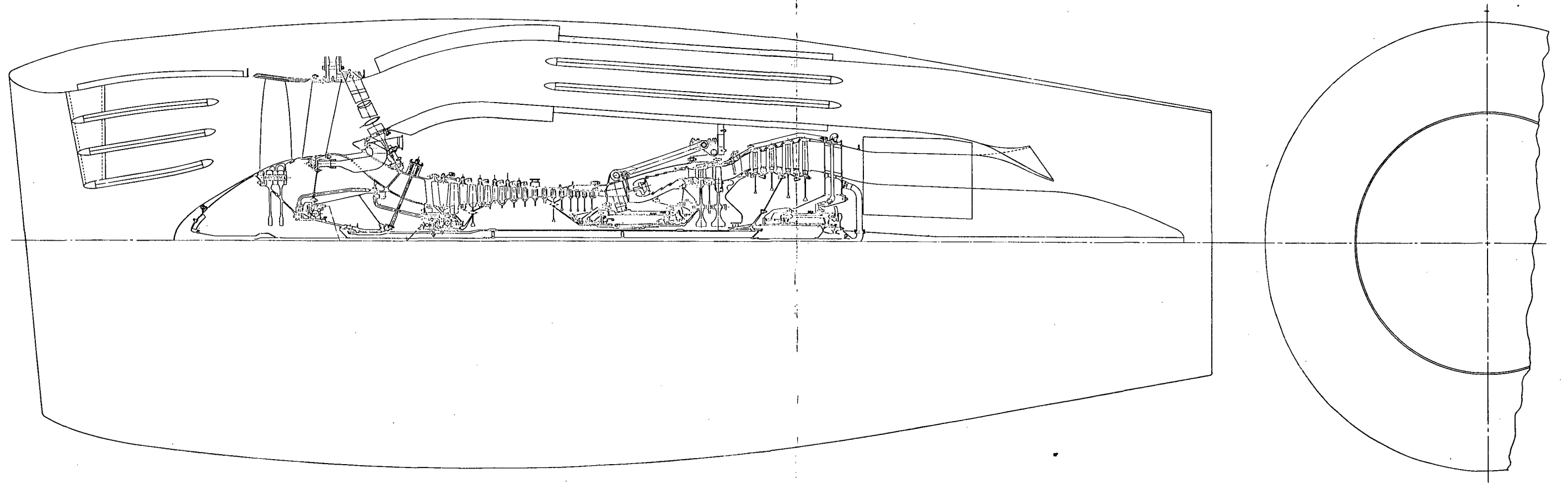


Figure 4 - Engine A Installed.

SECRET FOR EYES ONLY

FOLDOUT FRAME 1

FOLDOUT FRAME 2

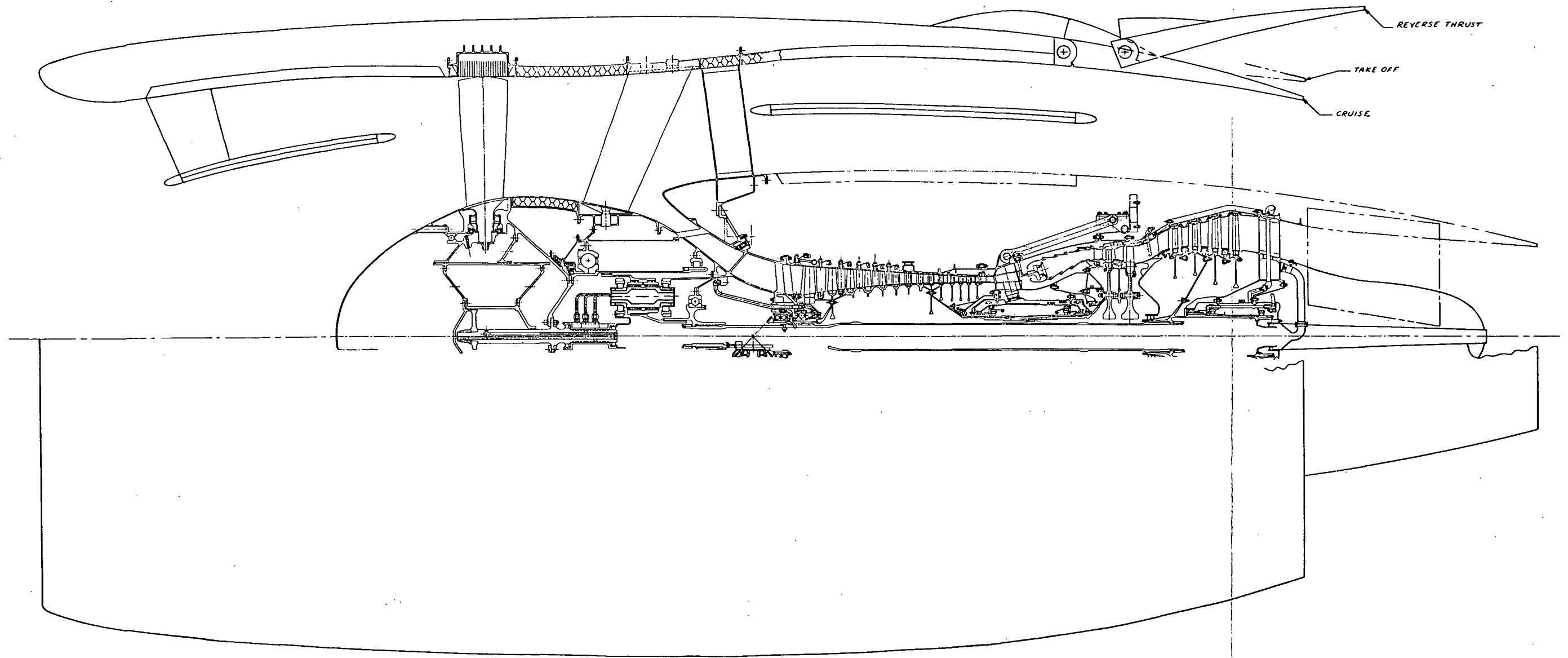


Figure 5 - Engine B Installed.

FOLDOUT FRAME

1

FOLDOUT FRAME

2

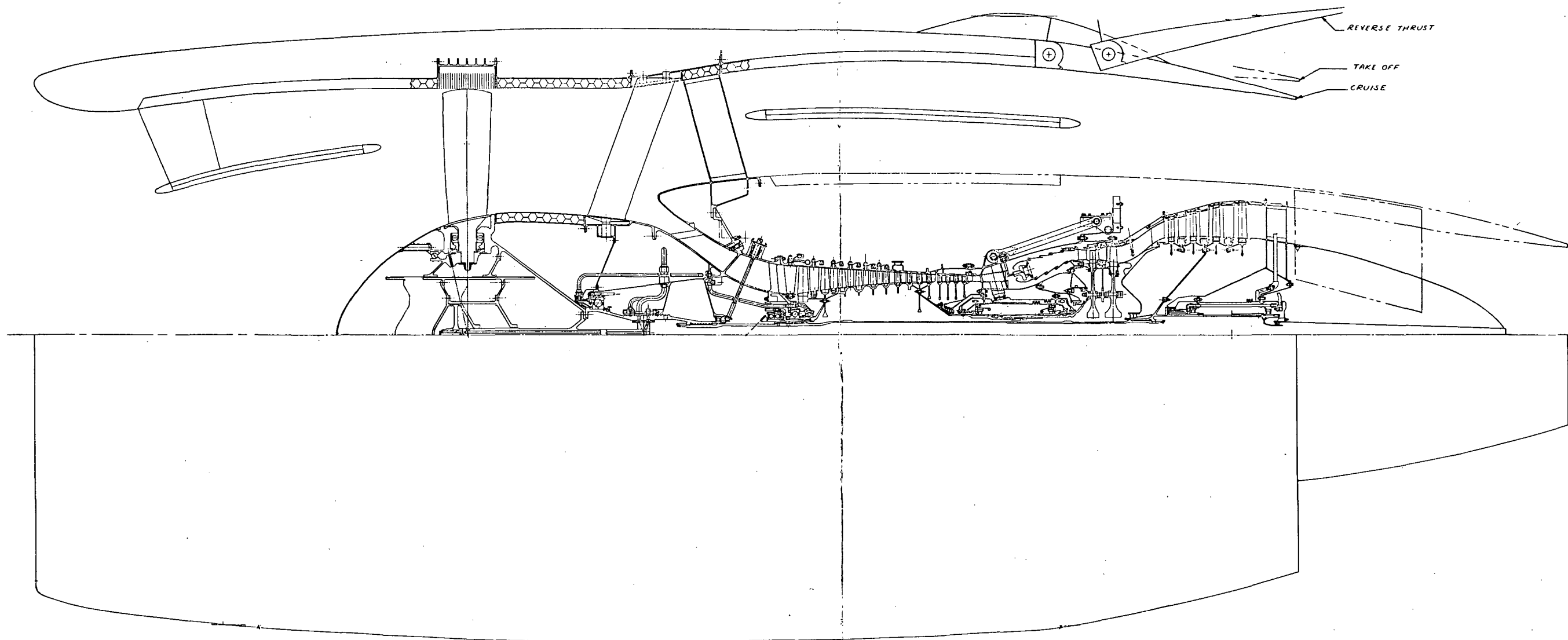


Figure 6 - Engine C Installed.